APPLICATION OF CONIFER NEEDLES IN THE RECONSTRUCTION OF HOLOCENE CO_2 LEVELS

DE TOEPASSING VAN CONIFERENNAALDEN BIJ DE RECONSTRUCTIE VAN HOLOCENE CO_2 CONCENTRATIES

(Met een samenvatting in het Nederlands)

PROEFSCHRIFT

ter verkrijging van de graad van doctor aan de Universiteit Utrecht, op gezag van de Rector Magnificus, Prof. dr. W.H. Gispen, ingevolge het besluit van het College voor promoties in het openbaar te verdedigen op vrijdag 16 januari 2004
des middags te 12.45 uur

door

LENNY LIESBETH RIA KOUWENBERG

geboren op 11 oktober 1973 te Leiden

PROMOTOR: PROF. DR. H. VISSCHER
Faculteit Biologie, Universiteit Utrecht

CO-PROMOTOR: DR. W.M. KÜRSCHNER
Faculteit Biologie, Universiteit Utrecht

The research in this thesis was carried out at the Laboratory of Palaeobotany and Palynology, Budapestlaan 4, 3584 CD Utrecht, the Netherlands. The research was supported by the Netherlands Council for Earth and Life Sciences (ALW) with financial aid from the Netherlands Organisation for Scientific Research (NWO), project no. 750.198.07.

CONTENTS

CHAPTER 1

General introduction and synopsis

Coupling of atmospheric CO_2 and global climate is supported by climate model outputs predicting a strong rise in global mean temperature as a result of the progressive injection of anthropogenic CO_2 into the atmosphere. In order to assess the effect of ongoing fast-paced addition of CO_2 to the climate system, the amplitude and frequency of natural CO_2 changes and their contribution to climate dynamics need to be documented. On glacial/interglacial and millennial time-scales, parallel variations of CO_2 and temperature have been observed in Antarctic ice-cores. In marked contrast, conflicting evidence exists for the presence of CO_2 fluctuations associated with documented centennial-scale cooling events in the Holocene. To clarify the nature of the link between CO_2 and climate on relatively short time-scales, precise, high-resolution reconstructions of the pre-industrial evolution of atmospheric CO_2 are required.

An increasingly applied method to detect and quantify short-term fluctuations in Holocene CO_2 levels is the analysis of stomatal frequency of fossil leaves derived from peat and lake deposits. For a wide variety of tree species, there is observational and experimental evidence of an inverse relation between numbers of leaf stomata and ambient CO_2 concentration. Adjustment of stomatal frequency to changes in atmospheric CO_2 allows plants to retain the most profitable balance between carbon uptake for photosynthesis and loss of water through evaporation. Quantification of CO_2 responsiveness of individual tree species over the last century enables estimation of Holocene CO_2 levels by measuring stomatal frequency of fossil leaves.

So far, stomata-based CO_2 reconstructions for the Holocene have mainly been derived from fossil leaves of broad-leaved trees and shrubs. However, because of the long-term dominance of conifers in temperate and boreal forest ecosystems, the use of fossil conifer needles could greatly improve the spatial and temporal coverage of such reconstructions. Although conifer needles are often found in Holocene peat and lake deposits due to their high preservation capacity, they were largely neglected after initial studies had suggested that stomatal frequency of conifers would not adjust to CO_2 mixing ratios above 280 ppmv. However, it should be noted that conifers exhibit a different mode of leaf development and subsequent epidermal morphology than the broad-leaved angiosperm taxa commonly used for stomatal frequency analysis. A presumed lack of response of conifer needles could well be a consequence of the application of conventional stomatal frequency quantification methods that are tailored to the stomatal pattern of broad-leaved plants. A re-assessment of the potential of conifer needles in atmospheric CO_2 reconstructions would require the development of new quantification strategies in which their complex stomatal patterning is taken into consideration. Because robust estimates of past climate data on the basis of fossil materials depend on the reliability and accuracy of proxy-validation, it is also essential to assess to what extent stomatal frequency of conifer needles can be influenced by biological or environmental factors other than atmospheric CO_2 concentration.

As a contribution to broaden the range of taxonomically, geographically, and ecologically contrasting plant species that may be applied in stomata-based CO_2 reconstruction, and with special emphasis on North American conifers this thesis, therefore, aims to (1) develop

suitable quantification strategies for the stomatal frequency response of selected conifer taxa to historical CO_2 increase; (2) validate the CO_2 response by assessing the influence of local biological and environmental parameters on stomatal numbers; (3) perform stomatal frequency analysis on fossil conifer needles from the Northwest Pacific area to obtain high-resolution CO_2 reconstructions for the Late Holocene; and (4) compare the obtained records, together with existing Holocene stomata-based CO_2 reconstructions, to global and regional climate records in order to examine the relation between atmospheric CO_2 and temperature on centennial time-scales.

In **Chapter 2** the stomatal frequency response of four native North American conifer species (*Tsuga heterophylla*, *Picea glauca*, *P. mariana*, and *Larix laricina*) to a range of historical CO_2 mixing ratios (290 to 370 ppmv) is analyzed. Because of the specific mode of leaf development and the subsequent stomatal patterning in conifer needles, the traditionally used stomatal index of these species is not affected by CO_2. In contrast, a new measure of stomatal frequency, based on the number of stomata per mm needle length, decreases significantly with increasing CO_2. For *T. heterophylla*, the stomatal frequency response to CO_2 changes in the last century is validated through assessment of the influence of other biological and environmental variables. Because of their sensitive response to CO_2, combined with a high preservation capacity, fossil needles of the investigated conifer species have great potential for detecting and quantifying past atmospheric CO_2 fluctuations.

Because in conifers density-based stomatal frequency measurements rather than stomatal index were found to respond to CO_2, the influence of cell expansion on the stomatal frequency must be determined. In **Chapter 3**, epidermal cell differentiation and specifically stomatal characteristics of *Tsuga heterophylla* needles during leaf development are described. Stomata first appear in the apical region and subsequently spread basipetally towards the needle base during development. The number of stomatal rows on a needle does not change during ontogeny, but stomatal density decreases nonlinearly with increasing needle area, until about 50 % of the final needle area. The total number of stomata on the needle increases during the entire developmental period, indicating that stomatal and epidermal cell formation continues until the needle has matured completely. This is fundamentally different from angiosperm dicotyledon leaf development, where in general leaf expansion in the final stages is due to cell expansion rather than cell formation. The lack of further change in either stomatal density or stomatal density per mm needle length (the stomatal characteristic most sensitive to CO_2 in conifers) in the final stages of leaf growth indicates that leaf maturation in conifers does not significantly affect stomatal density based CO_2 reconstructions.

Now that the inverse relation between atmospheric CO_2 concentrations and stomatal numbers on *Tsuga heterophylla* needles have been quantified and validated, paleo-atmospheric CO_2 concentrations over the period 800-2000 AD are reconstructed in **Chapter 4** from fossil *T. heterophylla* needles preserved in sediments of the small lake Jay Bath (Mount Rainier, Washington, USA). The stomatal frequency record reveals significant century-scale

fluctuations, with prominent minima in CO_2 of about 260 ppmv around 860 AD and 1150 AD, and smaller minima of 275-280 ppmv occurring around 1600 and 1800 AD. In between, CO_2 maxima of 300 ppmv around 1000 AD, 320 ppmv around 1300 AD, and 300 ppmv around 1700 AD are recorded. These features occur in harmony with global terrestrial temperature changes, as well as surface temperature fluctuations of the North Atlantic Ocean. The results reinforce the notion of a continuous coupling of CO_2 and climate during Holocene times.

In **Chapter 5**, extension of the stomatal frequency record of *Tsuga heterophylla* needles from Jay Bath to 200 AD reveals remarkably low stomatal numbers from 300 AD to 750 AD, lower even than modern values. Unlike fluctuations in the stomatal frequency record over the past 1200 years, these low stomatal numbers do not correspond to equivalent warm periods in global or regional climate records. They do coincide, however, with a major disturbance around Jay Bath. A vegetation reconstruction based on fossil needles shows early-successional species inhabiting the area between 300 and 700 AD, following a prominent disturbance. Therefore, initial establishment of *T. heterophylla* at the site occurred in a relatively open and exposed setting in constrast to the closed forest characteristic of later successional stages. The first generations of *T. heterophylla* probably experienced suboptimal growing conditions in this early-successional habitat. Notably spring water stress resulting from prolonged chilling of root systems in open montane habitats could have suppressed stomatal numbers. After 750 AD, the uninterrupted presence of a stable late-successional forest justifies interpretation of stomatal frequency data in terms of atmospheric CO_2 levels.

Reconstructing atmospheric CO_2 levels on the slopes of an active volcano, such as Mount Rainier warrants testing for the influence of volcanic CO_2 production on local CO_2 levels. In **Chapter 6** the likelihood of volcanic CO_2 presence at Jay Bath is discussed. Considering the location of Jay Bath, outside of the proximity of the crater or current geothermally active areas, the site has probably not experienced significant excess CO_2 from these sources. This is supported by carbon-isotope measurements on needles of *Tsuga heterophylla.* A contribution of substantial amounts of volcanic CO_2 in photosynthesis should leave a signature in ^{13}C or ^{14}C isotopes of plant organic matter. Carbon-isotope data over the past two millennia show no indication for the presence of magmatic CO_2. Therefore, the reliability of the stomatal frequency record from Jay Bath is not compromised by local volcanic activity.

Finally, in **Chapter 7**, the CO_2 reconstruction from Jay Bath over the past 1200 years is compared to other stomata-based CO_2 estimates that correspond to documented, centennial-scale Holocene cooling events. The majority of the reconstructions do not support the widely accepted concept of relatively stable CO_2 concentrations throughout the past 12,000 years. To address the critique that stomatal frequency variations could have been caused by local environmental changes or methodological insufficiencies, multiple stomatal frequency records were compared for three climatic key periods during the Holocene: (1) the Preboreal oscillation; (2) the 8.2 kyr cooling event; and (3) the Little Ice Age. Despite being obtained

with different calibration approaches, from taxonomically and ecologically contrasting plant species in Europe and North America, the highly similar fluctuation patterns in the paleo-atmospheric CO_2 records strengthen the integrity of leaf-based CO_2 quantification.

It may be concluded from this thesis that fossil needles of conifer species, in particular *Tsuga heterophylla*, can be applied in stomata-based atmospheric CO_2 reconstructions, and may especially be useful to reconstruct relatively high CO_2 levels. Among potential factors that may obscure the CO_2 responsiveness of conifer needles, notably environmental stress associated with open montane habitats should be taken into account. The conifer-based CO_2 reconstruction over the last 1200 years supports the notion of a coupling between CO_2 and climate on centennial time-scales during the Holocene.

N.B. The chapters of this thesis are or will be published as separate papers in scientific journals. As a consequence, some repetition of statement could not be avoided.

CHAPTER 2

STOMATAL FREQUENCY ADJUSTMENT OF FOUR CONIFER SPECIES TO HISTORICAL CHANGES IN ATMOSPHERIC CO_2

The species-specific inverse relation between atmospheric CO_2 concentration and stomatal frequency for many woody angiosperm species is being used increasingly with fossil leaves to reconstruct past atmospheric CO_2 levels. To extend our limited knowledge of the responsiveness of conifer needles to CO_2 fluctuations, the stomatal frequency response of four native North American conifer species (*Tsuga heterophylla*, *Picea glauca*, *Picea mariana* and *Larix laricina*) to a range of historical CO_2 mixing ratios (290 to 370 ppmv) was analyzed. Because of the specific mode of leaf development and the subsequent stomatal patterning in conifer needles, the stomatal index of these species was not affected by CO_2. In contrast, a new measure of stomatal frequency, based on the number of stomata per mm needle length, decreased significantly with increasing CO_2. For *Tsuga heterophylla*, the stomatal frequency response to CO_2 changes in the last century is validated through assessment of the influence of other biological and environmental variables. Because of their sensitive response to CO_2, combined with a high preservation capacity, fossil needles of *Tsuga heterophylla*, *Picea glauca*, *P. mariana*, and *Larix laricina* have great potential for detecting and quantifying past atmospheric CO_2 fluctuations.

INTRODUCTION

The current rise in atmospheric CO_2 levels has stimulated research on physiological responses of land plants to changes in the concentration of this greenhouse gas. In growth experiments with elevated CO_2 levels, the number of leaf stomata decreased for 40% of the species studied (Woodward and Bazzaz, 1988, Woodward and Kelly, 1995; Royer, 2001). This inverse relation between stomatal frequency and atmospheric CO_2 is even more apparent under lower-than-present experimental CO_2 levels (Woodward, 1987; Woodward and Bazzaz, 1988; Malone, 1993; Royer, 2001). A genetic basis for the response is provided by the identification of a CO_2-sensitive gene in *Arabidopsis thaliana* that is involved in the control of stomatal development (Gray et al., 2000).

The relation between stomatal frequency and atmospheric CO_2 concentration (mixing ratio; measured as parts per million by volume [ppmv]) is confirmed by studies of leaves that were grown under the lower CO_2 levels of the past 100 yr. Such leaves can be obtained from herbarium collections or subfossil leaf assemblages. The main advantage of historical leaf material over experimental material is that the stomatal frequency responses to CO_2 have occurred under natural conditions. Effects of experimental single-step CO_2-enrichment (typically CO_2-doubling) on seedlings may not be representative of long-term responses to incremental increases of 1 to 2 ppmv CO_2 per year or per growing season.

Notably leaves of woody angiosperm taxa show a negative correlation between mean stomatal frequency and the historical CO_2 rise from 280 to 360 ppmv (Woodward, 1987; Penuelas and Matamala, 1990; Paoletti and Gellini, 1993; Kürschner et al., 1996; Wagner et al., 1996; Wagner, 1998). Modelled response curves for species of *Betula* and *Quercus* predict different response limits to a CO_2 increase (~400 and ~340 ppmv, respectively), indicating that nonlinear stomatal frequency responses vary from one tree species to another (Kürschner et al., 1997). The models also suggest that the maximum effect of the current CO_2 increase on stomatal frequency has already been reached, thereby explaining the common lack of stomatal frequency responses in CO_2-doubling experiments.

Conifers and broad-leaved angiosperms have basic differences in stomatal formation and leaf development (Esau, 1977). In angiosperms, stomata and epidermal cells are initiated at multiple points on the developing leaf surface, resulting in a relatively random distribution of stomata on the entire leaf surface. Epidermal cells and stomata in conifer needles are all initiated at the base of the needle, developing henceforth in longitudinal files during needle growth (Croxdale, 2000). Conifers have a less-pronounced decrease in stomatal conductance than angiosperms in response to long-term, elevated CO_2 exposure (Saxe et al., 1998; Medlyn et al., 2001). Because stomatal conductance is in part determined by the number of stomata on the leaf surface (Jones, 1992), in theory different responses could be related to differences in the adjustment of stomatal frequency to CO_2 levels.

To date, only six experiments have been performed to test whether the typical arrangement of stomata in conifer needles affects stomatal frequency responses to atmospheric CO_2 (Royer, 2001). A frequency decrease in *Pinus sylvestris* under elevated CO_2 (Beerling, 1997; Lin et al., 2001) suggests that conifers also may have the capacity to adjust their stomatal numbers. However, stomatal frequency in other species (*Pinus pinaster*, *P. banksiana*, *P. palustris*, *Pseudotsuga menziesii*, and *Picea abies*) is not reduced at elevated CO_2 levels (Stewart and Hoddinott, 1993; Guehl et al., 1994; Dixon et al., 1995; Pritchard et al., 1998; Apple et al., 2000). This lack of reduction could indicate that in many conifer species, stomatal frequency is not very sensitive to CO_2 changes. On the other hand, the controlled-environment experiments may have been performed under CO_2 levels that are well above the response limit to a CO_2 increase.

In addition to experimental studies, the CO_2 responsiveness of two conifer species has been confirmed by analyses of fossil and herbarium materials. Van de Water et al. (1994) have reported elevated stomatal frequencies in fossil needles of *Pinus flexilis* corresponding to a CO_2 range from 180 to 290 ppmv. Recently, in a herbarium study on needles of *Metasequoia glyptostroboides*, stomatal frequency decreased linearly over a CO_2 range from 310 to 340 ppmv (Royer et al., 2001). Additional experiments on *Metasequoia* under CO_2 concentrations of 430 and 790 ppmv showed a nonlinear response, similar to the response curves of angiosperm species, levelling off at about 500 ppmv. Obtaining these response curves is hampered by the fact that most experiments involve a single-step doubling of CO_2. To compare the CO_2 response curves of conifers to those of angiosperms, the stomatal frequency must be measured over a gradual increase in CO_2.

Historical data sets enable the construction of accurate response curves that can be used as training sets for the quantification of past atmospheric CO_2 levels on the basis of stomatal frequency analysis of fossil leaves (Van der Burgh et al., 1993; Beerling et al., 1995; Kürschner et al., 1996; Rundgren and Beerling, 1999; Wagner et al., 1999; McElwain et al., 2002). Considering the dominance of conifers in temperate and boreal forest ecosystems, the ability to use fossil conifer needles for quantifying past CO_2 levels would greatly extend the spatial and temporal coverage of such reconstructions. In North America, well-preserved needles of *Tsuga heterophylla*, *Picea glauca*, *P. mariana*, and *Larix laricina* are often present in Quaternary lake and peat deposits (Dunwiddie, 1986; Cwynar, 1987; Mayle and Cwynar, 1995).

To assess the CO_2 responsiveness of conifer needles, as well as their potential as biosensors of paleo-atmospheric CO_2 fluctuations, the present study focuses upon the stomatal frequency response of these species to a range of historical CO_2 values (290-370 ppmv). Customized counting strategies are introduced to account for the typical stomatal patterning in conifers needles.

MATERIAL AND METHODS

Material

Stomatal frequency was analyzed for four native North American conifer species: *Tsuga heterophylla*, *Picea mariana*, *P. glauca*, and *Larix laricina*. The measurements were performed at two institutes: (1) on *Tsuga heterophylla* needles at the Laboratory of Palaeobotany and Palynology (Utrecht University) and (2) on the latter three species at the Department of Animal and Plant Sciences (University of Sheffield).

Some of the needles of *Tsuga heterophylla* used in the study were obtained from the collection of the National Herbarium of the Netherlands, complemented with needles from living trees collected in the field in 1998 and 2000. The material originates from 13 localities in the Pacific Northwest area of the USA and Canada; 8-11 needles from each locality were processed (Fig. 2.1). Additionally, assemblages of subfossil *Tsuga heterophylla* needles were derived from an 8-cm-long peat core taken at the margin of Jay Bath, a pond in Mount Rainier National Park, (Washington, USA; 46º46' N, 121º46' W). Eleven of the annual layers in this core, spanning a period from 1980 to 1998, yielded 3-5 *Tsuga heterophylla* needles each. A total of 160 *Tsuga heterophylla* needles from herbaria, living trees, and the peat core, were analyzed for stomatal frequency.

The material of *Picea glauca*, *P. mariana* and *Larix laricina* originates from herbarium sheets of the Royal Botanical Gardens Kew, cultivated trees in the United Kingdom, and living trees at various locations in the USA and Canada. Each locality provided 1-4 needles, for a total of 69 *Picea glauca/mariana* needles and 31 *Larix laricina* needles used in this study.

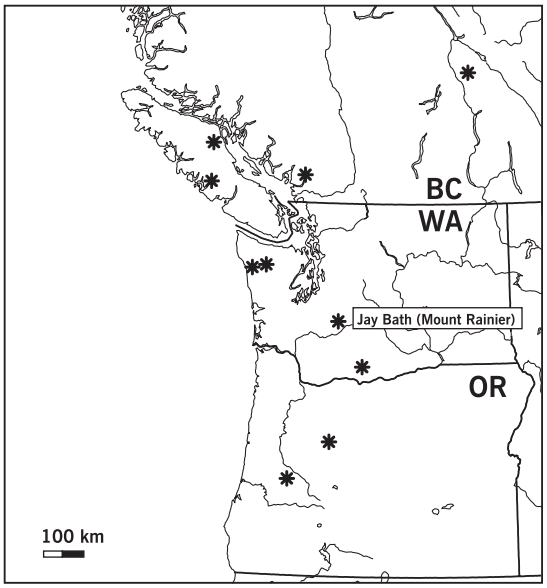

Figure 2.1: Source localities of the *Tsuga heterophylla* needles in the Pacific Northwest region. BC = British Columbia (Canada), WA = Washington (USA) and OR = Oregon (USA).

Methods
The needles of *Tsuga heterophylla* were bleached with a 4% natriumhypochloride solution to remove the mesophyll. The remaining cuticle was then stained with safranin and mounted in glycerin jelly on a microscopic slide. Computer-aided measuring of epidermal cell parameters on needle cuticles of *Tsuga heterophylla* was performed on a Leica Quantimet 500C/500+ Image Analysis system (Wetzlar, Germany). Stomata on *Picea* and *Larix* needles were counted directly from whole unprepared needles using a Leica epifluorescence microscope. Regression analysis and Student's t-test were performed using SPSS 8.0 for Windows statistical software (Chicago, Illinois, USA).

The presence of tephra from the 1980 eruption of Mt. St. Helens (Mullineaux, 1974, 1996) enabled a precise age assessment of the annual layers apparent in the peat core from Jay Bath.

The atmospheric CO_2 mixing ratios for the past 100 years that were used in the response curves were derived from instrumental measurements at Mauna Loa since 1957 (Keeling and Whorf, 2002) and shallow Antarctic ice cores (Etheridge et al, 1996; Indermühle et al, 1999). Records of temperature and precipitation at Mount Rainier were obtained from the IRI/LDEO Climate Data Library (website: http://ingrid.ldeo.columbia.edu).

Expression of stomatal frequency - Stomatal frequency is conventionally expressed as stomatal density (the number of stomata per unit leaf area) or as stomatal index (the proportion of stomata expressed as a percentage of total epidermal cells). Stomatal index is generally favored because it accounts for the influence of lateral cell expansion related to water availability on stomatal density (Salisbury, 1927; Kürschner, 1997; Kürschner et al., 1996).

The stomata on conifer needles are arranged in rows, occurring in either single files (*Larix laricina*) or grouped in bands (*Tsuga heterophylla*, *Picea glauca/mariana;* Fig. 2.2). Therefore, in contrast to broad-leaved species, stomatal placement and occurrence on conifer needles is not well characterized through the measurement of either stomatal density or index in small counting fields.

In *Larix laricina*, the arrangement of stomata in single files across the entire needle surface hampers the conventional use of small counting fields to determine stomatal density because variation in the number of rows might not be fully captured. Therefore, stomatal frequency in *Larix laricina* is expressed as the total number of stomata per mm needle length. Also, the typical stomatal pattern precludes the application of stomatal index.

The lower surface of the hypostomatal *Tsuga heterophylla* needles displays two broad bands of stomatal rows on each side of the central vein (Fig. 2.2), while four stomatal bands are present on the surface of the four-sided amphistomatal *Picea glauca/mariana* needles. In this way, the leaf surface is divided into stomate-free (midvein, leaf margins) and stomatal regions (the bands). Consequently, the stomatal frequency on the needles of these species

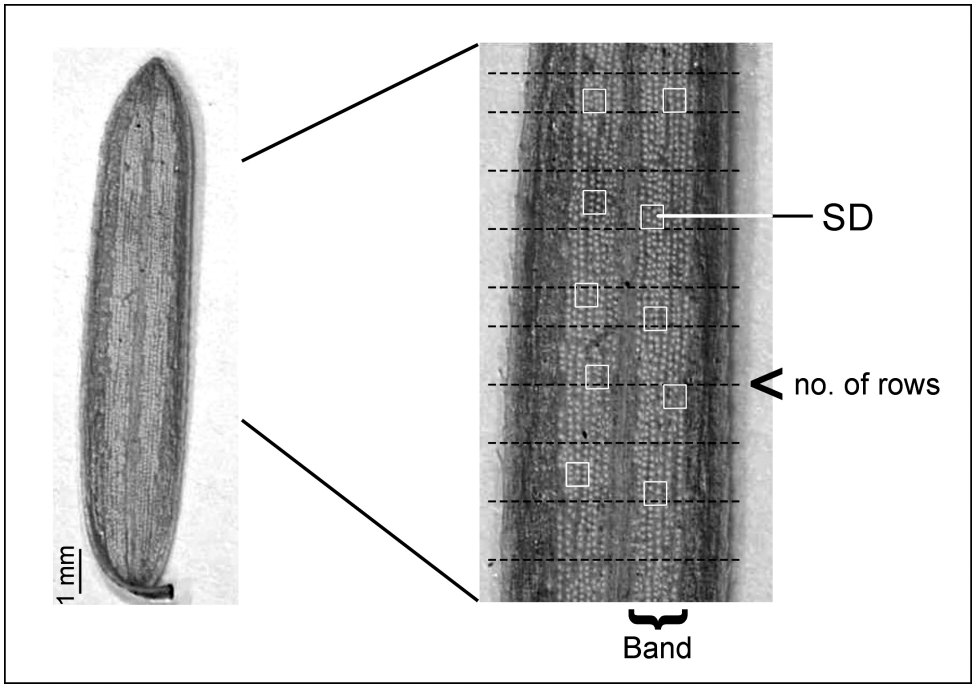

Figure 2.2: Abaxial surface of a *Tsuga heterophylla* needle viewed with a dissecting stereomicroscope. Band = band of stomatal rows on each side of the midvein. Dotted lines: approximate positions of the transects used for measuring the number of stomatal rows in both bands (number of rows). White squares: approximate positions of the counting fields used to measure stomatal density (SD).

not only varies in terms of stomatal density/index within the bands, but also by the extent of the stomatal regions on the needle surface. Thus, for *Tsuga heterophylla* and *Picea glauca/mariana* stomatal index and density within the bands were measured, as well as the width of the bands and the total number of stomata per millimeter needle length.

To account for the varied stomatal patterning in conifer needles, the following customized stomatal quantification methods were applied in this study.[1]

Stomatal density (SD) was measured as the number of stomata per square millimeter of leaf area). On *Tsuga heterophylla* needles, SD was measured in 10 counting fields (0.057 mm^2) within the stomatal bands at a magnification of 500×. For *Picea glauca/mariana* needles, SD was measured on the abaxial surface in 2-10 counting fields spanning the entire width of a band along the length of a calibrated 0.800-mm scale bar at a magnification of 200×.

[1]Methods have been developed independently in Utrecht and Sheffield

Stomatal Index (SI) was measured as (the number of stomata divided by the number of stomata plus epidermal cells) ×100. On *Tsuga heterophylla* needles, SI was calculated based on stomatal and epidermal cell counts in 12 counting fields spanning the width of a band along a 0.400-mm needle length. On *Picea glauca/mariana* needles, SI was calculated based on stomatal and epidermal cell counts in 2-10 counting fields spanning the width of a band along the length of a calibrated 0.800-mm scale bar.

Stomatal number per Length (SNL) was measured as (the number of abaxial stomata plus the number of adaxial stomata) divided by needle length in millimeters. On *Larix laricina* needles, SNL was measured in 2 - 10 counting fields along the length of a calibrated 0.800-mm scale bar at a magnification of 200×.

Stomatal Rows (SR) was measured as the number of stomatal rows in both stomatal bands. This method quantifies the extent of the stomatal regions on the *Tsuga* and *Picea* needles. Band width is highly dependent of the number of rows in a band, as measured in 35 perfectly preserved modern *Tsuga heterophylla* needles (n = 700; Pearson correlation, 0.953). Band width is expressed as number of rows rather than absolute width (in millimeters) because the former is easier to measure (especially in less well-preserved [fossil] needles). For *Tsuga heterophylla*, the number of rows in both bands was counted along 10 transects perpendicular to the needle axis and restricted to the middle third part of the needle because the number of rows decreases strongly at the tip and the base of the needles (Fig. 2.2). For the amphistomatal *Picea glauca/mariana*, mean number of rows per needle (on both sides) was determined.

Stomatal density per length (SDL) was determined using the equation SDL = SD × SR. Stomatal density per length combines stomatal density within the bands and the width of the bands, providing a measure of the total number of stomata per millemeter of needle length in *Tsuga heterophylla* and *Picea glauca/mariana* needles. Because SR is the number of rows instead of the true band width (in millimeters), SDL represents a general indication of the number of stomata per millimeters needle length, capable of reflecting changes in stomatal frequency. The expression of band width in number of rows rather than absolute distance also explains the apparent discrepancy of expressing SDL per square millimeters instead of per millimeter.

True stomatal density per length (TSDL) was determined using the equation TSDL = SD × band width (in millimeters). The number of stomata per millimeter of needle length (TSDL) can be approximated more accurately when the band width is expressed in millimeters instead of number of rows. The TSDL was calculated only for *Tsuga heterophylla*, using the linear relation between SR and band width (in millimeters) as measured in 35 perfectly preserved modern *Tsuga heterophylla* needles (n = 700; Pearson correlation, 0.953).

RESULTS

The SI calculated for needles of *Tsuga heterophylla* from four samples of herbarium material (Fig. 2.3A) did not change significantly over a CO_2 range from 290 to 367 ppmv (r^2 = 0.22; P = 0.531). By contrast, three other measured stomatal parameters decreased in relation to the CO_2 rise from 290 to 367 ppmv: SD (Fig. 2.3B), SR (Fig. 2.3C) and TDSL (Fig. 2.3D). The SD decreased from 205 to 177 stomata/mm^2 (r^2 = 0.5077; $P < 0.001$), a response rate of 1.99% decrease per 10 ppmv of CO_2 increase. The SR shows a response rate of −2.85% per 10 ppmv of CO_2 increase, based on the decrease in number of rows from 17.5 to 14.0 (r^2 = 0.3389; P = 0.002). The TSDL decreases from 237 to 164 stomata/mm; a response rate of −4.49% per 10 ppmv of CO_2 increase (r^2 = 0.5873; $P < 0.001$).

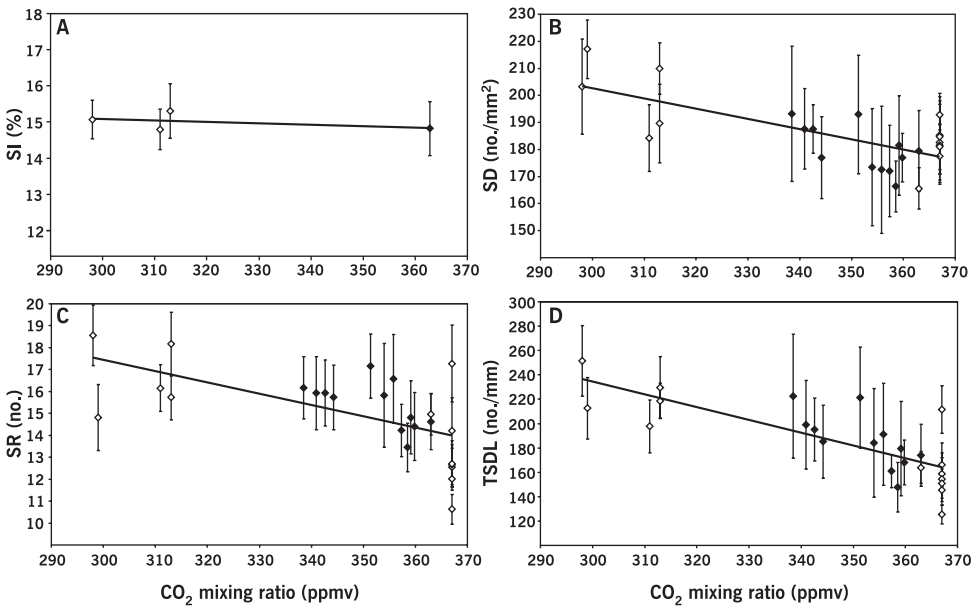

Figure 2.3: Response of stomatal parameters of *Tsuga heterophylla* to a CO_2 increase from 290 to 370 ppmv. Black diamonds represent subfossil and modern needles from Jay Bath (Mount Rainier, Washington, USA), open diamonds modern and herbarium needles from other localities. Error bars indicate ± 1 SE. Solid lines indicate best fit in classical regression analysis. **A**: Response of stomatal index (SI) of *Tsuga heterophylla* to a CO_2 increase from 290 to 370 ppmv. Mean SIs do not change significantly (SI = 0.0038 × [CO_2] + 16.19; r^2 = 0.22; P = 0.531). **B**: SD: stomatal density (SD = −0.3786 × [CO_2] + 316.25; r^2 = 0.4892; $P < 0.001$). **C**: SR: number of stomatal rows in both bands (SR = −0.0514 × [CO_2] + 32.875; r^2 = 0.3588; P = 0.002). **D**: TSDL: true stomatal density per millimeter of needle length (TSDL = −1.0501 × [CO_2] + 549.67; r^2 = 0.5873; $P < 0.001$).

The highly similar stomatal frequencies of *Picea glauca* and *P. mariana* allows their treatment as a single group. No significant relationship was observed between SI and CO_2 mixing ratio for these species (data not shown). Mean SDL in *P. glauca* and *P. mariana* decreased from 106 to 50 stomata/mm^2 (Fig. 2.4) in response to the CO_2 rise from 288 to 360 ppmv ($r^2 = 0.5048$; $P = 0.001$), resulting in a response rate of −7.34% per 10 ppmv of CO_2 rise for these species.

Larix laricina responds to the CO_2 increase from 283 to 319 ppmv with a decrease in mean SNL from 24.4 to 16.5 stomata/mm^2 (Fig. 2.5), a response rate of −8.09% per 10 ppmv of CO_2 increase ($r^2 = 0.3884$; $P = 0.023$).

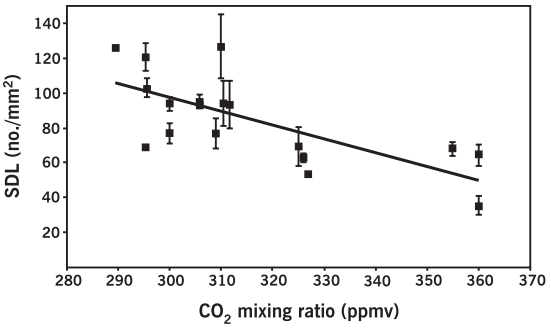

Figure 2.4: Response of stomatal density per millimeter of needle length (SDL) on *Picea glauca/mariana* needles to a CO_2 increase from 283 to 360 ppmv based on both adaxial and abaxial measurements. Error bars indicate ± 1 SE. Solid line indicates best fit in classical regression analysis (SDL = $-0.7949 \times [CO_2] + 335.41$; $r^2 = 0.5048$; $P = 0.001$).

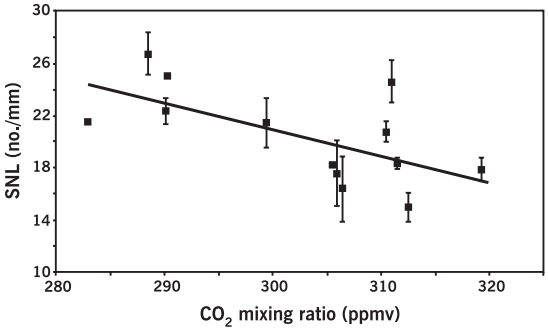

Figure 2.5: Response of stomatal number per millimeter of needle length (SNL) on *Larix laricina* needles to a CO_2 increase from 283 to 319 ppmv. Error bars indicate ± 1 SE. Solid line indicates best fit in classical regression analysis (SNL = $-0.1983 \times [CO_2] + 80.413$; $r^2 = 0.3884$; $P = 0.023$).

DISCUSSION

Counting strategies

In *Tsuga heterophylla* and *Picea glauca/mariana*, stomatal frequency is significantly reduced as a response to increasing CO_2. The SD decreases as does the stomatal region. The SI, on the other hand, although commonly used as the most sensitive indicator for CO_2-related change in stomatal frequency in broad-leaved angiosperm species, does not decrease as atmospheric CO_2 concentrations increase. Thus, the observed decrease in SD on the needles must be accompanied by a proportionally equal reduction in epidermal cells, keeping SI constant. This discrepancy in response between SD and SI can be explained by the mode of stomatal formation in conifers.

Conifer leaves develop linearly from a single growth center at the needle base, similar to monocots, instead of from multiple point sources on the leaf as in broad-leaved angiosperms (Croxdale, 2000). Epidermal cells appear in longitudinal files, with the cells at the tip of the leaf maturing first. Stomatal formation in conifers takes place during a late stage of leaf growth. Guard cells of *Pseudotsuga menziesii*, for example, do not become apparent until the needle has reached two-thirds of its final size (Owens, 1968). When the stomatal precursor cells form in specific rows, the epidermal cells in the adjacent files of cells divide asymmetrically to produce subsidiary cells lying directly next to the stomatal precursor cells and epidermal cells in the adjacent cell file (Fig. 2.6; Croxdale et al., 1992; Larkin et al., 1997).

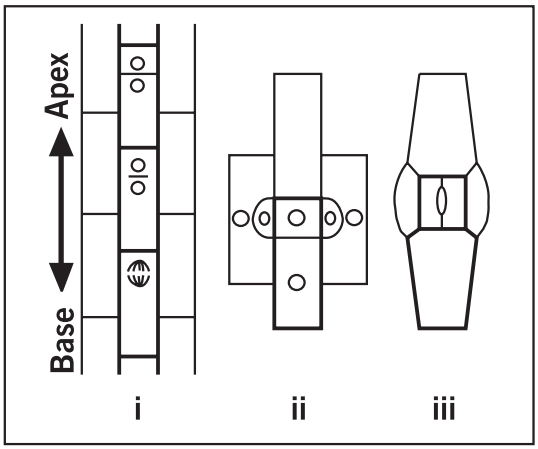

Figure 2.6: Stomatal patterning during leaf development in grasses (note: stomatal patterning in conifers and monocots is highly comparable [Croxdale, 2000]). **i** Adjacent cell files on a developing leaf. In the middle cell file asymmetric divisions occur with the stomatal initial cell forming towards the leaf tip and the larger cell product forming closer to the leaf base, resulting in an alternation of stomatal initials, which develop directly into a guard mother cell, and future epidermal neighbor cells. New transverse cell walls are offset from walls in adjacent files. **ii** Subsidiary cells form in asymmetric divisions in adjacent cell files on both sides of the guard mother cell. **iii** The guard mother cell divides symmetrically to form two guard cells that surround a pore. The lower neighbor cell originated in the asymmetric division in (i); the darker line outlines the two cells produced by that division. (Reproduced with permission from the American Society of Plant Biologists: Larkin et al., 1997).

In many conifer species and monocots, the latter epidermal cells can continue to divide a specific number of times creating a species-specific fixed number of epidermal cells in the "stomatal-epidermal complex" (Tomlinson, 1974). These complexes can contain between four and 12 epidermal cells each, depending on the species (Florin, 1931). When stomata are densely packed, as in *Tsuga* and *Picea*, nearly all epidermal cells encountered in the stomatal bands belong to the stomatal-epidermal complexes, except for a few very elongated pavement cells in rows of epidermal cells (Fig. 2.7). In these cases of densely packed stomata, the number of epidermal cells in the bands will mainly depend on the number of stomata present, keeping SI constant. The SD reflects stomatal initiation rate much better than SI. Because epidermal cells from the stomatal complexes should be excluded from the ratio, the application of SI as an expression of stomatal frequency in conifers should be restricted to species with a significant number of pavement epidermal cells. This phenomenon may also explain in part why little or no stomatal response has been observed in grasses growing in elevated CO_2. The number of subsidiary cells can be affected by CO_2 levels (Boetsch et al., 1996), but pavement and stomatal complex epidermal cells in mature conifer leaves cannot always be easily distinguished (Florin, 1931). Therefore, the size of the stomatal complexes and the number of pavement epidermal cells in a conifer species should be taken into account before using a SD- or SI-based counting strategy.

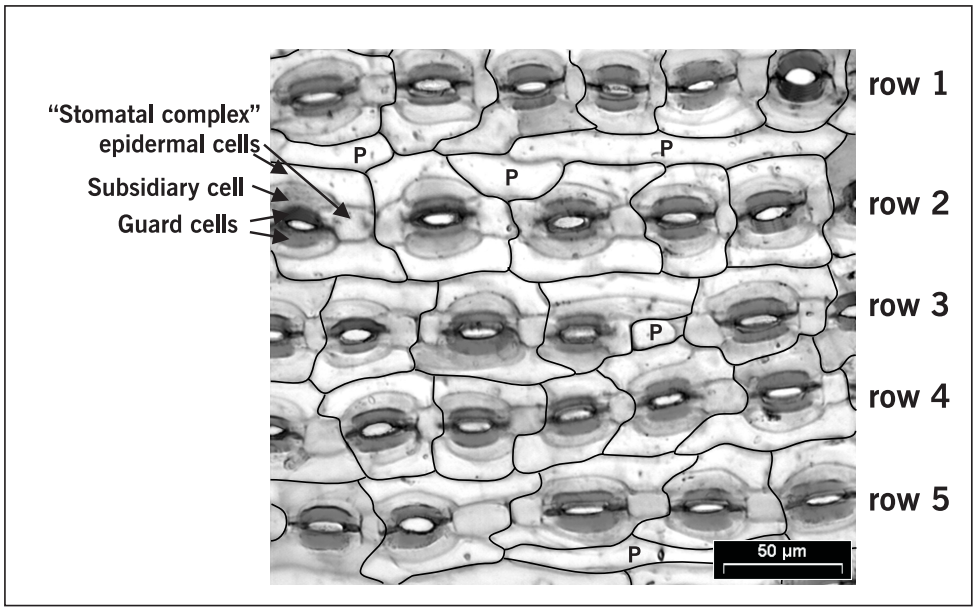

Figure 2.7: Abaxial cuticle of *Tsuga heterophylla*. Stomatal complexes are outlined in black. (P) indicates "pavement" epidermal cells (those not originating as part of a stomatal complex).

When the other stomatal parameters are considered, TSDL/SDL appears to be the quantification method most sensitive to CO_2. The SD in *Tsuga heterophylla* decreases with increasing CO_2, but at a lower response rate than TSDL, while the band width changes too, only with much greater variability than TSDL. In *P. glauca* and *P. mariana*, the same picture emerges, SR has a strong response to CO_2, but with high variability. The significance increases when SD and SR are combined in SDL (J. C. McElwain, personal observation). The TSDL/SDL is thus proposed as the most appropriate method to use in cases where the stomatal rows in a hypo- or amphistomatal conifer species are grouped in bands, as in *Tsuga heterophylla* and *Picea glauca*/*mariana*. As a further validation for the use of the number of rows as a proxy for band width, TSDL (based on actual measurements of band width in millimeters) was calculated for 35 modern *Tsuga heterophylla* needles. Measured TSDL and SDL correlate extremely well (Pearson correlation coefficient of 0.951), which indicates that the number of rows can be applied as a very useful proxy for band width. Actually, the number of rows might be an even more consistent proxy of stomatal region than the measured band width itself. When a few stomata lie away from the main band or large areas are devoid of stomata, the measurement of band width in stomatal rows rather than of absolute distance will minimize the overestimation of the stomatal region.

Concerning conifer taxa with single stomatal rows (such as *Pinus* and *Larix*), care should also be taken to capture the variability in the number of rows as well as the variability in the number of stomata per row. This can be achieved by measuring SNL, the total (abaxial and adaxial) number of stomata per millimeter of needle length. If small counting fields are used (less than half of the needle width) for conventional SD measurements, minor variations in the number of rows will not be reflected, and stomatal row numbers should be included in the quantification of stomatal frequency.

Validation of the stomatal frequency response to CO_2

In the present study SD-based counting strategies are applied instead of SI-based methods. The SD depends not only on stomatal initiation rate, but also on lateral cell expansion after stomatal formation, which can be strongly influenced by other environmental factors than atmospheric CO_2. To determine if the observed changes in stomatal frequency in the conifers can be ascribed to the rise in CO_2 over the last century, the potential influence of environmental and biological variations (geography, altitude, light regime, humidity, temperature, and ontogeny) on stomatal frequency has to be evaluated.

Geography - Because the conifer needles in this study were collected in varying geographical regions, interpretation of the observed responses could be complicated by differences in climate at the source localities and genotypic dissimilarities between different populations. Contrasting sampling strategies for *Tsuga heterophylla* vs. *Picea glauca/mariana* and *Larix laricina* were used to deal with the potential influence of variation in climate and populations on the stomatal frequency.

All *Tsuga heterophylla* needles (from living trees, herbarium sheets, and subfossil peat) were collected in the Pacific Northwest region of the USA/Canada and have thus grown under similar temperate conditions with high precipitation, minimizing the potential influence of large climatic variations. The modern samples (Fig. 2.3: 363 ppmvand 367 ppmv) were collected from living trees at several sites in British Columbia and Washington. The considerable variation in stomatal frequency in these modern samples may reflect intrinsic variability between trees, phenotypical responses to micro-climatic differences between these sites, and differences in local CO_2 mixing ratios present at forested sites (Tarnawski et al., 1994). Despite the variation in stomatal frequency, the TSDL (the most sensitive quantification method) of the modern samples is consistently low and the decreasing trend in mean stomatal frequency in the data set is substantial and significant.

Subfossil and modern needles, which were derived from a single population of trees around Jay Bath over the last 20 yr, are indicated by black diamonds in Fig. 2.3D. The TSDL changes in this restricted data set (within a single population) do not differ significantly from the TSDL decrease observed in the total data set, which includes data points from other localities (and populations). Thus, there are no indications that the observed stomatal frequency changes in *Tsuga heterophylla* reflect variations in stomatal frequency between different populations.

A reverse sampling strategy was employed for *Picea glauca/mariana* and *Larix laricina*. Herbarium material from these species was chosen from a wide range of localities in northern USA and Canada, within the species' natural climatic ranges and tolerances. Herbarium leaves of cultivated trees from Scotland, North America, and England were also included in the calibration data sets because no significant differences in stomatal frequencies were observed between trees growing in cultivation and in nature under the same CO_2 levels. By maximizing variation in climate and populations in the data set, the potential effect of biological and environmental factors other than CO_2 on stomatal frequency of *Picea* and *Larix* is expressed within the statistical confidence intervals of the regression data set. Because the decrease in stomatal frequency appears both within a single population and in a data pool of maximized environmental variation, the stomatal response to CO_2 of the studied conifer species is unlikely to be an artefact caused by differences in populations and climate associated with the geographical variation in the data sets.

Altitude – Although the CO_2 mixing ratio in air remains constant over altitudinal gradients, the CO_2 partial pressure (as measured in pascals) is lower at higher elevation because of the decrease in air pressure. Stomatal frequency responds to altitude-controlled changes in CO_2 partial pressure when CO_2 mixing ratio is unaltered (Woodward and Bazzaz, 1988). To check whether the observed stomatal frequency decrease in *Tsuga heterophylla* could be related to altitudinal differences in the data set (sea level to 1600 m), an alternative response curve was plotted using only needles grown at altitudes in the range of Jay Bath (1200 - 1600 m; Fig. 2.8). The stomatal frequency response in *Tsuga heterophylla* needles from this restricted altitudinal range is not significantly different from the response in the original

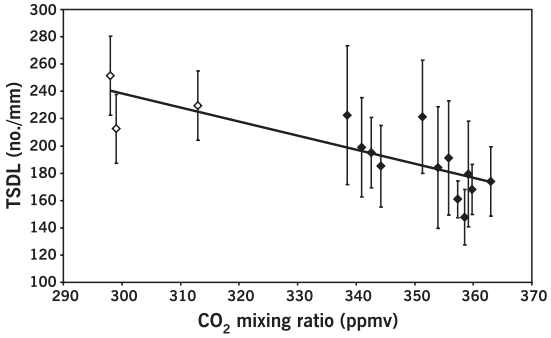

Figure 2.8: Response of true stomatal density per millimeter of needle length (TSDL) of *Tsuga heterophylla* to a CO_2 increase from 290 to 370 ppmv. The material depicted in this figure are those needles from figure 3D that grew at 1300-1600 m altitude. Black diamonds represent subfossil and modern needles from Jay Bath (Mount Rainier, Washington, USA), open diamonds represent herbarium needles from other localities. Error bars indicate ± 1 SE. Solid line indicates best fit in classical regression analysis (TSDL = $-1.0256 \times [CO_2] + 545.95$; $r^2 = 0.6223$; $P < 0.001$).

data set with needles from a broader altitudinal range (Fig. 2.3D). For *Picea glauca*, *P. mariana*, and *Larix laricina*, leaf material from herbarium sheets collected from high elevations was not included in the data sets to avoid the effects of decreased CO_2 partial pressure with increasing elevation on stomatal frequency. Thus, the observed stomatal frequency response in the conifer species is not significantly affected by the altitudinal variation in the data set.

Light intensity – Because light intensity is known to strongly influence epidermal morphology and SD (Nordhausen, 1903; Lichtenthaler, 1985; Kürschner, 1996, 1997), additional stomatal frequencies were measured for *Tsuga heterophylla* needles that were grown under sunny and shady light regimes at the botanical gardens in Utrecht (Netherlands). No significant difference in either SD, SR, or TSDL could be detected in the needles grown under contrasting light regimes (shade: 177 ± 36 stomata/mm, sun: 174 ± 18 stomata/mm; P = 0.883 for TSDL; L.L.R. Kouwenberg, unpublished data). Hence, the observed relation between CO_2 and TSDL in *Tsuga heterophylla* is not significantly affected by the varying light intensity under which the herbarium and fossil needles may have developed. The observed TSDL values of these needles are highly comparable to the modern material from the Pacific Northwest region of North America.

Water availability – Water availability determines cell expansion and thus stomatal density on leaf surfaces (Salisbury, 1927; Tichá, 1982). Therefore it must be considered whether the observed SD decrease in the data set could be a result of local changes in soil water availability during the last century. Annual and spring precipitation records measured at Longmire (Mount Rainier) from 1930 to 2002 were compared to the stomatal frequency records of *Tsuga heterophylla* (Fig. 2.9A). These records do not show any long-term unidirectional increase in precipitation that might have triggered the observed reduction in stomatal frequency.

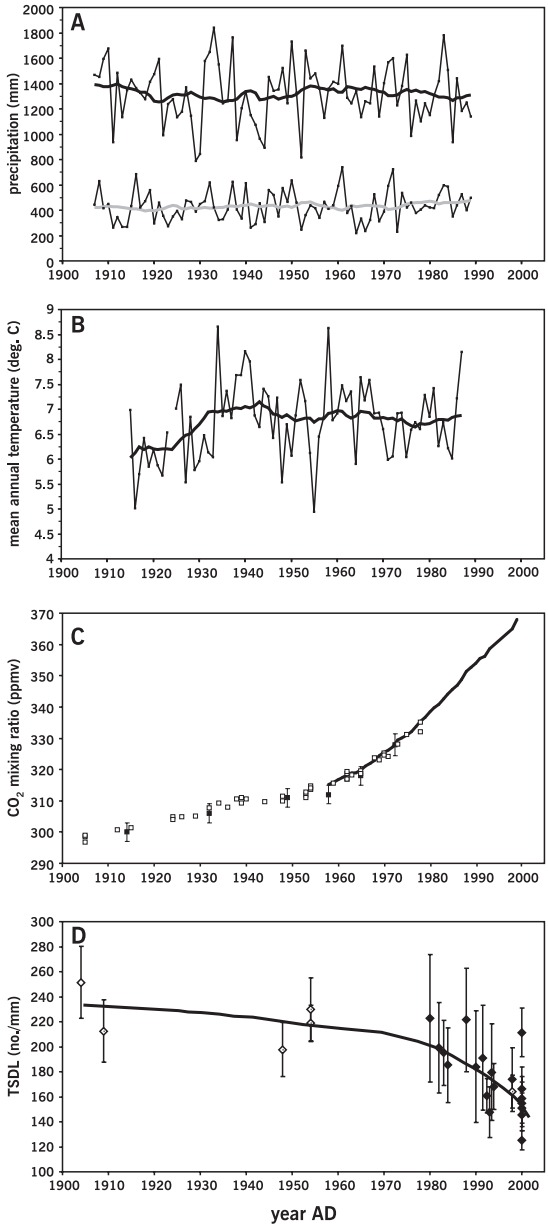

Figure 2.9: A: Precipitation at Longmire (Mount Rainier, Washington, USA), 1930–2002. The upper curve represents annual precipitation; the thick black line is the 19-yr running mean to emphasize the long-term trends. The lower curve represents spring precipitation (February–May); the thick gray line indicates the 19-yr running mean. **B**: Mean annual temperature at Longmire, 1915–2002. Thick black line represents the 19-yr running mean to visualize the long-term trend. Data in (A) and (B) from the IRI/LDEO Climate Data Library (website: http://ingrid.ldeo.columbia.edu). **C**: The atmospheric CO_2 mixing ratios from instrumental measurements at Mauna Loa, Hawaii, USA, since 1957 (black line; Keeling and Whorf, 2002) and Antarctic ice cores 1900–1990 (white squares are measurements from Law Dome [Etheridge et al., 1996]; black squares are measurements from Taylor Dome [Indermühle, 1999]). **D**: True stomatal density per millimeter of needle length (TSDL) for *Tsuga heterophylla*. Black diamonds represent subfossil and modern needles from Jay Bath (Mount Rainier), open diamonds represent modern and herbarium needles from other localities. Error bars indicate ± 1 SE. Thick line represents long-term trend (drawn by visual match).

Temperature – Experiments with *Betula pubescens* indicate that large temperature changes (from 12 to 30ºC) can cause a significant increase in stomatal formation as reflected in SI (Wagner, 1998). Thus, monthly temperature records from Longmire were also compared with the stomatal frequency records of *Tsuga heterophylla* (Fig. 2.9B). Both spring and annual temperatures increased 0.8°C between 1915 and 1940, but show no further long-term uni-directional change. Thus, differences in growing temperature are highly unlikely to have influenced the decrease in stomatal frequency.

Ontogeny – Marked variations in SD are reported for angiosperm leaves during leaf ontogeny (Tichá, 1982). Considering the specific leaf development and stomatal initiation in conifers, ontogenetical differences in stomatal frequency on conifer needles could be expected to be less pronounced. Measurements of SD, SR, and TSDL on developing *Tsuga heterophylla* needles from the same branch were indeed not significantly different in these stomatal frequency parameters for young and fully grown needles (mean needle length of 7.2 and 12.0 mm respectively (Chapter 3).

Stomatal frequency response rates

The four conifer species analyzed in this study show a significant reduction in stomatal frequency as a response to a CO_2 rise of 80 ppmv over the last century. The response rates, a 4.49% decrease in TSDL per 10 ppmv of CO_2 increase for *Tsuga heterophylla* and a 7.34% and 8.09% decrease in SDL for *Picea mariana/glauca*, and *Larix laricina*, respectively, are comparable with the SI response rates for angiosperm tree taxa commonly used for CO_2 analysis of fossil leaves (*Betula*: −5.47% of the SI per 10 ppmv of CO_2, *Quercus* −3.82%). Thus, over a CO_2 range between 290 and 370 ppmv, stomatal frequency adjustment in conifers can occur at a similar rate as in woody angiosperms. Furthermore, earlier suggestions that the response of conifers in general would level off at CO_2 values of 280 ppmv (Van de Water et al.,1994), are refuted by the observation that both *Tsuga heterophylla* and *Picea glauca/mariana* have not reached their response limit yet at the current CO_2 level of 370 ppmv. Thus, similar to angiosperms, conifers (*Pinus*, *Metasequoia*, *Tsuga*, *Picea*, *Larix*) may have species-specific response ranges. Several conifer species still respond to increases in CO_2 above the response limits for angiosperm species used for stomatal frequency analysis, making them very suitable for the reconstruction of paleo-atmospheric CO_2 concentrations well above present levels (Royer et al., 2001).

CONCLUSIONS

The capability of conifers to adjust their stomatal frequency to changes in atmospheric CO_2 mixing ratios has now been confirmed in four more conifer species. *Tsuga heterophylla*, *Picea glauca, P. mariana,* and *Larix laricina* show a strong reduction in stomatal frequency in accordance with a change in historical CO_2 levels from 290 to 370 ppmv. Because of their sensitive response over a broad range of CO_2 levels, combined with a high preservation capacity, fossil needles of the studied conifer species show great potential for paleo-atmos-

pheric CO_2 reconstructions. Considering the dominance of conifers in temperate and boreal forest ecosystems (in both the Northern and Southern Hemisphere), the spatial and temporal coverage of such reconstructions may thus be markedly extended. This is corroborated already by results of ongoing research in the Pacific Northwest region of the USA (Chapter 4) and Atlantic Canada (McElwain et al., 2002). Furthermore, the observation that all four conifer species have not yet reached their response limits to CO_2 suggest that paleo-CO_2 estimates derived from conifers rather than angiosperms may be preferable during those times in the Earth's history when greenhouse gas concentrations were much higher than present (such as during the Cretaceous).

The specific stomatal patterning on conifer needles has precluded the application of stomatal index measurements as a CO_2-sensitive expression of stomatal frequency. New quantification methods, based on the number of stomata per millimeter of needle length, are proposed as the most accurate measure of stomatal frequency in conifer species. In general, stomatal quantification methods should be tailored to specific leaf development and subsequent stomatal patterning of the species studied.

CHAPTER 3

EPIDERMAL CELL DIFFERENTIATION AND STOMATAL CHARACTERISTICS OF *TSUGA HETEROPHYLLA* NEEDLES DURING LEAF DEVELOPMENT

In order to validate the inverse relation between the number of stomata and atmospheric CO_2 levels observed in different plant species, the potential influence of other environmental conditions and ontogenetical development stage on stomatal densities must be investigated as well. Epidermal cell differentiation and specifically stomatal characteristics of *Tsuga heterophylla* (Raf.) Sarg. needles during different stages of budburst were measured. Stomata first appear in the apical region and subsequently spread basipetally towards the needle base during development. The number of stomatal rows on a needle does not change during ontogeny, but stomatal density decreases inversely with increasing needle area, until about 50% of the final needle area. The total number of stomata on the needle increases during the entire developmental period, indicating that stomatal and epidermal cell formation continues until the needle has matured completely. The lack of further change in either stomatal density or stomatal density per mm needle length in the final stages of leaf growth indicates that in conifers leaf maturation does not significantly affect stomatal density based CO_2 reconstructions.

INTRODUCTION

The pattern and frequency of stomata on any leaf surface are under tight genetic control, but may be modified by environmental parameters such as the availability of CO_2 (Croxdale, 2000; Glover, 2000). An inverse relation between stomatal frequency and atmospheric CO_2 concentration, initially detected by Woodward (1987), has been demonstrated in a wide variety of C_3-plants (Royer, 2001). Consequently, fossil leaf remains of these species, mainly long-lived dicotyledon angiosperms, are increasingly used to quantify past atmospheric CO_2 levels (e.g., Van der Burgh et al., 1993; Beerling et al., 1995; Kürschner et al., 1996; Rundgren and Beerling, 1999; Wagner et al., 1999; McElwain et al., 2002, Wagner et al., 2002).

In order to assess the reliability and accuracy of leaf-based CO_2 reconstructions, it is essential to investigate the potential influence of leaf development on stomatal frequency. Among angiosperms, stomatal patterning and its underlying mechanism has been studied in dicotyledons (reviews by Croxdale, 2000 ; Serna et al., 2002), as well as in monocotyledons (Tomlinson, 1974; Charlton, 1990; Chin et al., 1995; Croxdale., 1998). The epidermal pattern on any mature leaf is the result of division and expansion of epidermal cells, and the formation of stomata. The stomatal density (SD: number of stomata per mm^2 leaf area) on a developing leaf reflects the relative contribution of cell divisions and expansion to leaf growth.

In dicotyledons, the expansion of epidermal cells after the proliferative and formative divisions during leaf growth (creating epidermal and stomatal initial cells, respectively) strongly affects SD in the final growth stages of a leaf (Esau, 1977; Tichá , 1982; Croxdale, 2000). Consequently, SD on dicotyledon leaves is highly dependent on the age of developing leaves; this age effect has been quantified for several taxa (Tichá, 1982). In dicotyledon leaves, variation in SD is also caused by changes in the extent of leaf expansion due to differences in light intensity or water availability (Royer, 2001). In order to minimize the influence of variations in cell expansion, stomatal frequency analysis aimed at atmospheric CO_2 reconstruction now generally relies on Salisbury's (1927) stomatal index (SI: proportion of stomata expressed as a percentage of the total number of epidermal cells).

Leaves of monocotyledon species exhibit fundamentally different modes of growth and development. In contrast to dicotyledons, regions of cell division, stomatal formation, and cell expansion are spatially separated. Epidermal and stomatal initial cells are formed at the base of the elongated leaf by proliferative and formative epidermal cell divisions, while near the apex only expansion and maturation of the cells occur (Charlton, 1990; Croxdale et al., 1992; Chin et al., 1995; Croxdale, 1998). Quantitative information on changes in SD during monocotyledon leaf development is still lacking. Generally, well-preserved remains of monocotyledon leaves are rare in the fossil record. Only one study reports SD counts on late-glacial graminoid leaves in relationship to past atmospheric CO_2 levels (Wooller and Agnew, 2002).

In marked contrast, needles of a variety of conifers are frequently abundant in peat and lake deposits. Considering the long-term dominance of conifers in temperate and boreal forest ecosystems, the use of fossil conifer needles for quantifying past CO_2 levels could greatly improve the spatial coverage of such reconstructions. Analysis of fossil and herbarium material has already provided convincing evidence that species of *Pinus*, *Picea*, *Tsuga*, *Larix*, and *Metasequoia* have the capacity to adjust their stomatal frequency to changing CO_2 regimes (Van de Water et al., 1994; Royer et al., 2001; McElwain et al., 2002; Chapter 2).

Stomatal responses in conifers appear to differ considerably from responses in dicotyledon angiosperms. Observations in *Tsuga heterophylla*, *Picea glauca*, *P. mariana*, and *Larix laricina* indicate that CO_2 responsiveness is expressed by changes of SD and TSDL (number of stomata per mm needle length), but *not* by changes of SI (Chapter 2). Moreover, SD in these species is *not* affected significantly by variation in light intensity and moisture availability. These differences are likely to be determined by differences in mode of leaf development and subsequent stomatal patterning.

Conifers resemble monocotyledons rather than dicotyledons in leaf development (Esau, 1977). The specific epidermal and stomatal development in conifers has been the subject of only a few studies. Qualitative studies either describe the early leaf ontogeny in several conifer species without addressing stomatal patterning (Von Guttenberg, 1961; Owens, 1968), or focus on the development of individual stomatal complexes (Florin, 1931). Quantitative studies are restricted to stomatal frequency variation between mature conifer needles of different ages (Nestsyarovich, 1963; Watts et al., 1976).

To date, stomatal pattern and stomatal frequency on developing conifer needles have not been studied quantitatively. In the present paper we, therefore, measure stomatal numbers and stomatal characteristics in developing needles of *Tsuga heterophylla* in order (1) to describe the relative contribution of cell division and cell expansion to the typical conifer type of leaf growth; and (2) to determine whether the use of both young and mature needles would affect mean stomatal frequency values on which paleo-atmospheric CO_2 reconstruction are based.

MATERIAL AND METHODS

A branch displaying needles in several stages of budding was collected in April 2000 from a solitary *Tsuga heterophylla* tree at the Botanical Gardens of Utrecht (The Netherlands).

The needles were bleached with a 4% natriumhypochloride solution to remove the mesophyll. The remaining cuticle was then stained with saffranin and mounted in glycerin jelly on a microscopic slide. Computer-aided measurement of epidermal cell parameters on the *T.*

heterophylla needle cuticles was performed on a Leica Quantimet 500C/500+ Image Analysis system (Wetzlar, Germany). Regression analysis, Student's T-test and One way ANOVA were performed using SPSS 10.0 for Windows statistical software (Chicago, Illinois).

The needles, in different stages of leaf development, were categorized in five developmental classes:

1: From bud (the entire needle is still inside the bud [n = 4])
2: Just out of bud (the tip of the needle just emerged from the bud [n = 4])
3: Out of bud (the largest part of the needle is out of the bud [n = 4])
4: Small (the needle has completely emerged [n = 5])
5: Fully grown (the needle has reached the length of a mature needle [n = 5])

Needle length and width were measured along a calibrated scale bar and needle area was calculated as length × width. Relative needle length, width, and area were calculated using the average value of the fully grown needles as 100 %. Thus, individual fully grown needles can reach relative values over 100 %. Stomata on *T. heterophylla* needles are arranged in two broad bands consisting of multiple rows on just the abaxial needle surface (Fig. 3.1) on which the following stomatal parameters were measured.

Stomatal Density (SD) was measured as the number of stomata per square millimeter of leaf area. SD was measured in 16 counting fields (0.057 mm^2) within both bands along the length of the needle in completely budded needles (stage 4 and 5). In needles from stages 1-3, which had not completely budded, stomata had only matured at the tip of the needle. In these cases SD was measured at 7-10 counting fields at the needle tip, indicated as SD_{top}. For comparison, the average of the six SD measurements in the apical region of needles from stages 4 and 5 are also indicated as SD_{top}.

Stomatal rows (SR) was measured as the number of stomatal rows in both stomatal bands. This method quantifies the width of the stomatal bands and consequently the extent of the stomatal regions on the needle. SR is determined for each stomatal band at ten transects perpendicular to the mid vein in fully budded needles. The lower quality of preparation of needles from stages 1-3 restricted SR measurements to 2-6 per needle.

True stomatal density per millimeter needle length (TSDL) was determined using the equation TSDL = SD × band width (in millimeters; Chapter 2). To calculate TSDL for *T. heterophylla*, band width expressed in SR was converted to band width in mm, using the linear relation between SR and band width (mm) as measured in 35 perfectly preserved modern *T. heterophylla* needles (n = 700 ; Pearson correlation 0.953).
Whenever stages 1-3 are compared to 4 and 5, TSDL based on SD_{top} is used ($TSDL_{top}$).

The total number of stomata per needle (SN) was calculated using the equation TSDL × needle length (in millimeters).

Pore length (PL) was measured as the length of the stomatal pore in micrometers. PL was measured on 20 stomata per needle in both stomatal bands at × 640 magnification. In fully budded needles (stages 4 and 5) PL was measured at ten stomatal pores close to the tip (PL_{top}) and 10 pores closer to the base (PL). In needles from stages 1-3, 20 stomatal pores were averaged as well, but mature stomata were only present at the needle tip.

Subsidiary cell length (SL) was measured as the length (parallel to the mid vein) in micrometers of the subsidiary cells in the stomatal complexes neighbouring the stomata. SL was measured on 20 stomatal complexes in both stomatal bands at × 640 magnification in the tip and base region. SL could not be determined in partly budded needles (stage 1-3) since the epidermal cell walls are not clearly visible.

RESULTS

Qualitative observations

Stomata already appear on the epidermis when the needle is still entirely within the bud. In needles within the bud guard cells are present at the tip of the needle (Fig. 3.1A) and initiating stomata can be discerned in the middle region. In several rows of epidermal cells a pattern of undifferentiated stomatal cells and subsidiary cells is observed. When the needle increasingly emerges (stage 2/3; [just] out of bud) mature guard cells are present on the tip outside of the bud (Fig. 3.1B). Stomata are visible on the basal and middle regions, but they are immature in appearance being still very rectangular in shape. As soon as the needle is completely exposed (stage 4/5 small and fully grown) and a robust epidermis with a cuticle has developed, mature stomata with lignified guard cells cover the entire needle from tip to base (Fig. 3.1C).

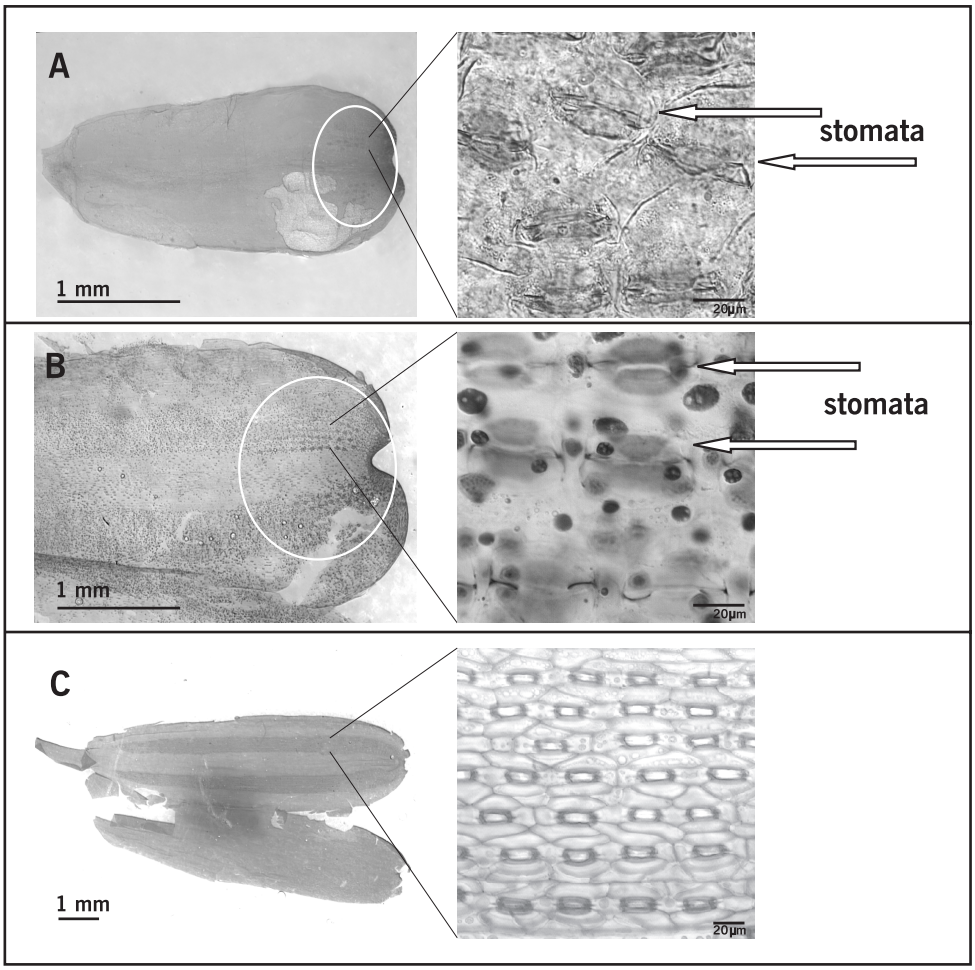

Figure 3.1: Epidermis of *Tsuga heterophylla* needle during ontogeny. **A**: Unbudded needle: stomata are visible at the tip indicated by the white circle (this region is enlarged at the right side). **B**: Budding needle: more mature stomata are present at the tip in the white circle, but not in the basal and mid section yet. **C**: Small needle: mature stomata are arranged in two bands on either side of the mid vein on the entire needle; mature stomata and epidermal cells are depicted in detail on the right side. Open white arrows indicate stomata.

Developmental classes

The measured needle characteristics and the statistics of comparison between individual classes are documented in Appendix A1. Average needle length of *Tsuga heterophylla* in this study increased from 2.65 ± 0.5 mm for needles still in the bud to 11.96 ± 0.9 mm for fully grown needles (Fig. 3.2A), corresponding to an increase in relative needle length from 22.2 ± 4.2 % to 100 ± 7.2 %. Average needle width also increased during needle growth from 1.4 ± 0. mm to 2.18 ± 0.1 mm (Fig. 3.2B; relative needle width: 62.5 ± 3.9% to 100 ± 6.0%). Average needle area increased from 3.6 ± 0.9 mm^2 to 26.1 ± 2.7 mm^2 (Fig. 3.2C), representing a relative increase from 14.0 to 100 %.

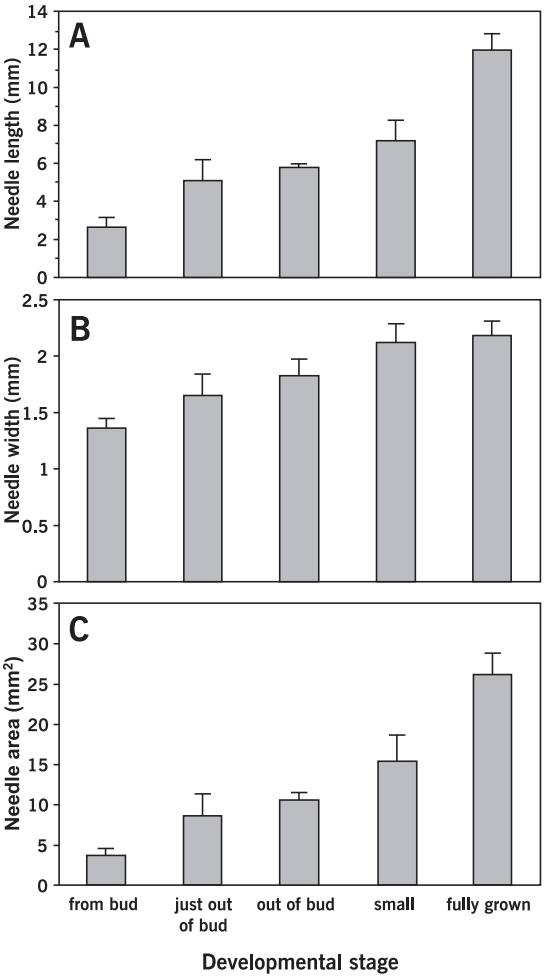

Figure 3.2: Needle dimensions during the ontogeny of *Tsuga heterophylla*. **A**: Average needle length. **B**: Average needle width. **C**: Average needle area (area = length × width). Error bars indicates 1 S.E.

SR does not change significantly between classes (Fig. 3.3A). SD decreases in budding needles, but it does not change any further from small to fully grown needles (Fig. 3.3B). Stomatal density near the tip of the needles is significantly higher than on the lower part (224.8 ± 32.3 mm^{12} vs 210.1 ± 31.8 mm^{-2} for all small and fully grown needles; $P = 0.005$). The relation between stomatal density and developmental class does not change when only stomatal density near the tip is compared. The number of stomata per mm needle length (TSDL) is significantly higher in unbudded needles than in the other classes and lowest in small and fully grown needles (Fig. 3.3C). The total number of stomata on a needle (SN) is higher on fully grown needles than in the other classes (Fig. 3.3D).

Pore length was higher in small and fully grown needles than in the other three classes (Fig 3.4A). PL_{top} (pore length measured at the tip of the needle) was slightly smaller, but not significantly than at the lower part of the needle. Subsidiary cell length was only measured in small and fully grown needles, and was significantly higher in fully grown needles (Fig 3.4B). Subsidiary cells at the tip were significantly shorter than the average SL over the entire needle ($P = 0.002$).

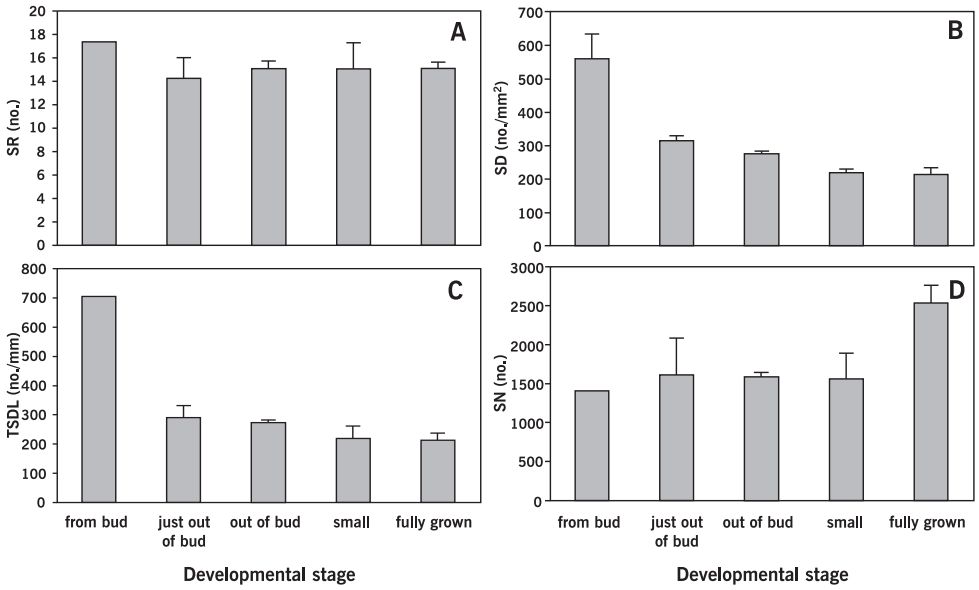

Figure 3.3: Stomatal frequency during the ontogeny of *Tsuga heterophylla* needles. **A:** Average number of rows on the needle (SR). **B:** Average stomatal density per mm^2 within stomatal regions (SD). **C:** Average number of stomata per mm needle length (TSDL). **D:** Average total number of stomata per needle (SN). Error bars indicate 1 S.E. SR and SD could not be measured on all the needles from the bud due to difficulties in discerning immature cell walls (n = 1 for SR, and n = 2 for SD).

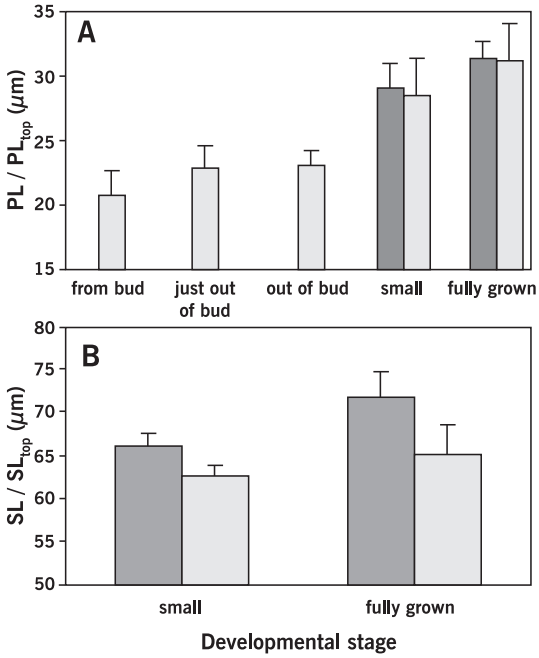

Figure 3.4: Ontogenetic changes in average (**A**) Stomatal Pore and (**B**) Subsidiary Cell lengths for *Tsuga heterophylla* needles of different developmental stages. Dark grey bars represent measurements on the entire needle including basal and mid region (PL and SL), light grey bars include only measurements from the apical region (PL_{top} and SL_{top}). Error bars indicate 1 S.E. In the younger needles (from bud, just out of bud and out of bud) mature stomata were only present at the tip, therefore no data from basal stomata could be obtained, and walls of subsidiary cells could not unambiguously be discerned to obtain reliable measurements.

Leaf development

In order to quantitatively describe the stomatal characteristics during needle development of *Tsuga heterophylla*, these characteristics are also presented in relation to relative needle area instead of developmental class.

SR does not change with increasing needle area (Fig. 3.5A; $r^2 = 0.000$). Stomatal density, as measured on the entire needle or just at the tip, shows a clear inverse relation with increasing area (Fig. 3.5B; $r^2 = 0.952$). The TSDL also inversely decreases during needle development (Fig. 3.5C; $r^2 = 0.874$). These two parameters decrease steepest in the early leaf development, and do not vary significantly (anymore) when the needles are completely exposed (at 50% relative leaf area). The total number of stomata per needle increases linearly with relative needle area (Fig. 3.5D; $r^2 = 0.695$).

Pore length also increases linearly with needle area (Fig. 3.6A; $r^2 = 0.800$) as does subsidiary cell length, which was only measured for needles with more than 50% relative needle area (Fig. 3.6B; $r^2 = 0.841$).

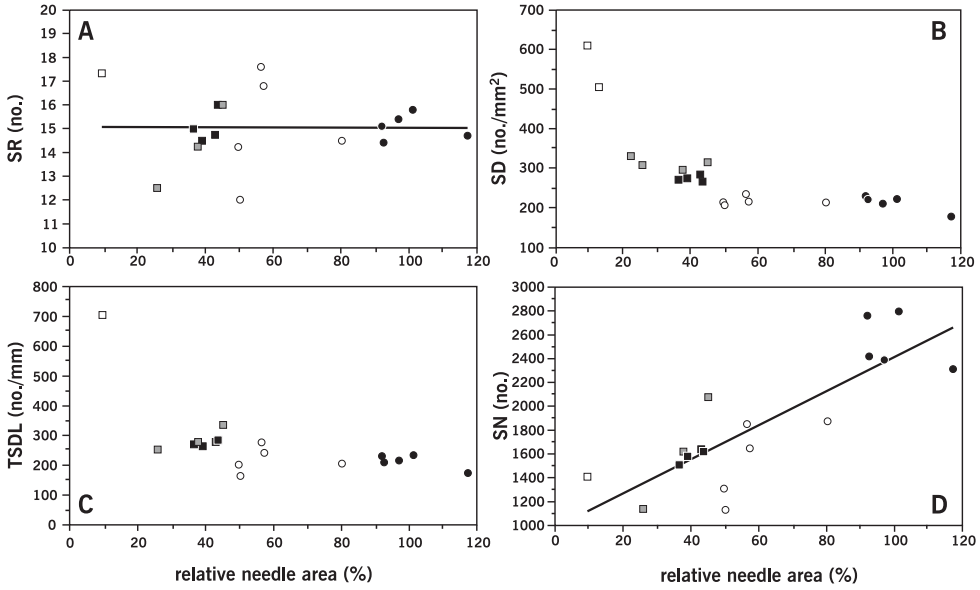

Figure 3.5: Ontogenetic changes in stomatal frequency as related to relative needle area (RNA). Data points represent individual needles in each developmental class. Black circles – fully grown needles; open circles - small needles; black squares - out of bud needles; grey squares – just out of bud needles; open squares – from bud needles. **A**: Number of rows on the needle. Linear regression: SR = −0.0002981 × RNA + 15.065; r^2 =0.000 (P = 0.981). **B**: Stomatal density per mm^2. Inverse regression: SD = 4270/RNA + 163.705; r^2 = 0.952 (P = 0.000). **C**: Number of stomata per mm needle length (TSDL). Inverse regression: TSDL = 5071.6/RNA + 147.041; r^2 = 0.874 (P = 0.000). **D**: Number of stomata per needle (SN). Linear regression: SN = 14.355 × RNA + 980.708; r^2 = 0.689 (P = 0.000).

DISCUSSION

Epidermal development in *Tsuga heterophylla*

Epidermal ontogeny in *Tsuga heterophylla* appears to be very similar to the general monocotyledon-type development (Fig. 3.7). Stomatal initiation occurs only at the basal part of the needle in specific rows of epidermal cells, while other rows without stomata contain only elongated epidermal cells. Subsidiary cells originate from cell division of the epidermal cells neighbouring the stomatal initial cell. The maturation of the stomata (division into guard cells, cell expansion and finally lignification of the guard cells) starts at the apex and progresses basipetally until also the basal stomata have matured in completely emerged needles. Cell initiation and cell expansion are thus spatially separated in different zones on the leaf, but take place simultaneously.

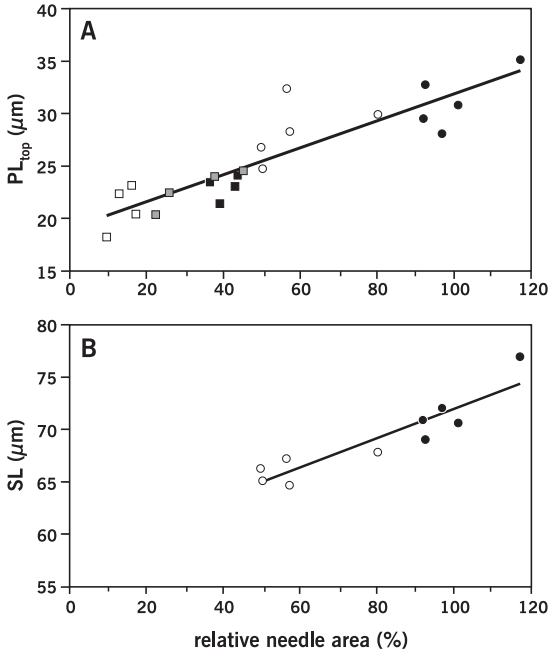

Figure 3.6: Ontogenetic changes in Stomatal Pore and Subsidiary Cell lengths for *Tsuga heterophylla* needles as related to relative needle area (RNA). Data points represent individual needles in each developmental class. Black circles – fully grown needles; open circles - small needles; black squares – out of bud needles; grey squares – just out of bud needles; open squares – from bud needles. **A**: Pore length of stomata in apical region. Linear regression: PL_{top} = 0.128 × RNA + 19.048; r^2 = 0.800 (P = 0.000). **B**: Length of subsidiary cells of fully grown and small needles. Linear regression: SL = 0.14 × RNA + 57.924; r^2 = 0.841 (P = 0.000).

The number of stomatal rows is already fixed in the first stages of stomatal development within the bud. During subsequent needle development no extra stomatal rows originate. Rows of stomata in mature needles appear further apart from each other than the rows in unbudded needles, without extra epidermal cell rows between them to increase leaf width. The increase in needle width during ontogeny (which is much smaller than the increase in needle length: 60 % vs 350 % from unbudded to fully grown), should then be the result of lateral expansion of the stomatal and epidermal cells.

During the entire growth period cell expansion occurs, but especially in the first stages as indicated by the inverse decrease in stomatal density per mm^2 with relative needle area. A decline in stomatal density would be expected to result from expansion of epidermal cells without the formation of new stomata. The observed decrease can be partly explained by the lateral expansion of subsidiary and epidermal cells. Longitudinal cell expansion also occurs during leaf growth, causing the increase in stomatal pore length during the whole period of needle development. Subsidiary cell length in the emerged needles also increases. However, the cell expansion indicated by the pore and subsidiary cell length increase between small and fully grown needles does not result in a significant decline in stomatal density. Perhaps the increase in pore and subsidiary cell length in the final stages is rather a result of change in cell shape than a change in cell area, or compensated for by a decrease in area of surrounding epidermal cells.

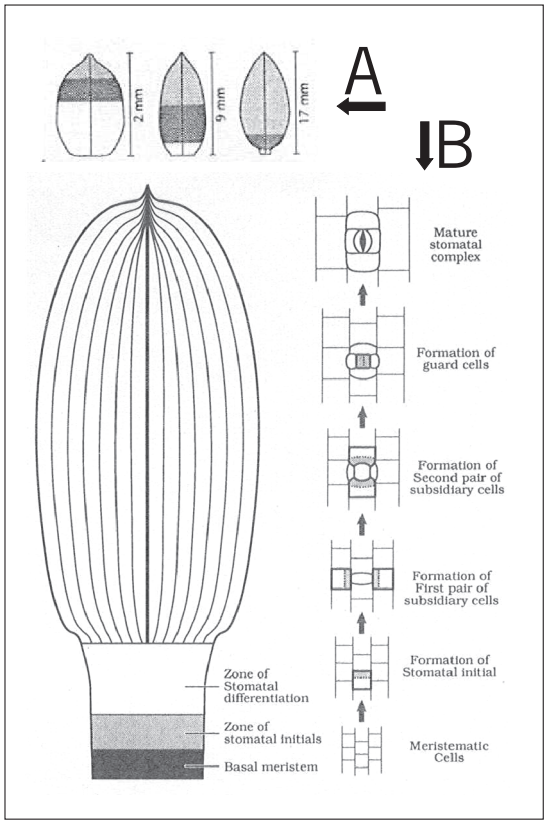

Figure 3.7: Schematic development in leaves of the monocotyledon *Tradescantia*. **A**: Diagram of a *Tradescantia* leaf at three stages of leaf development showing the region of fully formed stomatal complexes (light shading), the region of stomatal differentiation (dark shading) and the region where cell proliferation and stomatal patterning occur (no shading). Reproduced from Chin et al., 1995. **B**: Schematic diagrams (not to scale) showing the overall organization of the *Tradescantia* leaf (left) and the sequence of developmental events that result in the formation of a stomatal complex (right). Reproduced from Croxdale et al., 1992.

Because cell expansion has been shown to be relatively unimportant for increasing needle length once the leaves have emerged, the subsequent growth should result from continuous initiation of stomata and/or epidermal cells. The constant production of new stomata and subsidiary cells would explain why stomatal density remains unchanged during the final stages of leaf growth which would not be expected if cell expansion of existing epidermal cells was the dominant process. Indeed, the total number of stomata on the needle increases with increasing needle area during the entire ontogenetical period. The clear increase in SN apparent in figure 3.5D is mainly due to the large difference in SN of fully grown needles compared to the other stages. However, the total number of stomata on unbudded and very young needles is likely to be overestimated, because it is assumed in the calculation of SN that the entire needle length is covered with stomata. In very young needles stomata are only present on the upper part, thus the real number of stomata on such needles should be lower than the estimated number. In this case the observed increase in stomata per needle with

increasing leaf area becomes more pronounced through the entire developmental period. The consistent increase in SN during leaf growth indicates continuous formation of new epidermal and stomatal cells at the formative zone at the base of the needle.

Stomatal frequency in young conifer and angiosperm leaves

In contrast to conifers and monocotyledons, cell initiation and expansion in young dicotyledon leaves are not spatially separated and take place at different times during leaf development. In general, the period of main cell expansion occurs when cell initiation is finished although overlap is possible (Van Volkenburgh, 1999; Croxdale, 2000). In several studies on dicotyledon leaf growth it is noted that the majority of cells is already initiated when the leaf is 20-50% of its final area after which SD decreases due to expanding leaf area (Brouwer 1963, Gay and Hurd, 1975 Van Volkenburgh, 1987). However, ontogenetic changes in stomatal density vary considerably between different dicot species. In *Capsicum*, for example, stomatal initiation causes the stomatal density to increase until the leaf is at 50% of its final size before cell expansion becomes more important and the stomatal density decreases along with the final increase in leaf area (Schoch, 1972). Stomatal density in other species already starts to decrease at different rates at about 10 % of final leaf area. In general, stomatal density still decreases in the final phases of leaf growth due to cell expansion (Tichá, 1982). In *Tsuga heterophylla* the stomatal density does not decrease significantly when the needle area doubles from 50 to 100% because the later leaf growth is due to prolonged cell initiation rather than just the expansion of existing epidermal cells. The lack of a strong decrease in SD in maturing *T. heterophylla* needles as opposed to dicotyledons might also be related to the fact that main needle growth in conifer needles is most pronounced in one dimension (length), contrary to the two dimensional leaf growth in most angiosperm species.

Owens (1968) describes the epidermal development of the conifer *Pseudotsuga menziesii* whose needles are longer than those of *T. heterophylla* but otherwise very similar in epidermal morphology. In *P. menziesii* cell divisions become restricted to the epidermal rows which give rise to stomata, when the needle is 5 mm in length (about $1/6^{th}$ of its final length). A distinct cuticle and guard cells do not become evident until the needle reached two-thirds of it final length. The pattern of stomatal development, therefore, is similar to *T. heterophylla* but in the latter species mature guards cells are already present on the entire needle at half its final size. Thus, also in conifers the timing of stomatal development is variable between species.

Implications for stomatal frequency analysis

The decrease in stomatal density due to cell expansion in the final phase of leaf growth in dicots warrants caution when applying stomatal density measurements to reconstruct past atmospheric CO_2 concentrations (Tichá, 1982; Royer, 2001). Distinguishing young from mature leaves can be difficult, since mature stomata are always present on the entire leaf surface even though the epidermal cells might still be expanding. Careful sampling strategies and applying the stomatal index rather than stomatal density are often necessary to circumvent this problem. In *Tsuga heterophylla* mature stomata are only present along the

entire needle length after the needle has fully emerged from the bud. As soon as the entire needle is covered with mature stomata (at 50% relative needle area) no significant change in stomatal density per mm^2, stomatal rows, or stomatal density per mm needle length occurs. Very young needles, which do differ in stomatal frequency from mature ones, can easily be recognized because they only have mature stomatal complexes at the needle tip and are still partially in bud. Moreover, encountering needles with higher stomatal densities from early developmental stages in fossil assemblages should be unlikely, because their fragile epidermis has a relatively low preservation capacity. Thus, as long as the fossil needles to be used for stomatal frequency measurements have mature stomata on the entire needle and not just at the tip, ontogenetic differences will not significantly influence the reliability of paleoatmospheric CO_2 reconstructions based on mean stomatal density. This could also hold true for grasses and other monocotyledon taxa which have a highly similar leaf development.

CHAPTER 4

Atmospheric CO_2 fluctuations during the last Millennium reconstructed by stomatal frequency analysis of *Tsuga heterophylla* needles

The inverse relation between atmospheric CO_2 concentrations and stomatal numbers on *Tsuga heterophylla* needles was applied to reconstruct paleo-atmospheric CO_2 concentrations over the period 800-2000 AD from fossil *T. heterophylla* needles in a lake sediment core from Mount Rainier, Washington, USA. The stomatal frequency record revealed significant century-scale fluctuations, with prominent minima in CO_2 of about 260 ppmv present around 860 AD and 1150 AD, and smaller minima of 275-280 ppmv occurring around 1600 and 1800 AD. In between, CO_2 maxima of 300 ppmv around 1000 AD, 320 ppmv around 1300 AD, and 300 ppmv around 1700 AD are recorded. These features occur in harmony with global terrestrial temperature changes, as well as oceanic surface temperature fluctuations in the North Atlantic. The results obtained in this study reinforce the notion of a continuous coupling of CO_2 and climate during the Holocene, as previously suggested by stomatal frequency records from the last Deglaciation and Early Holocene.

INTRODUCTION

The notion of tightly co-varying atmospheric CO_2 levels and climate is reinforced by the prediction in climate models of both a strong rise in global mean temperature as a result of the continuous injection of anthropogenically produced CO_2 in the atmosphere ((1-7ºC; IPCC, 2001), as well as significant feedback effects of these CO_2 induced climate changes on the carbon exchange between oceanic, atmospheric and terrestrial reservoirs (Joos et al., 1999; Yi et al., 2001; Plattner et al., 2001; Dore et al., 2003).

Late Quaternary atmospheric CO_2 concentrations (mixing ratios) and isotopic temperature records reconstructed from Antarctic ice-cores show parallel variations on glacial-interglacial time scales (Raynaud et al., 1993; Petit et al., 1999). On millennial time scales, a similar co-variation has been recognized during the glacial periods (Stauffer et al., 1998; Fischer et al., 1999; Indermühle et al., 2000). In marked contrast, however, ice-core data suggest that during the interglacials, like the Holocene, global temperature variations and atmospheric CO_2 concentrations are decoupled. Long-term global temperature trends, such as the warm Holocene Hypsithermal and the successive Subatlantic cooling, have not been recognized in the Antarctic CO_2 records, which have their lowest values in the early Holocene around 8000 BP and then rise gradually from 260 ppmv to pre-industrial 280 ppmv (Indermühle et al., 1999a; Flückiger et al., 2002).

On centennial time scales, no significant ice-derived CO_2 fluctuations occur contemporaneously with well-documented cooling events such as the Younger Dryas, Preboreal Oscillation, and the 8.2 kyr BP event. Intriguingly, however, several Antarctic ice core records of the last millennium do show CO_2 changes of 5–20 ppmv that are broadly concurrent with the Medieval Climatic Optimum and Little Ice Age (Barnola et al., 1995; Etheridge et al., 1996; Indermühle et al., 1999a). Although these records could indicate a coupling between temperature shifts and atmospheric CO_2, data from different coring localities are not in agreement with respect to timing and magnitude of the CO_2 changes (Siegenthaler et al., 1988; Barnola et al., 1995; Etheridge et al., 1996; Indermühle et al, 1999a).

An alternative proxy for atmospheric CO_2 concentration is provided by means of stomatal frequency analysis, where the inverse relation between the number of gas pores on plant leaves and ambient CO_2 enables the reconstruction of past CO_2 levels (e.g. Woodward,1987; Kürschner et al, 1996; Wagner et al., 1996; Royer, 2001; Royer et al., 2001). Stomatal records show a much more dynamic CO_2 evolution during the last Deglaciation and Holocene than the ice-core measurements. Reconstructed centennial-scale CO_2 fluctuations in the order of 20-80 ppmv can be related to cooling events such as the Younger Dryas (Beerling et al., 1995; McElwain et al, 2002; Rundgren and Björck, 2003), Preboreal oscillation (McElwain et al., 2002; Wagner et al., 1999a), the 8.2 kyr event (Wagner et al., 2002) and the Little Ice Age (Rundgren and Beerling, 1999). These reconstructions contradict the concept of an Early-Holocene decoupling of CO_2 and temperature, postulated on the basis of ice-core records.

In the stomata-based reconstructions, and in some ice-core records, CO_2 fluctuations occur approximately synchronous with Holocene temperature changes. There may be a slight time-lag at the end of the Younger Dryas (McElwain et al., 2002), but insufficient temporal resolution and chronological uncertainty of the stomatal data and ice-core measurements has hampered accurate determination of the exact phase-relation between CO_2 and climate on centennial time scales.

In addition to leaves of angiosperm tree species, needles of conifers are increasingly used for detecting and quantifying past CO_2 changes (Van de Water et al., 1994; Royer et al., 2001; McElwain et al., 2002). In the present study we document the stomatal frequency analysis of a high-resolution record of fossil *Tsuga heterophylla* needles from North America. Spanning the period between 800 AD and 2000 AD, the results are used to ascertain whether global or extra-regional temperature trends for the last Millennium, inferred from both marine and terrestrial proxy records, are indeed associated with a dynamic atmospheric CO_2 regime.

MATERIAL AND METHODS

A record of fossil needles of the conifer *Tsuga heterophylla* over the past 1200 years was obtained from the upper 44 cm of a 91 cm sediment core, drilled in Jay Bath, a shallow pond (about 1.20 m water depth) on the southern flank of Mount Rainier (Washington, USA; 46º46' N 121º46' W; Fig. 4.1). These sediments contain rich and diversified needle assemblages (Dunwiddie, 1986). The needles can be identified at a species level. Relative-fre-

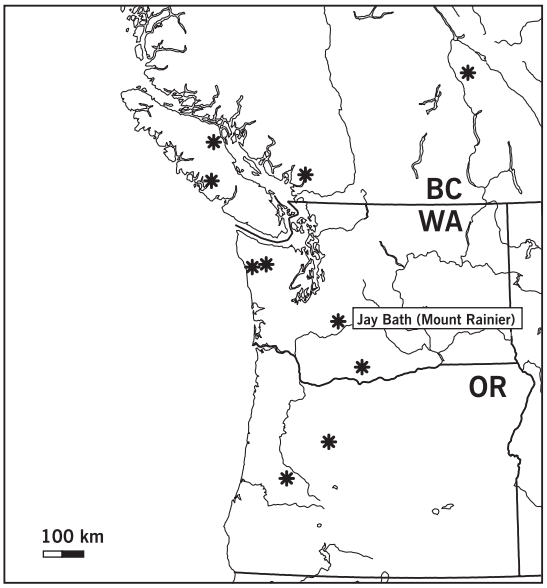

Figure 4.1: Source localities of the *Tsuga heterophylla* needles used in the training set and the location of Jay Bath (Mount Rainier National Park). BC = British Columbia (Canada), WA = Washington (USA) and OR = Oregon (USA).

quency patterns indicate that the needle record of the studied interval originates from a stable, late-successional forest dominated by *T. mertensiana*, *T. heterophylla* and *Abies amabilis.*

The core was cut into 1 cm thick sediment samples, which were sieved on a 250µm mesh sieve. *T. heterophylla* needles were identified and stored in ethanol. Needles for stomatal analysis were bleached with a 4% natriumhypochloride solution to remove the mesophyll. The remaining cuticle was then stained with safranin and mounted in glycerin jelly on a microscopic slide. Computer-aided measuring of epidermal cell parameters on needle cuticles of *T. heterophylla* was performed on a Leica Quantimet 500C/500+ Image Analysis system (Wetzlar, Germany).

In conifer needles, the number of stomata per mm needle length (TSDL) is the parameter most sensitive to changes in CO_2 concentrations (Chapter 2). The response rate of *T. heterophylla* needles to the CO_2 increase over the last century was used to quantify late-Holocene TSDL-based CO_2 changes (Fig. 4.2). All needles incorporated in the training set originate from the Pacific Northwest region (Fig. 4.1). Because of large altitudinal differences between the sites, CO_2 levels were expressed as partial pressure instead of mixing ratios: pCO_2 (Pa) = CO_2 mixing ratio (ppmv) × barometric air pressure P_B (Pa). Barometric air pressure is estimated according to Jones (1992): $P_B = 101.325/e^{[(z/29.3)/T]}$ where z is altitude above sea level and T air temperature in K (estimated from mean annual temperature at the closest weather station, corrected by a temperature lapse rate appropriate for the region in case of significant altitudinal difference between site and station).

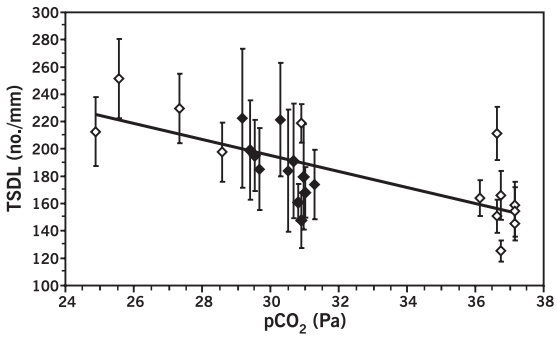

Figure 4.2: Response of stomatal parameters of Tsuga heterophylla to a pCO_2 increase from 24 to 38 Pa. CO_2 partial pressure was calculated as: CO_2 mixing ratio (ppmv) × total barometric pressure P_B (Pa). Barometric air pressure is estimated according to Jones (1992): $P_B = 101.325/e^{[(z/29.3)/T]}$ where z is altitude above sea level and T air temperature in K (estimated from mean annual temperature at the closest weather station, corrected by a temperature lapse rate appropriate for the region in case of significant altitudinal difference between site and station). CO_2 mixing ratios of 290–315 ppmv were derived from shallow Antarctic ice cores (http://cdiac.esd.ornl.gov/trends/co2/siple.htm; Neftel et al., 1985), mixing ratios of 315–368 ppmv are annual means from Mauna Loa monitoring (http://cdiac.esd.ornl.gov/ndps/ndp001.html). Black diamonds represent subfossil and modern needles from Jay Bath (Mount Rainier, WA), open diamonds modern and herbarium needles from other localities. Error bars indicate ± 1 SE. Solid lines indicate best fit in classical regression analysis. TSDL: true stomatal density per mm needle length (TSDL = $-5.8581 \times pCO_2 + 371.14$; $r^2 = 0.5124$; $P < 0.001$).

The stomatal frequency change in the training set is not attributable to changes in local precipitation or temperature (Chapter 2), or affected by difference in age between the needles (Chapter 3). The stomatal frequency response of plants to CO_2 is nonlinear and can best be described by a sigmoid function with upper and lower response limits, because the number of stomata on a leaf can neither be zero nor infinite (Kürschner et al., 1997). *T. heterophylla* apparently does not approach its response limits in the interval between 290 and 370 ppmv, as a linear regression produced a much better fit than non-linear models. Reconstructed CO_2 values were calculated using a classical linear regression, which allows a better performance at the extremes and with slight extrapolation than inverse linear regression (Osborne, 1991; Birks, 1995).

Reconstructed atmospheric CO_2 levels for the last millennium are expressed as mixing ratios rather than the reconstructed partial pressure to allow quantitative comparison with other CO_2 records. Mixing ratios were calculated by dividing the partial pressure by the air pressure at the site studied (1311 m altitude), calculated using the equation of Jones (1992). In this equation modern mean annual temperatures were used, because paleo-temperatures are not known over the whole period since 800 AD. However, temperature at the site has not varied more than approximately 1 ºC between 1500 AD and today (Graumlich and Brubaker, 1986), which would account for a negligible additional uncertainty in reconstructed CO_2 mixing ratio of not more than 0.15 ppmv.

Age-depth relations for the sediment core studied were determined by fitting a 4th order polynomial through a series of five AMS ^{14}C chronologies (calibrated using OxCal 3.8 [Bronk-Ramsey, 1995] and INTCAL98 calibration data [Stuiver et al., 1998]) and one tephra layer at 21 cm from the 1481 Mt. St. Helens eruption (dated by dendrochronology; Yamaguchi, 1983; Mullineaux, 1996). In this way a mean sedimentation rate of one cm per 27 years was obtained for the core (Fig. 4.3).

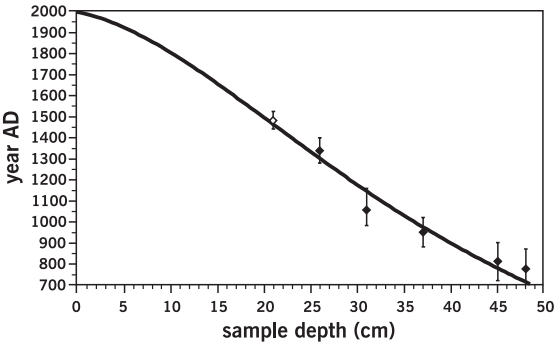

Figure 4.3: Age-depth diagram for Jay Bath core. White diamond represents tephra layer from 1481 Mt. St. Helens eruption (Yamaguchi, 1983; Mullineaux, 1996). Black diamonds represent ^{14}C AMS dates converted to calendar ages using Oxcal 3.8 . Black line shows 4th order polynomial [AGE = −0.00020094 × (DEPTH)^4+ 0.02951 × (DEPTH)^3 − 1.33288 × (DEPTH)^2 − 8.71619 × (DEPTH) +2000.22] providing best fit (r^2 = 0.9977). Error bars indicate 2 sigma (95.4%) probability ranges.

RESULTS

The reconstructed atmospheric CO_2 mixing ratios at Jay Bath since 800 AD are presented in figure 4.4. Pre-industrial CO_2 values fluctuate around a long-term average of 280-290 ppmv culminating in a sharp rise in CO_2 after 1850 AD from 280 ppmv to 370 ppmv. The CO_2 record is characterized by high-frequency variability. Focussing on centennial-scale changes (the 3 point moving average), prominent minima in CO_2 of about 260 ppmv are present around 860 AD and 1150 AD, and smaller minima of 275-280 ppmv occur around 1600 AD and 1800 AD. In between, CO_2 maxima of 300 ppmv around 1000 AD, 320 ppmv around 1300 AD, and 300 ppmv around 1700 AD are recorded.

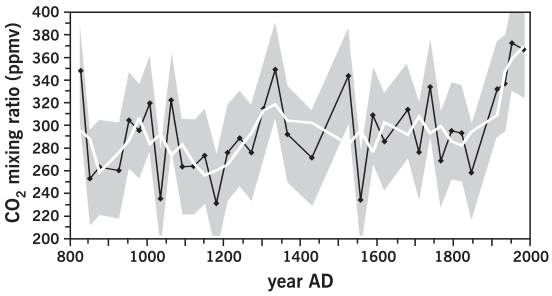

Figure 4.4: Reconstructed CO_2 mixing ratios based on stomatal frequency counts on *Tsuga heterophylla* needles for the time period from 800 AD to 2000 AD. Black line are the means of 3–5 needles per sample, thick white line represents a 3 point moving average. Grey area shows confidence interval of ± 1 RMSE.

DISCUSSION

The sharp rise in the stomata-based CO_2 curve (Fig. 4.5A) after 1850 AD corresponds excellently to the industrial CO_2 increase apparent in instrumental records (Keeling and Whorf, 2002) and shallow ice-cores (Neftel et al., 1985). This correspondence corroborates the reliability of the reconstruction. Mean pre-industrial CO_2 values are simular to those measured in Antarctic ice-cores (Etheridge et al., 1996; Indermühle, 1999a). However, with prominent maxima centred around 1000 AD, 1300 AD, and 1700 AD and minima around 860 AD, 1150 AD, 1600 AD, and 1800 AD, the centennial-scale CO_2 variability during the last millennium is much more pronounced in the stomata-based record than in ice-core data. In the Law Dome ice core these reconstructed fluctuations have not been detected (Etheridge et

al., 1996). On the other hand, CO_2 records from ice-cores D47 and D57 from Adelie Land (Antarctica) exhibit a rapid increase (of 15 ppmv) during the 13th century AD (Barnola et al., 1995). The discrepancies between the different ice-core and stomatal records may partly be explained by varying age distributions of the air in the bubbles due to the enclosure time in the firn-ice transition zone, which depends on local temperatures and accumulation rates. In different ice cores, this effect creates a site-specific attenuation of the signal as well as a difference in age between the air and surrounding ice, hampering the construction of well-constrained time-scales (Schwander et al., 1996; Spahni, et al., 2003). Other potential factors that may create dissimilarities between the records include the application of different extraction methods for CO_2, and post-depositional physicochemical reactions in the ice that can increase as well as decrease the CO_2 concentration in air bubbles (Anklin et al., 1995; Stauffer and Tschumi 2000).

Terrestrial climate changes of the last Millennium conventionally related to the Medieval Warm Period and the Little Ice Age occurred at different times in different parts of the world. Regional cooling trends were often interrupted by periods of relative warmth. It is not attempted, therefore, to correlate reconstructed global CO_2 fluctuations with these regional events. CO_2-temperature correlations on a global or extra-regional scale are illustrated in figure. 4.5.

A comparison of the stomata-based CO_2 reconstruction to a multi-proxy global mean temperature reconstruction (Mann and Jones, 2003) reveals some striking correlations, most remarkably so in the timing of the warm periods and the CO_2 maxima around 950 AD and 1300 AD (Fig. 4.5B). The overall picture suggests a clear co-variation between CO_2 and global temperature. However, detailed matching of the records is hampered by the fact that the Southern Hemisphere contribution to the global mean temperature estimation is based on limited proxy data, as well as the uncertainties in the chronology of the CO_2 record (on the scale of several decades).

To understand cause and effect in the CO_2-temperature coupling, appropriate regional climate records were selected for comparison with the reconstructed CO_2. The timing of CO_2 maxima and minima in the stomata-based record is synchronous (within uncertainty limits) to changes in North Atlantic Ocean sea surface temperature as recorded offshore Mid-Atlantic USA (Cronin et al., 2003; Fig. 4.5C) as well as offshore West Africa (DeMenocal et al., 2000; Fig. 4.5D). The observed synchroneity suggests that the North Atlantic ocean could very well serve as source and sink at the time of centennial-scale atmospheric CO_2 variations. Exchange of CO_2 between atmosphere and ocean is highly dependent on physicochemical factors affecting the solubility of CO_2 in the ocean surface waters such as alkalinity, dissolved inorganic carbon (DIC) content, salinity and temperature (Takahashi et al., 1993; Raven and Falkowski, 1999; Plattner et al., 2001). Because higher temperature induces lower CO_2 solubility, SST decrease would draw down CO_2 from the atmosphere into the surface waters, resulting in lower atmospheric CO_2 levels. Oceanic carbon cycle models incorporate a temperature factor of about 4% change in oceanic pCO_2 per degree tempera-

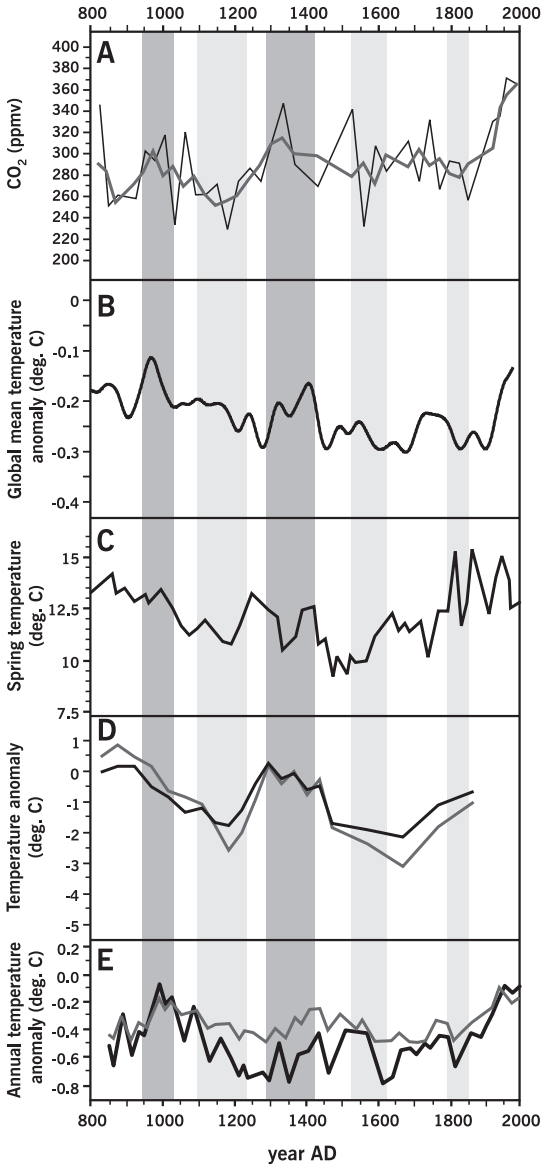

Figure 4.5: Comparison between reconstructed CO_2 mixing ratios and Northern Hemisphere climate records. **A**: CO_2 mixing ratios from stomatal counts on *Tsuga heterophylla* needles from Jay Bath. Thin black line are means of 3–5 needles per sample depth, thick grey line 3 point moving average to emphasize centennial scale trends. **B**: Global mean temperature anomaly (45 year running average) from multi-proxy records based on 1961–1990 reference period (Mann and Jones, 2003). **C**: Sea surface temperatures of Chesapeake Bay (Mid Atlantic USA) reconstructed from Mg/Ca ratios of ostracods (Cronin et al., 2003). **D**: Sea surface temperature anomalies offshore West Africa as reconstructed from foraminiferal assemblages (DeMenocal et al., 2000). Black line are cold season anomalies, grey line warm season anomalies **E**: Summer temperature anomalies in tree ring records from the Northern hemisphere. (Uppermost) grey line from Briffa et al. (2000); (lowermost) black line from Esper et al. (2002). Dark grey shading indicates periods of relatively high CO_2 mixing ratios, light grey shading periods of relatively low CO_2 mixing ratios (panel A).

ture change (equivalent to 11.2 ppmv at a starting level of 280 ppmv; Plattner et al., 2001). For example, a modelled cooling of 2.7 ºC in the Atlantic Ocean (north of 20ºN latitude) during the Younger Dryas produced a local atmospheric pCO_2 decrease of 2.7 Pa (equivalent to 27 ppmv at sea level; Takahashi et al., 1993; Marchal et al., 1999). The SST fluctuations over the last Millennium at the two sites on opposite sides of the Atlantic ocean are of

a similar magnitude (2-3 ºC; Fig. 4.5). Provided that SST at these sites reflects SST changes in the whole North Atlantic, temperature-driven changes in CO_2 flux between ocean surface waters and atmosphere may be invoked as a plausible mechanism to explain at least a substantial part of the reconstructed CO_2 variations over the last Millennium. Additional potential oceanic sources of CO_2 comprise climate-induced changes in salinity, carbonate chemistry (DIC and alkalinity levels), circulation, and marine biological productivity in the Atlantic or the other ocean basins (Siegenthaler and Wenk, 1984; Sarmiento and Orr, 1991; Marchal et al., 1998; Plattner et al., 2001).

The reconstructed CO_2 minima and maxima also show remarkable similarities to Northern Hemisphere temperature trends based on extra-tropical tree-ring records (Briffa, 2000; Esper et al., 2002). A link between CO_2 and terrestrial temperature would be most prominent in Northern Hemisphere records because models of the spatial distribution of a future temperature rise due to anthropogenic CO_2 production indicate that the greatest warming is expected to occur at high latitudes on the Northern Hemisphere continents (IPCC 2001). Models of evolution of CO_2 and Northern Hemisphere temperature in response to changes in radiative forcing over the last Millennium show that temperature changes in the order of magnitude as indicated by the tree-ring record of Esper et al. (2002) are associated with CO_2 changes of at least 20 ppmv (Gerber et al., 2003). Such changes are outside the range of CO_2 variability in ice-cores but compatible with the stomata-based record.

The minimum in the CO_2 record at 1150 AD and the maximum around 1400 AD seem to correspond to terrestrial temperature changes that occur 50-100 years later. However, any exact determination of leads and lags between CO_2 and temperature is impeded by the lower resolution and lower chronological accuracy of the stomata-based reconstruction in comparison to the tree-ring temperature records.

CONCLUSIONS

The centennial-scale variability in atmospheric CO_2 concentration linked to documented global and regional temperature change since 800 AD, recognized in this study, corroborates continuous coupling of CO_2 and climate during the Holocene. For the first time, CO_2 changes inferred from stomatal frequency analysis, have been related to coeval variation in Atlantic sea surface temperatures, providing evidence that CO_2 fluctuations over the last Millennium at least partly originated from temperature-driven changes in CO_2 flux between ocean surface waters and atmosphere. Because CO_2 variation also shows similarities with terrestrial temperature trends in Northern Hemisphere regions most sensitive to global warming, it may be speculated that in the last Millennium CO_2 could have served as a forcing factor for terrestrial temperature.

CHAPTER 5

INFLUENCE OF ENVIRONMENTAL STRESS FACTORS ON STOMATAL FREQUENCY OF FOSSIL *TSUGA HETEROPHYLLA* NEEDLES FROM MOUNT RAINIER (WASHINGTON, USA).

An extremely low number of stomata per mm needle length is encountered between 300 AD and 700 AD in the *Tsuga heterophylla* record at Jay Bath. These low stomatal numbers do not appear to result from extremely high atmospheric CO_2 levels at the time, but do coincide conspicuously with the establishment of the species during a period of major disturbance at the site. The open, exposed setting in the montane environment after this disturbance probably provided highly stressed growth conditions for the pioneering, early-successional *T. heterophylla* trees. Spring water-stress related to prolonged low soil temperatures, would be the most plausible explanation for an acclimational stomatal frequency response to reduced water uptake. Thus, environmental stress factors associated with early-successional montane habitats show the potential to obscure stomatal frequency changes in response to atmospheric CO_2. This complication should be taken into account when selecting leaf material from high-elevation sites for stomatal frequency analysis. Over the past 1200 years, the presence of a stable late-successional forest at Jay Bath, indicates that the latter part of the stomatal record was not influenced by extreme growth conditions and can thus be regarded as a reliable reflection of atmospheric CO_2 levels.

INTRODUCTION

The inverse relation between numbers of leaf stomata and ambient CO_2 enables the reconstruction of past atmospheric CO_2 levels (e.g. Woodward,1987; Kürschner et al, 1996; Wagner et al., 1996; Royer, 2001; Royer et al., 2001). Stomatal frequency analysis of leaves buried in peat and lake deposits is therefore increasingly applied as a practical tool for detecting and quantifying short-term changes in the Holocene CO_2 regime (e.g. Rundgren & Beerling, 1999; Wagner et al., 1999a; Wagner et al., 2002).

In addition to leaves of angiosperm tree species, well-preserved needles of a variety of conifers may occur abundantly in Holocene deposits. Because of the long-term dominance of conifers in temperate and boreal forest ecosystems, stomatal frequency analysis of conifer needles may widen the spatial coverage of stomata-based CO_2 reconstructions. Analysis of herbarium material and fossil assemblages has demonstrated that species of *Pinus, Picea*, *Tsuga*, *Larix* and *Metaseqoia* have the capacity to adjust their stomatal numbers to changing CO_2 regimes (Van de Water et al., 1994; Royer et al., 2001; McElwain et al., 2002; Chapter 2). Recently, analysis of a needle record of *Tsuga heterophylla* (western hemlock) from North America confirmed a centennial-scale CO_2 variability between 800 and 2000 AD (Chapter 4). Within uncertainty limits, CO_2 maxima and minima in the stomata-based reconstruction correlate with global temperature changes based on multi-proxy records, long-term changes in North Atlantic sea surface temperature, as well as terrestrial temperature trends on the Northern Hemisphere derived from tree-ring records (Chapter 4).

The 1200-year needle record of *T. heterophylla* was recovered from sediments of Jay Bath, a shallow pond on the southern flank of Mount Rainier (Washington, USA). These sediments contain rich and diversified needle assemblages. The needles can be identified at a species level, and relative-frequency patterns reflect changes in the composition of the conifer-dominant vegetation during the past 6000 years (Dunwiddie, 1986; 1987). Following the apparent dieback of a forest dominated by *Abies amabilis* around 200 AD, rapid expansion of *T. heterophylla* into the area gave rise, after a few centuries, to the formation of the modern forest dominated by *Tsuga mertensiana*, *T. heterophylla* and *A. amabilis.*

Although generally regarded as a shade-tolerant, late-succesional species, *T. heterophylla* can be found in all stages of succession. It is an agressive pioneer because of its quick growth in full overhead light and its ability to survive on a wide variety of seedbed conditions (Packee, 1990). In general, mean stomatal frequency in *T. heterophylla* is not affected significantly by environmental variables other than CO_2 (Chapter 2). However, it should be noted that under suboptimal growth conditions, the effect of CO_2 on stomatal frequency of conifer needles may be obscured by the influence of environmental stress factors. Observations on needles of *Pinus, Abies*, and *Picea* along altitudinal gradients (Hultine and Marshall, 2000; Schoettle and Rochelle, 2000; Qiang et al., 2003), suggest that adverse montane growth conditions inhibit formation of needle stomata as an acclimational response to restrict water loss.

At the flanks of Mount Rainier, growth conditions of *T. heterophylla* in open, exposed early-successional habitats are likely to be different from those in the sheltered, late-successional closed forest. In order to assess the reliability of CO_2 reconstructions on the basis of *T. heterophylla* needles, it seems essential to determine whether or not stomatal chracteristics are influenced by environmental stress factors associated with early-successional habitats in montane areas. In the present paper we therefore extend the stomatal frequency analysis of the Jay Bath needle assemblages to the onset of the *T. heterophylla* record around 200 AD.

MATERIAL AND METHODS

A 91-cm sediment core containing conifer needles was obtained from Jay Bath, a shallow (about 1.20 m water depth) pond, situated at an altitude of 1311 m on the southern flank of Mount Rainier (Washington, USA; 46º46' N 121º46' W; Fig. 5.1). One-cm thick sediment samples were sieved on a 250µm mesh sieve and the encountered macrofossils were identified [conifer needles were identified at species level (Dunwiddie, 1985), seeds at the genus level] and stored in ethanol. Residues were checqued for charcoal fragments and mineral grains.

Needles of *Tsuga heterophylla* were isolated for stomatal analysis. They were bleached with a 4% natriumhypochloride solution to remove the mesophyll. The remaining cuticle was then stained with safranin and mounted in glycerin jelly on a microscopic slide. Computer-aided measuring of epidermal cell parameters on needle cuticles was performed on a Leica Quantimet 500C/500+ Image Analysis system (Wetzlar, Germany). Stomatal frequency was measured as the number of stomata per millimeter needle length, (TSDL: for analytical details, see Chapter 2). Pore length was measured on 30 stomata per needle at a magnification of ×640.

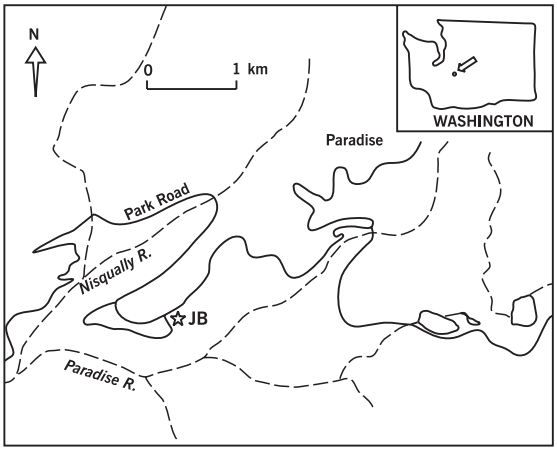

Figure 5.1: Location of Jay Bath (JB) on Mount Rainier, Pierce County, Washington (Reproduced from Dunwiddie, 1986).

Maximum stomatal conductance G_{max} is mainly determined by the density and geometry of stomata and can be calculated as 1/R (R = stomatal resistance; Jones, 1995); and according to Parlange and Waggoner (1970):

$$R = 1/nD\,(d/Bab + \ln(4ab/Ba)) \qquad \text{Eqn. } \mathbf{1}$$

where a (m) represents the major axis radius (PL), b (m) the minor axis radius, D (m^2/s) the diffusive coefficient of CO_2 in air, d (m) length of the diffusive pathway i.e. the depth of the stomatal tube plus the diameter of the substomatal cavity and n the stomatal density (n/m^2).

Age-depth relations for the sediment core were determined by fitting a 4th order polynomial through a series of ten AMS ^{14}C chronologies (calibrated using OxCal 3.8 [Bronk-Ramsey, 1995] and INTCAL98 calibration data [Stuiver et al., 1998]) and two dated tephra layers (Yamaguchi, 1983; Mullineaux, 1996). In this way an average sedimentation rate of one cm per 26 years was obtained for the core (Fig. 5.2).

Student's t-tests and regression analysis was performed using SPSS 10.0 for Windows statistical software (Chicago, Illinois, USA).

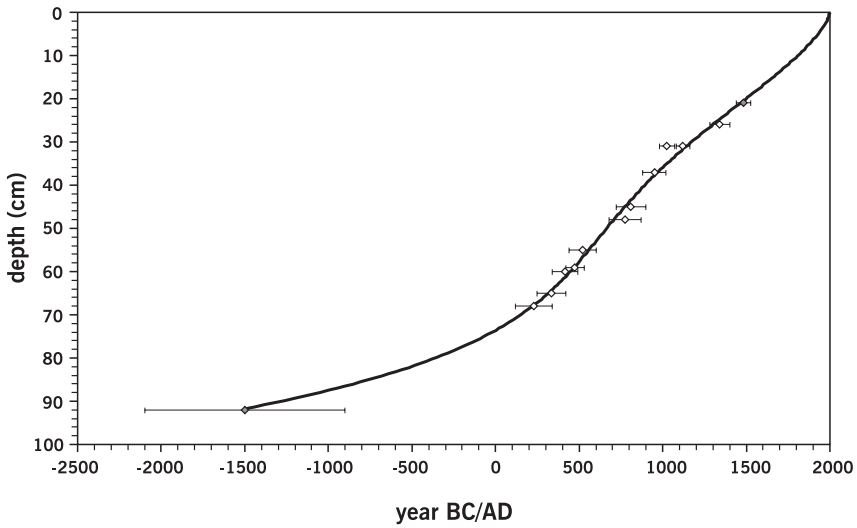

Figure 5.2: Age-depth diagram for Jay Bath sediment core. White diamonds represent AMS dates, converted to calendar age using OxCal 3.8 [Bronk-Ramsey, 1995] and INTCAL98 calibration data [Stuiver et al., 1998]. Error bars indicate 95.4% probability interval. Grey diamonds represent dated tephra layers from nearby Mt. St. Helens (Yamaguchi, 1983; Mullineaux, 1996). Black line is the most likely age-depth model, a 4th order polynomial function [AGE = $-0.00020094 \times (\text{DEPTH})^4 + 0.02951 \times (\text{DEPTH})^3 - 1.33288 \times (\text{DEPTH})^2 - 8.71619 \times (\text{DEPTH}) + 2000.22$; $r^2 = 0.9977$].

RESULTS

Stomatal frequency record

TSDL and pore length measurements, calculated maximum stomatal conductance are summarized in Appendix A2. TSDL ranges between 159 and 266 stomata per millimeter needle length (Fig.5.3A). Stomatal frequency (TSDL) shows centennial scale variations along the depth of the core. Extremely low TSDL values occur over the last 200 years and between 300 and 700 AD.

Average pore length ranges from 24.8 to 31.2 :m (Fig. 5.3B). TSDL and pore length are overall negatively correlated ($PL = -0.0275 \times TSDL + 33.74$; $r^2 = 0.2375$).

The calculated maximum stomatal conductance (G_{max}) varied between 8.5 and 15.1 mm s^{-1} (Fig. 5.3C). The periods before 750 AD and after 1800 AD are characterized by low G_{max}.

CO_2 reconstruction

By using the relation between stomatal density per mm needle length and atmospheric CO_2 mixing ratios as quantified in a training set over the last century, stomatal frequency fluctuations of *T. heterophylla* needles from Jay Bath can be converted to CO_2 levels (Fig. 5.4). The calculated CO_2 record starts with values around 300 ppmv between 200 and 300 AD, but rises drastically up to 390 ppmv within 100 years. Over the next 300 years CO_2 levels decline again to values that strongly fluctuate around the average pre-industrial level of 280–290 ppmv. A centennial-scale CO_2 variability is punctuated by minima centred around 860, 1150, 1600, and 1800 AD, and maxima around 1000, 1300, and 1700 AD. After 1850 AD there is a sharp rise from 280 ppmv to a modern CO_2 value of 370 ppmv (see also Chapter 4).

Macrofossil record

Figure 5.5 shows the presence of needles of selected conifer species in the Jay Bath core since the deposition of the Mt. St Helens Y-ash layer at approximately 1400 yr BC. Accessory elements (not depicted) are *Chamaecyparis nootkatensis* and *Pinus monticola*. Relative frequencies are expressed as a percentages of the total needle sum (see Dunwiddie, 1986). An important change in the composition of needle assemblages takes place between 200 and 300 AD, when dominance of needles of *Abies amabilis* is rapidly taken over by needles of *Abies procera* and *Tsuga heterophylla*. There are no large fragments of charcoal in the investigated samples; coarse mineral grains occur in the 200–300 AD interval.

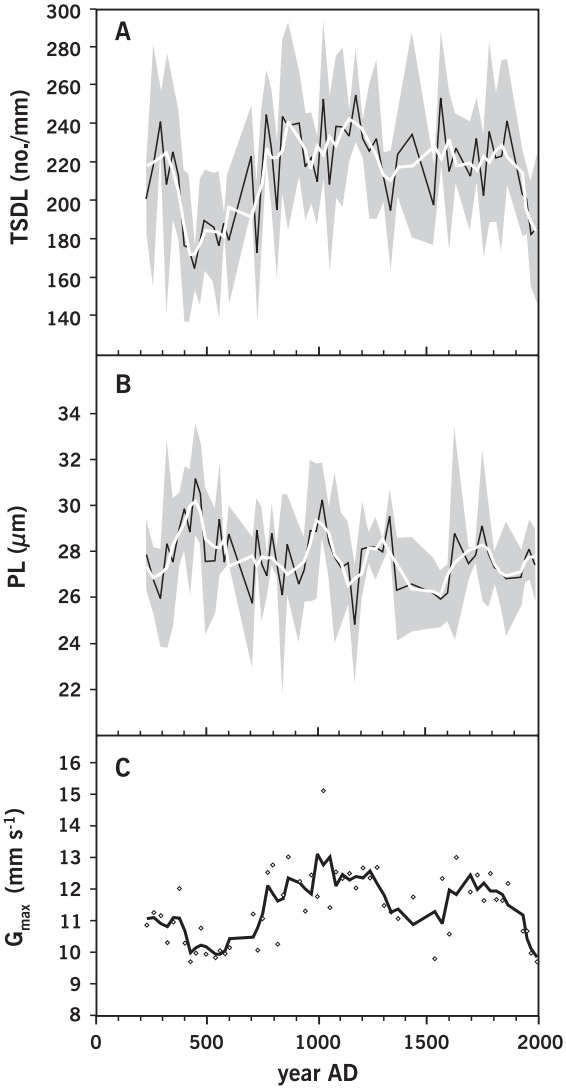

Figure 5.3: A: Stomatal density per mm needle length (TSDL, in n/mm) of *Tsuga heterophylla* needles from Jay Bath (Washington, USA). Black line represents mean values of 3–5 needles per depth interval. The grey band indicates ± 1 se. The white line represents a 3 point moving average. **B**: Pore length (PL in µm) of *Tsuga heterophylla* needles from Jay Bath (Washington, USA). Black line represents mean values of 3–5 needles per depth interval. The grey band indicates ± 1 se. The white line represents a 3 point moving average. **C**: Estimated maximum stomatal conductance (G_{max} in mm s^{-1}) based on TSDL and PL measurements of figure 5.2, using equation 1 ($G = 1/R$; $R = 1/nD\,(d/\pi ab + \ln(4ab/\pi a)$; a = PL (m); b was not directly measured, but calculated as $b = 0.109 \times a + 5.3184 \times 10^{-6}$ (measured in 50 stomata), D (m^2/s) is the diffusive coefficient of CO_2 in air (1.47×10^{-5} m^2s^{-1} at 20°C and 101.3 kPa), d (m) is the length of the diffusive pathway (not measured, but estimated as

0.1 mm) and *n* the stomatal density (n/m^2). Because in conifers stomata are not distributed uniformly on the leaf, TSDL is expressed per mm needle length. Needles of *Tsuga heterophylla* are ± 2 mm in width, so n (n/m^2) was calculated as TSDL (n/mm^{-1}) × 0.5 mm^{-1} (needles per mm) × 10^6. White diamonds are average conductance per depth (3–5 needles), black line is a 3 point moving average. Calculated G_{max} is in the same order of magnitude as measured G_{max} of *T. heterophylla* (1.08 mm s^{-1}; Korol, 2001). The deviation between estimated and measured values may be attributed to underestimation of *d* (length of the stomatal pathway), partial or patchy closure of stomata during the measurements, the additional resistance of the boundary layer, which was not included in the estimatations, and probably also the difference in altitude and environment between Jay Bath and the experimental forest sites in Montana and Idaho.

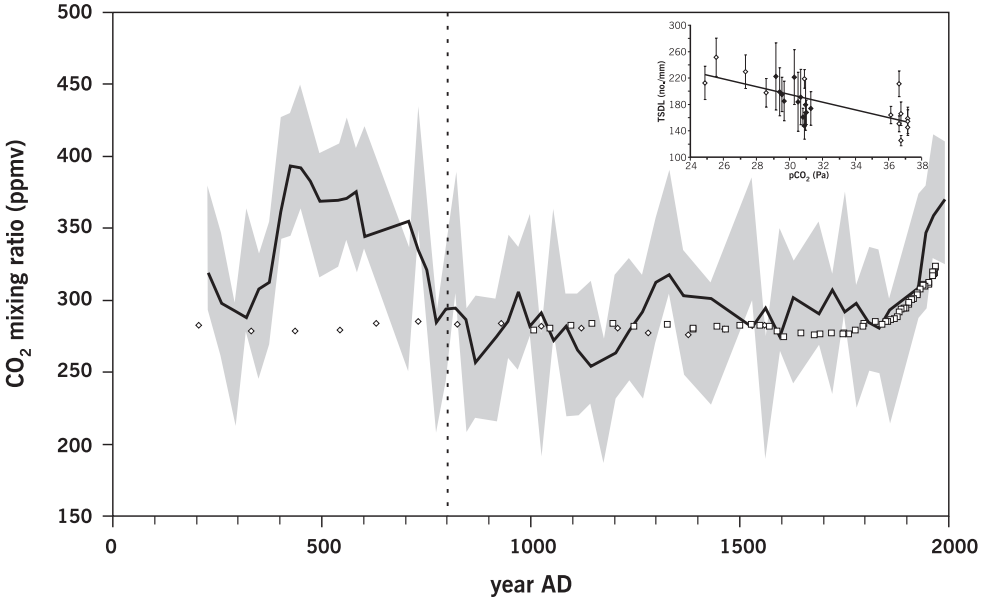

Figure 5.4: Reconstruction of paleo-atmospheric CO_2 levels when stomatal frequency of fossil needles is converted to CO_2 mixing ratios using the relation between CO_2 and TSDL as quantified in the training set. Black line represents a 3 point running average based on 3–5 needles per depth. Grey area indicates the RMSE in the calibration. White diamonds are data measured in the Taylor Dome ice core (Indermühle et al., 1999); white squares CO_2 measurements from the Law Dome ice-core (Etheridge et al., 1996). Inset: Training set of TSDL response of *Tsuga heterophylla* needles from the Pacific Northwest region to CO_2 changes over the past century (Chapter 4).

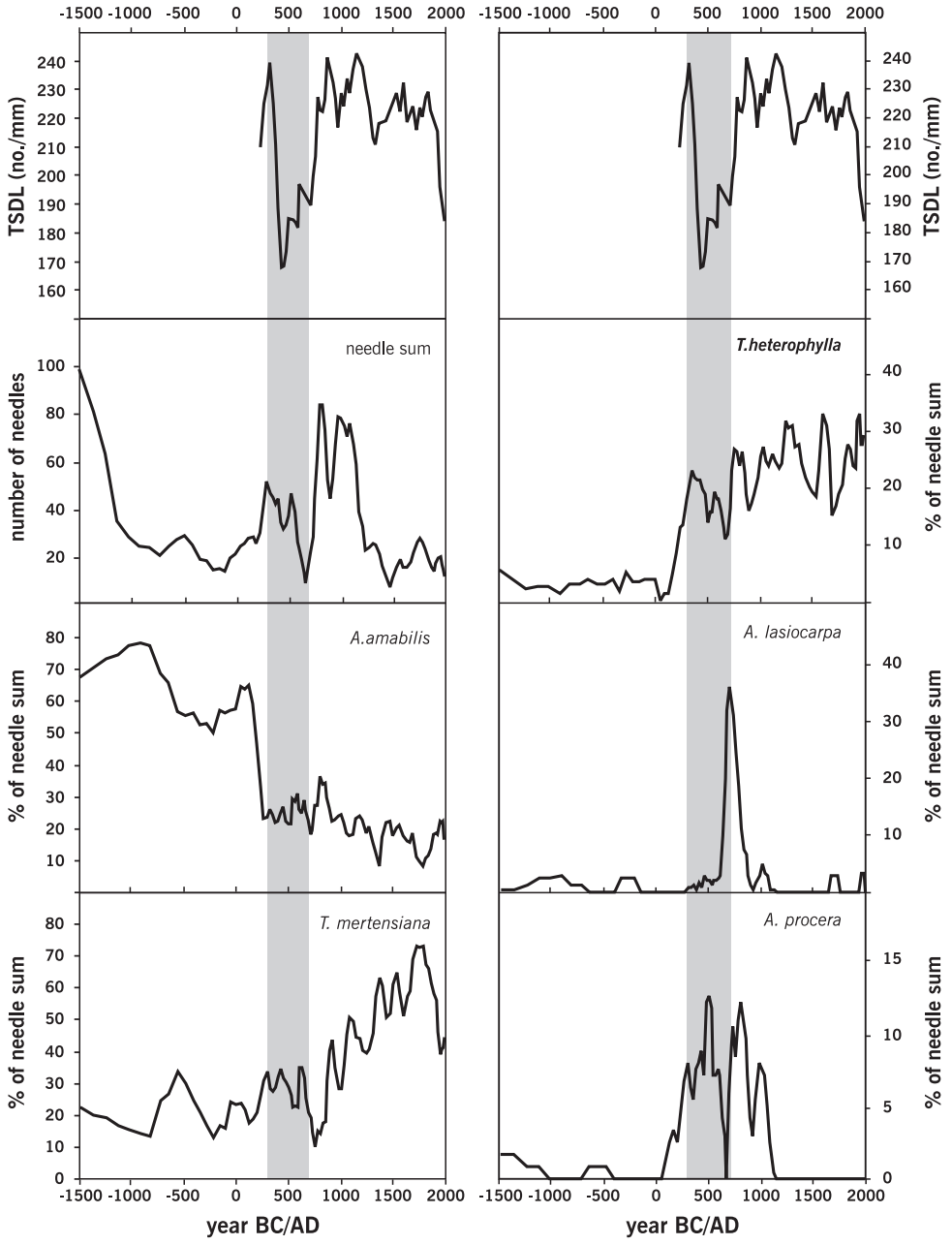
TSDL (no./mm)
number of needles
needle sum
T.heterophylla
% of needle sum
A.amabilis
A. lasiocarpa
T. mertensiana
A. procera
year BC/AD

DISCUSSION

The sharp rise in the stomata-based CO_2 curve after 1850 AD corresponds to the industrial CO_2 increase apparent in instrumental records (Keeling and Whorf, 2002) and shallow ice-cores (Neftel et al., 1985). This correspondence corroborates the reliability of the use of *T. heterophylla* needles in the reconstruction of past atmospheric CO_2 levels. The reconstructed fluctuations over the preceding 1200 years of the record could be linked to climate changes in this time period (Chapter 4) and have been reproduced for a significant part in a data set based on oak leaves from the Netherlands (Van Hoof, in prep.).

When going further back in time, due to extremely low stomatal frequency values in *T. heterophylla* needles, the reconstructed curve would suggest a major CO_2 excursion of about 100 ppmv between 300 and 750 AD. In the following paragraphs the reality of this excursion is discussed in relation to other CO_2 proxy records, documented global climate change, local CO_2 production, regional climate variation, and local stand dynamics.

CO_2 data from ice cores

Figure 5.4 shows the atmospheric CO_2 curve inferred from *T. heterophylla* needles plotted together with CO_2 data derived from the Antarctic Law Dome and Taylor Dome ice-cores (Etheridge et al., 1996; Indermühle et al., 1999a). Although centennial-scale CO_2 fluctations of the last millennium are not apparent in the ice-core data, a mean value of about 280 ppmv in the stomata-based reconstruction corresponds to the long-term pre-industrial record from Antarctic ice. The absence of centennial-scale fluctuations in the ice-core reconstructions may be explained by varying age distributions of the air in the bubbles related to the enclosure time in the firn-ice transition zone (Schwander, 1996; Spahni, et al., 2003) and/or post-depositional physicochemical reactions in the ice that may increase as well as decrease the CO_2 concentration in air bubbles (Anklin et al., 1995; Stauffer and Tschumi 2000).

In contrast to the last millennium, CO_2 reconstructions before 800 AD show a marked discrepancy between ice-core data and the needle-based record. Whereas ice cores continue to show CO_2 values of about 280 ppmv, stomata-based CO_2 levels seem to be consistently well above 300 ppmv during a period of 400 years. The magnitude of the CO_2 excursion (in-

Figure 5.5: Abundance of selected conifer species in the sediment core from Jay Bath. Values on y-axis are the percentage of needle equivalents of the selected species [entire needles, or combinations of top, midsection and base approximately equalling a needle in length (Dunwiddie 1986)] relative to the total needle sum . Three point running means are shown to facilitate comparison to the fossil needle record of Dunwiddie (1986), which was based on 2.5 cm slices of sediments. Because needles of C. *nootkatensis* and *P. monticola* break up in small fragments and are thus difficult to express in needle equivalents, these species were not included in the figure. Depicted at the top of both columns is the 3 point running average of the TSDL record. Grey area indicates the period of abnormally low stomatal numbers.

crease of 100 ppmv to a maximum level of almost 400 ppmv), as well as the exceptional high rate of the increase (about 10 ppmv / 10 years, which is twice the rate of the anthropogenic CO_2 increase during the past 200 years), question the authenticity of this CO_2 event.

Global temperature records

Reconstructed CO_2 fluctuations over the last 1200 years in the Jay Bath record correlate broadly with global temperature changes based on multi-proxy records (Mann and Jones, 2003), most remarkably in the timing of the warm periods and the CO_2 maxima around 1000 and 1300 AD (Fig. 5.6A; see also Chapter 4). Within uncertainty limits, changes in North Atlantic Ocean sea surface temperature as recorded offshore West Africa (DeMenocal et al., 2000) and North America (Cronin et al., 2003) are synchronous with CO_2 maxima and minima in the stomata-based record (Chapter 4). This also applies to terrestrial temperature trends on the Northern Hemisphere derived from tree-ring records (Briffa, 2000; Esper et al., 2002; Chapter 4). These correlations suggest that CO_2 fluctuations over the last millennium at least partly originated from temperature-driven changes in CO_2 flux between ocean surface waters and atmosphere (Chapter 4).

A prolonged period with elevated CO_2 levels between 300 and 750 AD, on the other hand, would not match reconstructed temperature trends. Although there is some evidence for relatively high Southern Hemisphere temperatures between 500 and 750 AD (Mann and Jones, 2003), the global record shows no indication of pronounced warming during this period (Fig. 5.6A).

Since the reconstructed enhanced CO_2 levels between 300 and 750 AD are incongruent with global climate changes, the extremely low stomatal frequency of *T. heterophylla* in this period is unlikely to reflect pronounced changes in the global atmospheric CO_2 regime.

Local volcanic CO_2 production

Because Mount Rainier is a currently active volcano, volcanically produced CO_2 could potentially be responsible for enhanced CO_2 levels in the Jay Bath area. It is known in other parts of the world, that plants can be exposed to natural elevated CO_2 concentrations, due to their proximity to CO_2-emitting springs and vents. Such sites contain local communities that may have persisted for generations at extreme CO_2 levels (reported values as high as 35,000 ppmv). However, stomatal frequency responses are not always apparent (Miglietta and Raschi, 1993; Tognetti et al., 2000). As a result of the non-linear nature of the relation between stomatal frequency and atmospheric CO_2 many species may already have reached their response limit at present-day CO_2 levels, so that further CO_2 increase cannot be detected on the basis of stomatal frequency analysis (Kürschner et al., 1997). On the other hand, there are also species in which excessive CO_2 has causes significant reduction of the stomatal frequency (Fernandez et al., 1998); Tognetti et al., 2000).

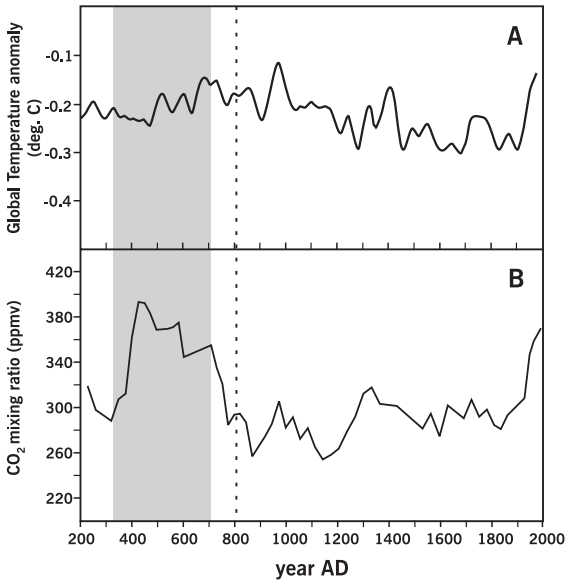

Figure 5.6: A: Global mean temperature anomaly from multi-proxy records based on 1961–1990 reference period (Mann and Jones, 2003) **B**: Reconstruction of paleo-atmospheric CO_2 levels based on stomatal frequency analysis of fossil *Tsuga heterophylla* needles. Black line represents a 3 point running average based on 3–5 needles per depth.

The question whether or not stomatal frequency data from Jay Bath could have been influenced by by local CO_2 emissions is discussed in Chapter 6 on the basis of carbon-isotope data from the studied sediment core. Over the past two millennia, there are no signals of excess volcanogenic CO_2 in the $\delta^{13}C$ record of organic matter. Moreover, no indication of a volcanic imprint on the ^{14}C measurements was found, while incorporation of significant amounts of volcanogenic CO_2 during photosynthesis would have caused an artificial aging in the order of at least a thousand years. Thus, interpretations of the stomatal frequency record from Jay Bath are not compromised by effects of Mount Rainier volcanic activity.

Regional climate variation

The expansion of *T. heterophylla* on Mount Rainier might have been associated with an increase in summer temperatures and/or a longer growing season. However, conifer taxa like *T. mertensiana*, adapted to colder/drier conditions, do not show a concurrent decline (Dunwiddie, 1986). The measured increase in temperature of 1 ºC during the first half of the last century did not affect stomatal numbers of *T. heterophylla* (Chapter 2).

Also pollen records from Mount Rainier do not show any significant vegetation changes that may reflect drastic changes in temperature or precipitation regimes during the last two millennia (Dunwiddie, 1986). It is unlikely, therefore, that low stomatal frequency of *T. heterophylla* between 300 and 750 AD could be the result of regional climate variation. Moreover, it should be noted that in experimental studies stomatal indices were not influenced by temperature (Reddy et al., 1998), or only after extreme increase that could not occur in nature (Wagner, 1998).

Local Stand Dynamics

Ecology of conifers on Mount Rainier

Jay Bath is located in the upper range of the *Abies amabilis* vegetation zone (Dunwiddie, 1986). In this zone, ranging from 900-1600 m altitude at Mount Rainier, late-successional forests are currently dominated by *A. amabilis* and *Tsuga mertensiana* as shade-tolerant competitors (Franklin and Dyrness, 1973). *Tsuga heterophylla* is very shade-tolerant as well and generally regarded as a late-successional element. However, the species also grows fast in full overhead light and can thus be present in both early and late successional stages (Fischer and Bradley, 1987; Packee, 1990).

Abies lasiocarpa is prominent in late-successional stages together with *T. mertensiana* in the *T. mertensiana* vegetation zone at higher elevations, because it is very tolerant of harsh conditions with short growing seasons, summer frost and heavy snowpacks at higher elevations. In lower elevation settings in the Cascade Range, such as Jay Bath, *A. lasiocarpa* can chiefly be found as a shade-intolerant species in early successions, invading disturbed sites (Franklin and Mitchell, 1967; Franklin and Dyrness, 1973). In temperate, high moisture conifer forests, *Abies procera* is dominant in early conifer successions, as it is unable to grow under closed canopies (Franklin and Dyrness, 1973; Stewart, 1986).

Late Holocene vegetation at Jay Bath

In contrast to pollen records that reveal regional vegetation history, macrofossil records reflect changes in the local vegetation around the pond. The relative abundance of needles of the different species in the sediment provides a reliable estimate of their respective basal area at the locality (Dunwiddie, 1987).

Vegetation development at Jay Bath since 4000 BC based on pollen and needle records has previously been described by Dunwiddie (1986). In the period after the deposition of the basal lahar (volcanic mudflow), an early successional vegetation consisting of *Pinus* spp., *Pseudotsuga menziesii*, *Abies lasiocarpa*, and *A. procera* occupied the newly formed landscape. *Abies amabilis* gradually became more prominent, but the continued presence of these disturbance-tolerant species, typical of early successions, suggest that the vegetation at the stand was subjected to frequent fires under a warmer and/or more arid climatic regime, as supported by regular charcoal finds.

The macrofossil record in the present study (Fig 5.5), starting immediately after deposition of the Y-tephra at approximately 1400 BC, is in very good agreement with Dunwiddie's (1986) results, but has a higher resolution and enhanced chronological accuracy. After the Y-tephra deposition, the needle record reflects the presence of a late-successional forest dominated by *A. amabilis* and *T. mertensiana* and without any disturbance-tolerant species. Before 200 AD *T. heterophylla* is sparsely present. But following a significant decline of *A. amabilis*, the element becomes prominent at the site. The concomitant expansion of *Abies procera* and, subsequently, *A. lasiocarpa* in the record between 300 and 1000 AD indicates forest succession after a major disturbance. Consequently, the initial expansion of *T.*

heterophylla can be related to its pioneering abilities in an open, early-successional habitat (Packee, 1990). After this period, the lack of disturbance-related tree species reflects highly stable late-successional habitats over the last 1300 years up to the present-day forest of *T. mertensiana, T. heterophylla, A. amabilis, and Chamaecyparis nootkatensis* (the latter species is not included in the macrofossil diagram).

Timing and nature of the disturbance

Disturbance, reflected by the decline of *A. amabilis* and the proliferation of *A. procera*, becomes apparent between 200 and 300 AD. Establishment of *A. procera* requires major stand openings. The trees generally live for 400–600 years, occasionally persisting under closed canopies, where they are unable to regenerate (Franklin and Dyrness, 1973). An open stand structure probably prevailed at Jay Bath until 600-700 AD. *A. lasiocarpa* reaches its peak between 600 and 800 AD. These trees are much slower growing and probably did not reach sufficient height to contribute significantly to the needle record until they had reached an age of about 100 years (Alexander et al., 1984), which suggests that the species established at the site around 500 AD. Because *A. lasiocarpa* trees usually die before they are 250–400 years old (Alexander, 1987), no more seedlings germinated after around 700 AD.

A. lasiocarpa is very tolerant of short growing seasons, frosts and heavy snowpack, and seeds need overwintering in or under snow to germinate. The inability of *A. lasiocarpa* seedlings to survive after 700 AD could be related to amelioration of harsh, exposed local conditions by forest closure at the stand, enabling *T. heterophylla*, *T. mertensiana,* and *A. amabilis* to outcompete *A. lasiocarpa*. The timing of reconstructed presence of *A. procera* and *A. lasiocarpa* at Jay Bath indicate that open conditions prevailed at Jay Bath after the disturbance at around 300 AD, and that a closed forest stand was not re-established until 700 AD. Open conditions at the site are confirmed by the presence of coarse-grained mineral material in the sediment at the time of initial vegetation change.

Various types of disturbances may affect forest composition on Mount Rainier. Large catastrophic fire is the main large-scale disturbance factor. In general, fires occur once every 400–500 years (Hemstrom and Franklin, 1982). Included in estimates of the fire regime are fires set by Indians. Indian tribes inhabited the surrounding area for the last 10,000 years, using fire to concentrate game, increase berry harvest and improve hunting visibility and grazing. Such fires could have reached Mount Rainier, but there is some doubt whether man-made fire was important in the western Cascades (Hemstrom and Franklin, 1982). European settlers did not arrive until the 19th century.

No large charcoal fragments evidencing local fires have been found in the sediment record after the Y-ash. Absence of fire may be due to the cooler and moister climate compared to that of the pre-Y ash period (Dunwiddie, 1986). Other important forest disturbances that could have affected local stand structure, include avalanches, lahar flows, windthrow and

pathogens such as insects or woodrot (Hemstrom and Franklin, 1982). Core data from Jay Bath exclude avalanches or lahars. Because of the apparently selective dieback of *Abies amabilis*, pathogens could be a realistic option.

Effect of post-disturbance conditions on stomatal numbers of T. heterophylla
Although the exact nature of the disturbance can not be established, the local vegetation record clearly shows that *T. heterophylla* initially became prominent in an early-successional open habitat. The period of renewed forest establishment coincides with lower stomatal numbers on fossil *T. heterophylla* needles (indicated by the grey area in Fig 5.5). As soon as a stable, late-successional forest stand was present again, stomatal numbers reach their average values over the past 1200 years. It may therefore be hypothesized that the lower stomatal numbers were a response to growth in open, exposed conditions instead of a sheltered closed forest.

In the central Rocky Mountains (Hultine and Marshall, 2000; Schoettle and Rochelle, 2000), and the Qilian Mountains in China (Qiang et al., 2003) it was demonstrated that the stomatal frequency of *Pinus flexilis*, *P. contorta*, *Abies lasiocarpa* and *Picea crassifolia* is influenced by suboptimal growth conditions. Stomatal frequency decreases towards the upper elevational limits of the species. In *P. crassifolia* the decrease, concerning both stomatal density and number of stomatal rows, follows an expected increase that corresponds to decreasing CO_2 partial pressure (Qiang et al., 2003). The observed decrease has been related to adverse growing conditions that characterize high altitudes, more particularly to water stress (Schoettle and Rochelle, 2000).

Open habitats have a much more extreme growing environment than closed forest stands, with higher temperature gradients, lower soil temperatures, a more severe frost regime, lower humidity and no shelter from high (UV)-irradiance (Tucker et al., 1987; Man and Lieffers, 1999). Although influence of factors such as UV-stress and wind stress can not be ruled out, water stress related to prolonged chilling of root systems seems to be the most prominent environmental stress factor that could explain low stomatal frequency and low stomatal conductance of *T. heterophylla*, when growing in open montane habitats. Boreal and montane conifers are particularly sensitive to adverse effects of low (< 8ºC) soil temperature on tree water uptake. Growth-chamber and field experiments with *Picea engelmannii* (De Lucia, 1986) and *Pinus sylvestris* (Mellander, 2003; Strand et al., 2002) indicate that root chilling will reduce water uptake and net photosynthesis in the critical transition of winter dormancy to the growing season. Prolonged exposure of roots to soil temperatures between 0ºC and 1ºC strongly reduces stomatal conductance.

In the Mount Rainier region, low soil temperature in the early growing season is probably the main limitation for conifer growth in open early-successional habitats habitats. Mount Rainier is known for heavy snowfall (Graumlich and Brubaker; 1986). In an open vegetation on the southern flank of the mountain, snowpack cover is anticipated to continue into the active growth phase of plants. In order to successfully compete in such habitats, trees

should be equipped with a plastic phenotype capable of adjusting stomatal numbers to prevent excess water loss during the spring. The fact that *T. heterophylla* is competitive in both early- and late-succesional habitats is consistent with the wide physiological plasticity of the species.

CONCLUSIONS

The extremely low number of stomata per mm needle length in the *Tsuga heterophylla* record at Jay Bath between 300 and 700 AD does not appear to result from extremely high atmospheric CO_2 levels at the time, but coincides with the establishment of the species during a period of major disturbance at the site. The open, exposed setting after this disturbance probably provided highly stressed growth conditions for pioneering, early-successional *T. heterophylla* trees. Spring water-stress related to low soil temperature, would be the most plausible explanation for an acclimational stomatal frequency response to reduced water uptake.

Thus, environmental stress factors associated with early-successional montane habitats show the potential to obscure stomatal frequency changes in response to atmospheric CO_2. This complication should be taken into account when selecting leaf material from high-elevation sites for stomatal frequency analysis. It is essential to concomitantly analyze the local successional forest developments that correspond to a montane leaf record. For the Jay Bath record, the late-successional closed forest, prevalent at the site from 800 AD until present, indicates that stomatal numbers of *Tsuga heterophylla* over the past 1200 years are not affected by these extreme growth conditions, and can be relied upon to reflect atmospheric CO_2 changes.

CHAPTER 6

TESTING FOR VOLCANIC SIGNATURES IN THE CARBON ISOTOPE COMPOSITION OF LATE HOLOCENE *TSUGA HETEROPHYLLA* NEEDLES FROM MOUNT RAINIER (WASHINGTON, USA)

Stomatal frequency data from fossil needles of *Tsuga heterophylla* from Jay Bath, a shallow pond on the southern flank of Mount Rainier (Washington, USA) have recently been interpreted in terms of atmospheric CO_2 levels. The volcanic activity of Mount Rainier warrants testing for the influence of volcanic CO_2 production on local CO_2 concentrations at this locality. Because Jay Bath is not located in the proximity of the crater or current geothermally active areas, the site has not likely experienced significant excess CO_2 from these sources. Magmatic CO_2 contains no ^{14}C and has (on Mount Rainier) a heavier isotope composition than bulk atmospheric CO_2. Consequently, plant organic matter that is formed under volcanic influence should reveal a ^{12}C and ^{14}C depleted carbon isotope composition. Carbon isotopic analysis on needles of *Tsuga heterophylla* over the past two millennia show no indication for the presence of magmatic CO_2 through local soil outgassing or any other source. Thus, the reliability of the stomatal frequency record from Jay Bath is not compromised by local volcanic activity.

INTRODUCTION

For an ever-increasing number of tree species there is observational and experimental evidence of an inverse relation between numbers of leaf stomata and atmospheric CO_2 concentration. As a corollary, stomatal frequency analysis of fossil tree leaves is now successfully used for detecting and quantifying short-term fluctuations in Holocene CO_2 levels that are not evident in the CO_2 record from Antarctic ice cores (Etheridge et al., 1996; Indermühle et al., 1999a). In paleo-atmospheric studies, the CO_2 responsiveness of leaves of individual tree species is generally calibrated against the Mauna Loa record of mean global CO_2 increase (Keeling and Whorf, 2002). It is essential, however, to realize to what extent local ambient CO_2 levels mirror global atmospheric CO_2 mixing ratios.

Small scale variability in CO_2, up to approximately 10 ppmv, is always present between sites from contrasting geographical areas, because of the interhemispherical and seasonal gradients in atmospheric CO_2 levels. Additionally, photosynthesis and respiration of the local vegetation causes variation in ambient CO_2 at different canopy levels. These differences also amount to only a few ppmv above the understory level (Chapter 5; Royer, 2001).

A much larger enhancement of local ambient CO_2 levels occurs in regions of volcanic and geothermal activity. Volcanic CO_2 emissions are much more concentrated in CO_2 than the atmosphere (from a few percent up to over 90% by volume, as compared to 0.0036 % in air), and thus can locally increase the CO_2 content of ambient air significantly. Consequently, reconstructed CO_2 levels from a geothermally active area could be of local volcanic origin rather than of a global atmospheric signature. Thermal activity could also perhaps enhance the amount of soil-derived CO_2 present at the site. Therefore, local CO_2 production should be considered as a complicating factor in attempts at global atmospheric CO_2 reconstruction on the basis of fossil leaves from sites in geothermally active regions.

In various parts of the world, trees living in the proximity of CO_2-emitting lakes, springs and vents have been studied for stomatal frequency responses to extreme CO_2 levels (reported values are as high as 35,000 ppmv). Results are varied, but in some species excessive CO_2 causes significant reduction of the stomatal frequency (Fernandez et al, 1998; Tognetti et al., 2000). When studying fossil leaves from sites in volcanic or geothermal areas, therefore, it should be decided whether or not stomatal frequency data could have been influenced by by local CO_2 emissions.

Recently, a 2000-year needle record of the conifer *Tsuga heterophylla* was recovered from sediments of Jay Bath, a shallow pond on the southern flank of Mount Rainier, one of the recently active volcanoes of the Cascade Range in Washington, USA (Fig. 6.1). *Tsuga heterophylla* demonstrates a good response to CO_2 (Chapter 2), and stomatal frequency data covering the last two millennia have been interpreted in terms of changing CO_2 regimes (Chapter 4; Chapter 5). However, extremely low stomatal numbers between 300 and 750 AD need special attention, because these would translate to CO_2 levels up to 400 ppmv. It is

unlikely that such values would correspond to global CO_2 levels of that time interval. The possibility of local CO_2 production by the geothermal system of Mount Rainier should be taken into consideration.

In volcanic areas, a contribution of magma-derived CO_2 to photosynthesis affects the carbon isotopic signature of the plant material. Volcanic CO_2 contains no ^{14}C, affecting the $^{14}C/^{12}C$ ratio in plants growing near fumaroles (Sulerzhitzky, 1970; Bruns et al., 1980; Saupé et al., 1980; Rubin et al., 1987) or in areas of diffuse soil degassing (Pasquier-Cardin, 1999). Furthermore, magmatic CO_2 also deviates in ^{13}C content from atmospheric CO_2, which can be detected in plant material influenced by sufficient volcanic outgassing (Pasquier-Cardin, 1999). This demonstrated influence of volcanic CO_2 on carbon isotope signature of present vegetation may be applied to test for past occurrences of magma-derived CO_2 outgassing.

To assess the potential influence of geothermal activity on past CO_2 levels at Jay Bath, the amount and spatial distribution of CO_2 emissions from summits and geothermal areas of Mount Rainier and comparable volcanoes are reviewed. Results of carbon isotope measurements on fossil *T. heterophylla* needles are discussed in order to determine whether or not significant amounts of volcanogenic CO_2 could have influenced the stomatal frequency data from Jay Bath.

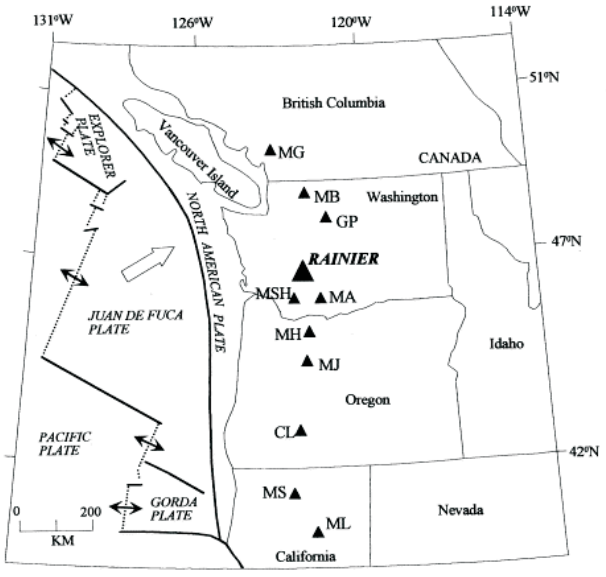

Figure 6.1: Volcanoes of the Cascade Range in the Northwest Pacific area of the USA and Canada. MB = Mount Baker, RAINIER = Mount Rainier, MSH = Mount Saint Helens and ML = Mount Lassen.

GEOTHERMAL SETTING

Mount Rainier is the highest of the Cascade volcanoes (4392 m), the third most voluminous (Sherrod and Smith, 1990) and the second most seismically active (Moran et al., 1995). Tephra deposits in the area provide evidence of irregular eruptive episodes during the Holocene (Mullineaux, 1974), most prominently between 6500 and 4000 years BP and between 2700 and 2200 years BP. The most recent eruptive activity occurred between 1820 and 1850 AD, and Mount Rainier is expected to erupt again in the next few centuries (Foxworthy and Hill, 1982).

Volcanic CO_2 at Mount Rainier could be emitted by different sources: plumes from the summit (during active as well as quiescent periods), fumaroles in the summit or on the flanks, or diffuse soil degassing. Few measurements of actual CO_2 outgassing at Mount Rainier have been carried out, only at fumaroles near the summit (Zimbelman et al., 2000). Therefore, estimations on the extent of CO_2 outgassing in plumes and on the flanks of Mount Rainier will be supplemented by reviewing information on CO_2 degassing at other volcanoes.

Summit outgassing

Quiescent outgassing from the summits of Hawaiian volcanoes Mauna Loa and Kilauea has been measured extensively. The plume degassing from the summit contained enhanced CO_2 values in an area of several km downslope, ranging from 1-5 ppmv right after an eruption to 0.1 - 0.6 ppmv in quieter periods (Ryan, 1995; Gerlach and McGee, 1998).

However, the Cascade volcanoes are andesitic volcanoes, which produce more CO_2 than the basaltic Hawaiian volcanoes. The crater plume of Mt. Etna, for example, is characterized by a maximum excess CO_2 concentration of about 10 ppmv, rapidly diminishing within 3 km of the summit (Allard et al., 1991). During the 1980 eruptive period of Mt. St. Helens, the closest neighbour of Mt. Rainier, the plume within the crater contained 400-1300 ppmv CO_2 (Casadevall, 1981; Evans, 1981; Harris et al., 1981); but airborne detection in the plume showed CO_2 excess of 15 ppmv right above the summit, decreasing to 5 ppmv at 1 km distance, and all volcanic CO_2 had been diluted further than 2 km away (Harris et al., 1981). Another Cascade volcano, Mt. Baker, produced no more than 2 ppmv excess CO_2 in its 4 km wide plume during a non-active period (McGee et al., 2001). These data imply that significant volcanic CO_2 concentrations in plumes only occur very close to the summit (Symonds et al., 1994), and that Jay Bath, at a distance of 9 km downslope (Fig. 6.2), probably never experienced elevated CO_2 levels due to outgassing of Mount Rainier's summit.

Fumaroles and geothermal areas

Gas from fumaroles in the crater of Mt. St. Helens contained CO_2 concentrations of 800-1200 ppmv in cooler samples and 100.000 to 500.000 ppmv in hot samples (828ºC), and fumaroles in the summit ice-caves of Mt. Rainier produced on average 4000 ppmv CO_2 (Zimbelman, 2000). The CO_2 from fumaroles is usually rapidly diluted by air declining to a

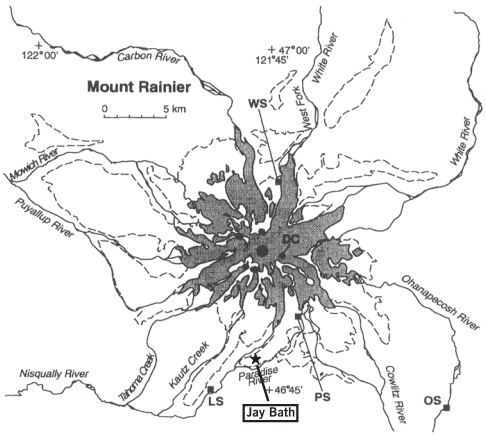

Figure 6.2: Map of localities of geothermal activity at Mount Rainier. A large fumarole field occurs at the top of the young summit cone (large dot), fumaroles and heated ground at Disappointment Cleaver (DC) and areas on the upper flank (small dots). Thermal springs (squares) occur on the lower flank of the volcano near Paradise (PS) and Winthrop (WS) Glaciers and beyond the volcanic edifice at Longmire (LS) and Ohanapekosh (OS). Dashed area = present extent of Mount Rainier lava flows; shaded area = glacier cover. Location of Jay Bath is indicated with an asterisk. (Frank, 1995).

few ppmv above background within a few hundred metres from the source vent (Francis et al., 2000). Presently, the only fumaroles on Mt. Rainier are located at the summit and the upper flanks, 2000 m above Jay Bath (Fig. 6.2; Frank, 1995).

Active geothermal manifestations at a lower altitude consist of thermal springs enriched in sulfate and carbon dioxide (Fig. 6.2). The springs at Longmire meadow were reported to have produced much excess CO_2 in 2001. Volcanic CO_2 emanating from lakes in Germany and vents in Italy, exhibiting substantially elevated CO_2 levels at the site, cannot be detected anymore at distances greater than 50-150 m away from the source (Bruns et al., 1980; Miglietta and Raschi, 1993; Tognetti et al., 2000).

As Jay Bath is located four km to the northeast and 500 m uphill from Longmire, the influence of the present fumaroles and geothermal areas on CO_2 concentrations at Jay Bath seems highly limited. However, it may perhaps not be ruled out that in the past a geothermal area very close to Jay Bath existed.

Diffuse soil outgassing

Even when no visible geothermal manifestations such as plumes are present, volcanoes can emit CO_2 through the soil. At the Italian volcanoes Mt. Etna and Volcano Island as much CO_2 emanates from the soil as in the plume, locally enhancing atmospheric CO_2 by up to 10 ppmv (Baubron et al, 1990; Allard et al., 1991). At the Furnas Volcanic Centre on the Azores soil carbon dioxide pulses of 100-60.000 ppmv on the time scale of hours to days raised ambient CO_2 levels permanently (Oskarsson et al.,1999; Pasquier-Cardin et al., 1999). Diffuse CO_2 soil degassing at Mammoth Mountain (California) caused massive tree kills and

hazardously high CO_2 concentrations (1-89%) in confined spaces such as tents and cabins (Farrar et al., 1995). However, the CO_2 was rapidly diluted, the peak CO_2 excess that could be measured airborne was 5 ppmv, with a larger plume of 1-3 ppmv (Gerlach et al., 1999).

Like the other CO_2 emission sources, diffuse soil degassing only seems to significantly influence CO_2 levels outside of the immediate vicinity by a few ppmv. At present, no areas of soil degassing on Mount Rainier are known. Although no evidence for recent soil degassing at Jay Bath, such as tree kills, has surfaced, past occurrence of this phenomenon at Jay Bath remains a possibilty.

Overall, volcanic CO_2 emissions appear to have a restricted area of influence. Since Jay Bath is located 9 km from the summit and 4 km from the nearest region of geothermal activity, it is unlikely that currently volcanic emission raises the CO_2 level more than a few ppmv. This value is lower than the natural CO_2 variation within a forest (Tarnawski et al., 1994; Royer, 2001) and lies well within the confidence limits of the reconstructive accuracy of the stomatal frequency analysis. However, it cannot be ruled out that in the past geothermal activity or diffuse soil degassing have occurred at Jay Bath. To ascertain whether these phenomena were indeed present, carbon isotopic ratios of fossil needles were checked for a magmatic CO_2 signature.

MATERIAL AND METHODS

A 91 cm sediment core containing an assemblage of fossil needles of *Tsuga heterophylla* was obtained from Jay Bath, a shallow (about 1.20 m water depth) pond on the southern flank of Mount Rainier (Washington, USA; 46º46' N 121º46' W; Fig. 6.1). Sediment samples were sieved on a 250μm mesh sieve whereafter the encountered macrofossils were identified (conifer needles were identified to the species level [Dunwiddie, 1985], seeds to the genus level) and stored in ethanol.

Plant material from selected depths was subjected to AMS ^{14}C dating and ^{13}C analysis following standard procedures at the Van der Graaff Institute, Utrecht, The Netherlands. ^{14}C activities are reported as radiocarbon ages BP, normalized to a ^{13}C value of −25 ‰. Radiocarbon ages were then converted to calendar ages using OxCal 3.8 [Bronk-Ramsey, 1995] and INTCAL98 calibration data [Stuiver et al., 1998].

For additional ^{13}C analysis of cuticles and mesophyll, *T. heterophylla* needles were thoroughly rinsed, cuticle and mesophyll were separated and then oven dried for 10 hours at 120ºC. Depending on the amount of cuticle material available, measurements were made on 5 needles per depth separately or material from several needles was combined. The mesophyll measured consists of combined material from five needles per depth. Analyses were per-

formed on a Fisons NA1500NCS Elemental Analyser coupled with a ThermoFinnigan Delta plus isotope ratio mass spectrometer. Plant ^{13}C values are expressed in per mil relative to the PDB standard with an accuracy of 0.1 ‰.

Isotopical ^{13}C fractionation was calculated from $\delta^{13}C$ values according to Farquhar et al.(1989):

$$\Delta = (\delta^{13}C_{CO2} - \delta^{13}C_{plant})/(1 - \delta^{13}C_{plant}) \quad \text{Eqn. } \mathbf{1}$$

Where $\delta^{13}C_{plant}$ are the measured ^{13}C values of the plant material and $\delta^{13}C_{CO2}$ is the ^{13}C value of the photosynthesized CO_2.

Student's t-tests and regression analysis was performed using SPSS 10.0 for Windows statistical software (Chicago, Illinois, USA).

RESULTS

The results of the ^{14}C and ^{13}C activity measurements on the plant material are presented in table 6.1.$\delta^{13}C$ measurements of the plant material range from −25.1 to −28.0 ‰. $\delta^{13}C$ values of seed and wood samples were less depleted than those of leaves, but not significantly (−26.1‰ vs −26.6‰; $P = 0.213$). Mesophyll of *Tsuga heterophylla* was significantly more depleted than cuticles of the same samples (−27.0‰ vs −25.7‰; $P = 0.041$).

DISCUSSION

$\delta^{13}C$ evidence for incorporation of volcanic CO_2

All $\delta^{13}C$ measurements made on plant material from the Jay Bath core are plotted in figure 6.3. Because stomatal numbers on *Tsuga heterophylla* needles are sensitive to changes in atmospheric CO_2 concentration, local volcanic CO_2 production should show up in a CO_2 reconstruction based on the inverse relation between stomatal density per mm needle length (TSDL) and CO_2 concentrations over the last century (Chapter 2; Chapter 5). High local CO_2 levels accompanied by deviating isotopic signatures would imply that past volcanic CO_2 production was of influence at Jay Bath. The CO_2 minima and maxima over the last 1200 years correlate with temperature changes in Northern hemisphere oceanic and terrestrial climate records (Chapter 5) and have partly been reproduced in independent CO_2 reconstructions from a European site (Chapter 7). These CO_2 fluctuations are therefore considered to reflect global atmospheric CO_2 mixing ratios. Local volcanic CO_2 production would, however, especially be of interest to explain the very low stomatal numbers before 800 AD. At first sight, no correlation between reconstructed local CO_2 and $\delta^{13}C$ seems present. Nonetheless, variability in $\delta^{13}C$ values is very high, and to obtain a clearer picture sources of this variation will be discussed first.

depth (cm)	fraction analysed	age (^{14}C yrs BP)	δ^{13}C [‰]	Δ [‰][a]
0	cuticle Tsuga heterophylla	–	−27.4 ± 0.52	19.0
11	needles Tsuga mertensiana	409 ± 29	−25.9	18.9
17	needles Tsuga mertensiana	548 ± 41	−26.9	19.9
26	needles Tsuga mertensiana	664 ± 38	−26.3	19.3
31	needles Tsuga mertensiana	997 ± 32	−27.0	20.0
37	needles Tsuga mertensiana	1085 ± 42	−27.0	20.0
45	4 seeds of Abies amabilis	1263 ± 38	−26.3	19.3
45	cuticle Tsuga heterophylla	–	−26.3 ± 1.01	19.3
45	mesophyll Tsuga heterophylla	–	−28.0	20.9
48	needles Abies procera	1202 ± 32	−27.4	20.3
55	twig	1604 ± 41	−25.1	18.1
56	cuticle Tsuga heterophylla	–	−25.1 ± 0.70	18.1
56	mesophyll Tsuga heterophylla	–	−26.0	19.0
59	needles Tsuga mertensiana	1560 ± 28	−27.9	20.8
60	needles Abies amabilis	1637 ± 35	−26.2	19.2
61	cuticle Tsuga heterophylla	–	−26.6	19.6
61	mesophyll Tsuga heterophylla	–	−27.2	20.2
64	1 seed of Abies amabilis	1698 ± 33	−26.8	19.8
66	cuticle Tsuga heterophylla	–	−25.2 ± 0.81	18.2
66	mesophyll Tsuga heterophylla	–	−26.7	19.7
68	cone fragments	1748 ± 43	−25.8	18.8

Table 6.1: Measurements of ^{14}C activity, δ^{13}C values and calculated fractionation of plant material from selected depths at Jay Bath. [a]$\Delta = (\delta^{13}C_{CO2} - \delta^{13}C_{plant})/(1 - \delta^{13}C_{plant})$ (Farquhar et al., 1989); $\delta^{13}C_{CO2} = -7.9$ ‰ recently and $\delta^{13}C_{CO2} = -6.5$ ‰ from 2000 to 100 BP (Francey et al., 1995; Indermühle et al., 1999a).

δ^{13}C measurements were first performed on the samples also used for ^{14}C analysis, consisting of needles and seeds from *Tsuga mertensiana*, *Abies amabilis* and *Abies procera*, supplemented by wood from unknown taxa (Table 6.1). However, δ^{13}C of C_3 species usually ranges between −25 and −29‰, up to extremes of −22‰ and −34‰ (Bender, 1971; Ehleringer

et al., 1993; Lambers et al., 1998) and fractionation differences occur between plants parts; in general leaves tend to have lighter isotopic composition (1-2‰ more depleted in ^{13}C) than stems, roots or wood (Craig, 1953; Park and Epstein, 1960; Lowdon, 1969; Smith and Epstein, 1970). Although originating from different species, seeds and wood samples in this study did have slightly less depleted $\delta^{13}C$ values than needles, but the difference was not signifi-

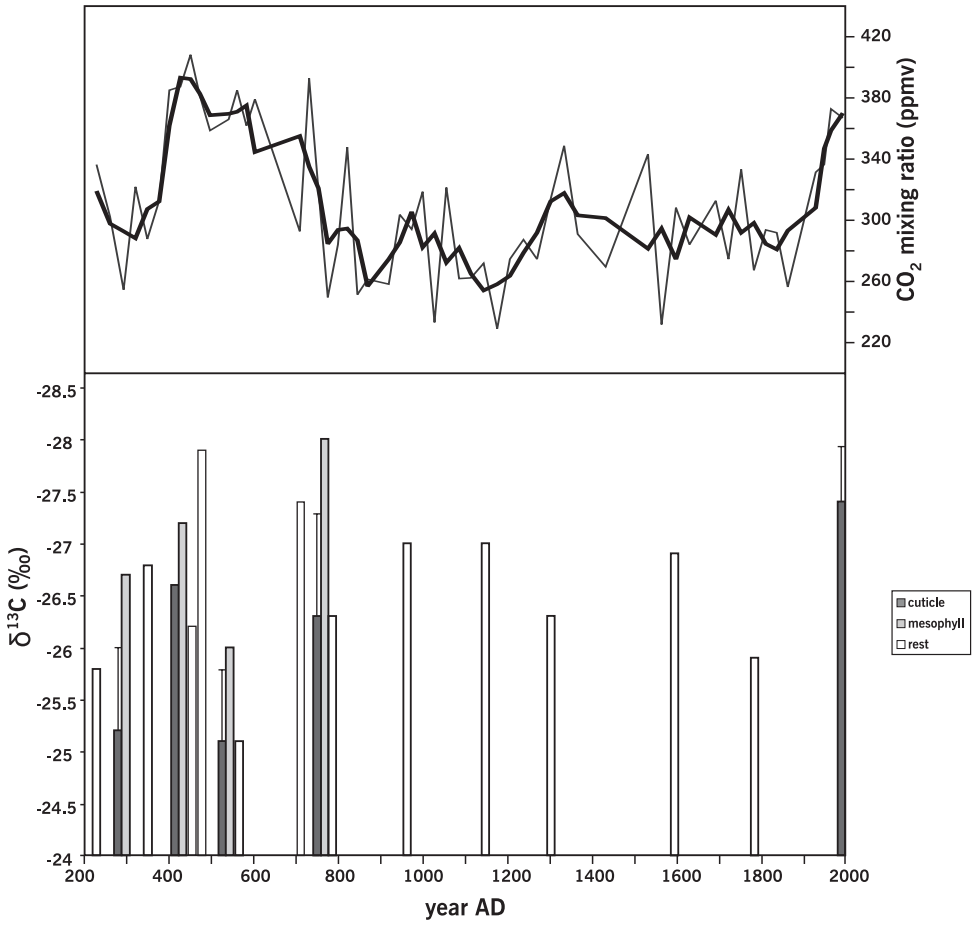

Figure 6.3: $\delta^{13}C$ values of plant material plotted against age (age model depicted in figure 6.4). Dark grey bars represent measurements on cuticles of *Tsuga heterophylla* needles (error bars indicate ± 1 SE) and light grey bars represent measurements on mesophyll from *Tsuga heterophylla* needles. White bars represent measurements on needles of *T. mertensiana*, *A. amabilis* and *A. procera*, and seeds and wood of *Tsuga* and *Abies*. For comparison, reconstructed CO_2 values based on stomatal frequency analysis of fossil *Tsuga heterophylla* needles are also included (Chapter 5). Thin black line represents means of 3–5 needles per depth, thick grey line a 3 point moving average.

cant (−26.1 ‰ vs −26.6 ‰ for needles; $P = 0.213$). To minimize concealment of a volcanic $\delta^{13}C$ signature, additional measurements were performed on *T. heterophylla* cuticles and mesophyll separately (grey bars in figure 6.3). Selective preservation differences between mesophyll and cuticular material might otherwise create an isotopical gradient with increasing depth in the $\delta^{13}C$ values of fossil needles. Indeed, the mesophyll in the needles is significantly more depleted in ^{12}C than the cuticles of the same samples (−27.0‰ vs −25.7 ‰; P= .041). This is consistent with the results of Wilmer and Firth (1980) that the epidermal tissue of leaves of several species was slightly more negative than the mesophyll. Observed differences in $\delta^{13}C$ values between samples are consistently present in the cuticle as well as in the mesophyll.

$\delta^{13}C$ in *T. heterophylla* cuticles changes with depth ($r^2 = 0.526$; $P = 0.001$), but only because modern samples are significantly more depleted than fossil needles. This can be explained by the difference in $\delta^{13}C$ signature between pre-industrial and current atmospheric CO_2 (−6.5‰ vs −7.9‰[Francey et al., 1995; Indermühle, 1999a]). When the C isotope discrimination [$\Delta = (\delta^{13}C_{CO2} - \delta^{13}C_{plant})/(1 - \delta^{13}C_{plant})$; Farquhar et al., 1989] is calculated, which is independent of the ^{13}C signature of the atmospheric CO_2, no significant change in fractionation between the recent and fossil samples is present (Table 6.1).

The carbon isotope signature of magmatic CO_2 varies, but is usually quite different from the current $\delta^{13}C$ value of atmospheric CO_2 (about −7.9‰). Most magmatically derived CO_2 is much heavier (more depleted in ^{13}C) in signature (Table 6.2), with a typical value of about −4.5‰, but the exact signature is dependent on the magma source. Mount Rainier, like the other Washington volcano Mt. St. Helens, deviates from the general picture with lighter $\delta^{13}C$ values (−11.1 to −12.4‰) in its magmatic CO_2 than those of other volcanoes. The low values probably reflect the influence of a subducted organic matter component to the deep carbon reservoir beneath Mount Rainier (Zimbelman et al., 2000).

The incorporation of substantial amounts of volcanic CO_2 during photosynthesis should theoretically be discernable in the carbon isotope signature of the plant material. Attempts to recognize a magmatic CO_2 signature in the $\delta^{13}C$ composition of plants have so far shown mixed results. At some localities where magmatic CO_2 was sufficiently less negative in $\delta^{13}C$ compared to air, plant material was less depleted in ^{13}C (Bruns, 1980; Rubin, 1987). However, plants in other volcanic areas did exhibit no obvious effect of volcanic carbon on the $\delta^{13}C$ measurements (Sulerzhitzky, 1970, Bruns et al., 1980, Saupé et al., 1980).

The lack of a clear volcanic $\delta^{13}C$ signal in these studies might very well be due to either too small a difference in $\delta^{13}C$ content between magmatic and ambient CO_2 or the inclusion of measurements on different plant species and plant parts in these data sets. The carbon isotopic measurements on plants in volcanic regions were usually carried out on few plants of different species and often on different parts of the plants (roots, leaves, etc.) resulting in probably too large a range of $\delta^{13}C$ values to be able to detect a volcanic carbon signal of a few per mil. In a region of magmatic CO_2 soil degassing on the Azores, $\delta^{13}C$ was measured

Location	Country	$\delta^{13}C$ (‰)
Monte Amiata[a]	Italy	8.6 (mean for Italy −4.5)
Thera hot source[b]	Greece	0
Yellowstone[c]	Midwest USA	−2.5 to −4.9
Mount Kilauea[d]	Hawaii, USA	−3.0 to −3.6
Furnas[e]	Azores	−3.3 to −6.1
Mount Etna[f]	Italy	−3.7
Mammoth Mountain[g]	California, USA	−4.5
Eifel lakes[b]	Germany	−4 to −5
Mount Lassen[h]	California, USA	−9.5
Mount St. Helens[i]	Washington, USA	−9 to −10
Mount St. Helens[j]	Washington, USA	−8.4 to −10.8
Mount Rainier[k]	Washington, USA	−11.1 to −12.5

Table 6.2: Measured $\delta^{13}C$ values of magmatic CO_2 from several localities as reported in previous studies. [a]Saupé, 1980; [b]Bruns, 1980;[c]Werner, 2003; [d]Rubin, 1987; [e]Pasquier-Cardin, 1999; [f]Allard, 1991; [g]Sorey, 1998; [h]Janik, 1983; [i]Casadevall, 1981; [j]Evans, 1981; [k]Zimbelman, 2000.

on leaves from plants of the same species growing at sites representing a range of volcanic carbon outgassing (Pasquier-Cardin, 1999). Three species showed no correlation between $\delta^{13}C$ and volcanic carbon uptake as indicated by ^{14}C aging, but three other species exhibited a clear enrichment in ^{13}C as a response to varying degrees of volcanic carbon exposure (less depleted in ^{13}C), averaging 0.18‰ by percent of volcanic carbon in the plant.

The difference in $\delta^{13}C$ between air and magmatic CO_2 at Mount Rainier should be large enough to create recognizable changes in $\delta^{13}C$ if substantial amounts of volcanic CO_2 were present in the atmosphere at Jay Bath. For example, 90 ppmv of excess volcanic CO_2 on top of a background level of 290 ppmv would cause 24% of the photosynthesized CO_2 to have a $\delta^{13}C$ signature of −11.8 ‰ instead of the pre-industrial atmospheric CO_2 $\delta^{13}C$ value of −6.5 ‰, if atmospheric and volcanic CO_2 were well mixed. The source CO_2 would have had a mean $\delta^{13}C$ signature of −7.77 ‰, causing a depletion of −1.27 ‰. If 50 ppmv of volcanic CO_2 were to be added to atmospheric background levels of 290 ppmv, the needles should be more depleted by 0.78 ‰. $\delta^{13}C$ values of all fossil material ranges from −25 to −28 ‰ and

within the restricted data sets of *Tsuga heterophylla* cuticles and mesophyll differences of 1.5 ‰ and 2.0 ‰ respectively are present. However, despite a large variation, $\delta^{13}C$ values do not correlate with reconstructed CO_2 concentrations (Fig. 6.3). Thus, the $\delta^{13}C$ measurements provide no evidence for the outgassing of substantial amounts of volcanic CO_2 at Jay Bath during the last two millennia.

^{14}C evidence for incorporation of volcanic CO_2

CO_2 from a magmatic source contains no or extremely low amounts of the cosmogenic isotope ^{14}C (Sulerzhitzky, 1970; Saupé et al., 1980; Rubin et al., 1987). Consequently, if plants incorporate volcanic carbon dioxide, without ^{14}C, the organic matter from these plants will reveal older ages when carbon-dated than after photosynthesis using purely atmospheric CO_2. Depletion of ^{14}C and subsequent aging (from several hundred to up to 4000 yr BP) has been recognized in plants growing near fumaroles and other CO_2-emanating areas (Sulerzhitzky, 1970; Bruns et al., 1980; Saupé et al., 1980; Rubin et al., 1987). Also in areas without visible CO_2 production, but instrumentally measured diffuse CO_2 soil degassing,

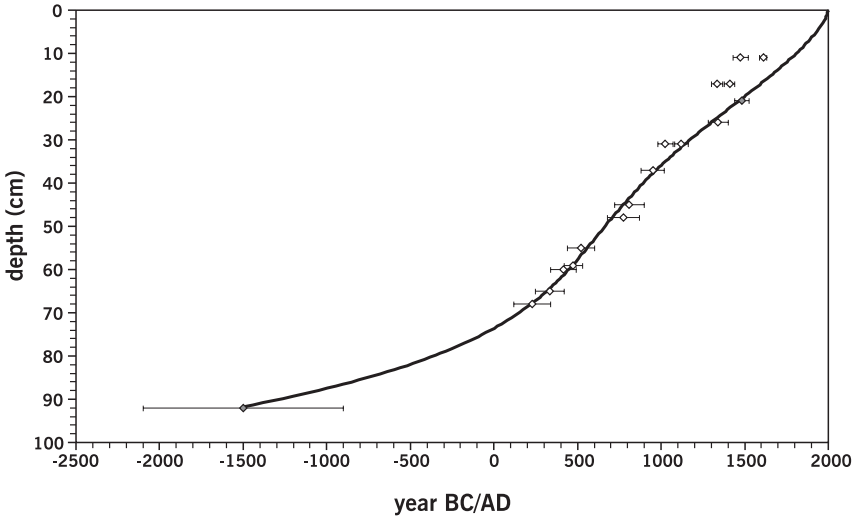

Figure 6.4: Age-depth diagram for Jay Bath sediment core. White diamonds represent AMS dates, converted to calendar age using OxCal 3.8 (Bronk-Ramsey, 1995) and INTCAL98 calibration data (Stuiver et al., 1998). Error bars indicate 95.4% probability interval. Grey diamonds represent dated tephra layers from nearby Mt. St. Helens (Yamaguchi, 1983; Mullineaux, 1996). Black line is the most likely age-depth model, a 4th order polynomial function [AGE = $-0.00020094 \times (\text{DEPTH})^4 + 0.02951 \times (\text{DEPTH})^3 - 1.33288 \times (\text{DEPTH})^2 - 8.71619 \times (\text{DEPTH}) + 2000.22$; $r^2 = 0.9977$], based on all dates, except those from 11 and 17 cm.

^{14}C depletion and aging of plants up to 4400 years has been evidenced, broadly correlating to the intensity of gas manifestations (Pasquier-Cardin et al., 1999). Low ^{14}C activity in cold springs in Oregon has also been interpreted as a result of diffuse emissions of magmatic CO_2 although no volcanic activity has occurred in the area for 1300 yr (James et al., 1999).

When the ^{14}C measurements on organic material from Jay Bath (Table 6.1) are converted to calendar ages and plotted against sample depth, nearly all ages show a close fit to a 4th order polynomial function (Fig. 6.4). Organic material containing volcanic carbon should deviate significantly from this curve, by an average of 89.7 yr/percent volcanic carbon, as calculated from aging measurements on several evergreen species growing in temperate, wet areas of soil degassing (Pasquier-Cardin et al.,1999). Only the samples from 11 and 17 cm are outliers from the estimated age-depth model.

Artificial aging as a result of photosynthesizing volcanic CO_2 can be calculated following the equation: $x_v = 1 - e^{(\ln 2 \times (V/a))/-T}$ [x_v = proportion of volcanic CO_2 in air or plant; V = aging, T = 5568 yr and a = 1.03 to account for the true ^{14}C decay period of 5570 yr (modified after Pasquier-Cardin, 1999)]. If, for example, volcanic CO_2 excess levels of 90 ppmv or 50 ppmv are assumed, on top of background pre-industrial global atmospheric CO_2 levels of 290 ppmv, then the organic material would appear 2171 years or 1278 years older, respectively. No such deviation is encountered in the Jay Bath ages. The differences between measured and modelled age for samples 11 and 17 is in the order of 100-200 years, which could be equivalent to elevation of background ambient CO_2 levels of 290 ppmv by 3-7 ppmv volcanic CO_2 excess. Thus, the ^{14}C record provides evidence against the local production of substantial amounts of volcanic CO_2 at Jay Bath during the past two millennia.

Effect of soil- CO_2

Higher soil temperatures as a consequence of subsurface magmatic activity could perhaps increase rates of organic matter recycling. The degradation of organic matter produces excess CO_2 above the forest floor, which is more depleted (−20‰) than ambient CO_2. Consequently, $\delta^{13}C$ measurements at the lowest levels in the canopy show much more depleted values (Buchmann et al., 1997). An increase of 50 ppmv of soil-respired CO_2 would mean that 14.7% of the source CO_2 would have a $\delta^{13}C$ value of −20 ‰ instead of −6.5 ‰. If soil and atmospheric CO_2 are well-mixed, source CO_2 for photosynthesis would have a $\delta^{13}C$ of −8.5 ‰, depleting plant $\delta^{13}C$ by an extra 2 ‰. No such consistent depletion can be observed in figure 6.3, and it remains questionable whether increased soil-CO_2 would affect needles through the entire canopy up to 30-40 m.

Another (small) potential effect of subsurface magmatic activity might be an increase in root-zone CO_2 concentration. The fixation of DIC (dissolved organic carbon) in the roots decreases $\delta^{13}C$ in leaves by about 0.5 to 1 ‰ (depending on nitrogen source) when root-zone CO_2 concentration was raised to 0.5 and 1 volume % (Viktor & Cramer, 2003). As no

information is available on the amount of root-zone CO_2 usually present at Jay Bath, and how much could be added by volcanic production, no attempt can be made to check whether $\delta^{13}C$ measurements could be influenced by this factor.

CONCLUSIONS

No evidence for substantial volcanic CO_2 production of Mount Rainier affecting the atmosphere at Jay Bath during the last two millennia has been encountered. First of all, the site is probably located too far away from the summit and known fumarolic areas at Mount Rainier to have experienced excess CO_2 from these sources of more than a few ppmv. A review of volcanic effects on carbon isotopes of plant material indicates that this approach shows the potential to detect past local volcanic CO_2 production. No signal of volcanic CO_2 is present in the $\delta^{13}C$ record. Moreover, no indication of a volcanic CO_2 imprint on the ^{14}C measurements is found, while incorporation of significant amounts of volcanic CO_2 during photosynthesis would have caused an artificial aging in the order of a thousand years or more. Thus, the reliability of the stomatal frequency record from Jay Bath is not compromised by local volcanic activity.

CHAPTER 7

Reproducibility of Holocene atmospheric CO_2 records based on stomatal frequency analysis

The majority of the stomatal frequency based CO_2 estimates for the Holocene do not support the widely accepted concept of comparably stable CO_2 concentrations throughout the past 12,000 years. To address the critique that these stomatal frequency variations result from local environmental change or methodological insufficiencies, multiple stomatal frequency records were compared for three climatic key periods during the Holocene, namely the Preboreal oscillation, the 8.2 kyr cooling event, and the Little Ice Age. The highly comparable fluctuations in the paleo-atmospheric CO_2 records, which were obtained from different continents and plant species (deciduous angiosperms as well as conifers) using varying calibration approaches, provide strong evidence for the integrity of leaf-based CO_2 quantification.

INTRODUCTION

A variety of land plants is capable of sustained adjustment of the number of leaf stomata to changing atmospheric CO_2 concentrations. Measured on fossil leaves and calibrated against modern training sets, stomatal frequency data are increasingly applied as a proxy for palaeo-atmospheric CO_2 reconstructions. The quality and quantity of fossil leaf remains preserved in lake and peat deposits of Holocene age allows the generation of stomatal frequency records from sites all over the Northern Hemisphere.

The majority of the stomatal frequency based CO_2 estimates for the Holocene do not support the widely accepted concept of relatively stable CO_2 concentrations throughout the past 12,000 years (Indermühle et al., 1999). The available high resolution CO_2 reconstructions based on plant fossils suggest that century-scale CO_2 fluctuations contributed to Holocene climate evolution (Wagner et al., 1999a; Rundgren and Beerling., 1999; McElwain et al., 2002; Wagner et al., 2002; Rundgren and Björck, 2003; Chapter 4).

Within the ongoing discussion on the alternative concept of a dynamic CO_2 regime, the approach of translating observed shifts in stomatal frequencies in terms of atmospheric CO_2 changes has often been questioned. It has been suggested that these shifts are a consequence of environmental factors other than CO_2 or an artifact of improper assembling and calibration of the modern training sets (Birks et al., 1999; Indermühle et al., 1999b). These comments emphasise the necessity to examine the amplitude and duration of reconstructed CO_2 fluctuations by comparing stomatal frequency records based on taxonomically and ecologically contrasting plant species. The global nature of the CO_2 signal should be revealed by records originating from a wide geographical range.

In the present review, we discuss the reliability of stomatal frequency derived CO_2 records by comparing available data from three different time slices in the Holocene which are known to be phases of major climatic change on the Northern Hemisphere. The first in a series of century scale Holocene climate deteriorations evident in marine, terrestrial, and ice core derived climate reconstructions is the so-called Preboreal oscillation, a short-lived cool pulse recorded at ~ 11.2 kyrs BP, soon after the end of the Younger Dryas (Björck et al., 1997; INTIMATE, 1998). The most prominent and best documented cooling in the Holocene is centred around 8.2 kyrs BP (Alley et al., 1997; Barber et al., 1999), where fresh water pulses from the melt-down of the Laurentian ice-sheet are thought to have reduced the thermohaline circulation in the North Atlantic for approximately 300 years. Well known from historical records and direct instrumental measurements is the pre-industrial cooling trend of the last millennium, commonly addressed as the Little Ice Age. Interrupted by periods of relative warmth, cool pulses occurred at different times in different parts of the world. In many Northern Hemisphere regions, the Little Ice Age culminated in a series of cool pulses between the 14th and the 18th century AD.

For all of these three events multiple stomatal frequency records are available. By directly comparing the results from the contrasting studies, we illustrate that the harmonious variation in stomatal frequency responses cannot be a result of local environmental changes or methodological insufficiencies, but do have their origin in a common, at least hemispherically acting forcing factor, namely atmospheric CO_2 dynamics throughout the Holocene.

MODERN CALIBRATION DATA SETS

The most critical issue in calculating atmospheric CO_2 concentrations from fossil stomatal frequency data is the accuracy of the modern calibrations data sets. These training sets enable quantification of the response rates of individual species to atmospheric CO_2 changes and, therefore, serve as reference data for CO_2 estimates from fossil leaves. An unique opportunity to study the leaf morphological adaptation of plants to changing ambient CO_2 is provided by the well documented continuous CO_2 increase from pre-industrial values of approximately 280 ppmv to 375 ppmv present day level. Analysis of herbarium leaf specimens of exactly known age allows to tie up known historical CO_2 and corresponding stomatal frequencies. Uncertainties in the herbarium data sets due to varying sample localities can be reduced by adding data from continuous, but often less well dated, leaf sequences accumulated in e.g. young peat deposits (Wagner et al., 1996).

Fossil and herbarium leaves grown during the industrial CO_2 rise, however, do not cover CO_2 levels below 280 ppmv, which hampers the statistical modelling of the stomatal response to lower CO_2 concentrations. To obtain data from the lower CO_2 range, the plants' response to CO_2 partial pressure (in Pa) rather than CO_2 mixing ratio (in ppmv) can be utilized (Woodward & Bazzaz, 1988). Because partial pressure decreases with elevation due to the reduced air pressure, inclusion of leaf material grown at higher altitudes allows extension of the historical training set to CO_2 levels below 28 Pa (equivalent to 280 ppmv at sea level). If the leaf material in the modern training set as well as the fossil assemblages originate from localities at the same elevation, expression of CO_2 levels in either partial pressure or mixing ratio will be of no consequence. However, if leaves from different altitudes are included in the training set or stomatal frequency record, CO_2 levels must be calculated as partial pressure for stomatal frequency calibration (Fig. 7.1B). The estimated local barometric pressure at the site where the fossil material was derived from, can then be used to reconvert the reconstructed CO_2 partial pressure to mixing ratio, to enable quantitative comparison with other CO_2- reconstructions.

In this manner significant changes in stomatal frequency under changing atmospheric CO_2 have been demonstrated for many woody angiosperms, of which deciduous trees such as *Betula*, *Quercus*, and *Ginko*, as well as common high latitude shrubs like *Salix* and *Dryas*, show the most pronounced responses. Conifers exhibiting a prominent decrease in stomatal frequency with increasing historical CO_2 include *Tsuga*, *Picea*, *Larix*, and *Metasequoia* (see

Royer, 2001; Chapter 2). Although desirable, a general model for fossil CO_2 estimates embracing multiple genera can not be generated, due to the highly individual responses of the various genera (Kürschner et al., 1997; Rundgren and Björck, 2003).

For broad-leaved plant species the ratio between stomata and the total amount of epidermal cells on the leaf surface (the stomatal index) has been proven to be the most sensitive parameter to quantify their response to CO_2 changes. By applying the cell ratio rather than the pure number of stomata, undesirable effects of lateral epidermal cell expansion due to contrasting light regimes, leaf age or temporary hydrological conditions are circumvented (Poole and Kürschner, 1999). Because of the specific stomatal patterning in the narrow-leaved conifers, the number of stomata per mm needle length rather than the stomatal index responds to atmospheric CO_2 levels. Although this parameter is density-based, leaf age and environmental conditions do not mask the adjustment to CO_2 levels (Chapter 2; Chapter 3).

While the conifer species studied show a linear decrease in stomatal frequency under present day atmospheric CO_2, the majority of broad-leaved species currently used for CO_2 reconstructions indicate a decrease in CO_2 sensitivity at values above approximately 320 ppmv (Kürschner et al., 1997). The response patterns on species or genus level determined in the modern training sets require the application of taxon-specific statistical treatments for the individual plant categories to guarantee the best fit of the models for palaeo-CO_2 estimations. Two contrasting examples of models for inferring palaeo-CO_2 based on modern training sets of broad-leaved trees and conifers, both incorporating herbarium material as well as sub-fossil leaves from peat sequences, are presented in Fig. 7.1.

Analysis of modern *Betula pendula* and *Betula pubescens* leaves has demonstrated a distinct reduction of the stomatal index over the post-industrial CO_2 increase from 290 ppmv to 370 ppmv, with a levelling off in the CO_2 response at values higher than 350 ppmv (Fig. 7.1A). The good correspondence of the stomatal index response evidenced for the two closely related species allows treatment of *B. pendula* and *B. pubescens* as one single group in the model (Fig. 7.1A, Wagner et al., 2000). In order to accommodate the partial non-linearity of the data while maintaining the best fit, the model for CO_2 estimations from fossil material is based on a log-transformation of both SI and CO_2 values in the training set (Fig. 7.1A).

The stomatal frequency response of *Tsuga heterophylla* in contrast is best described using a linear rather than a non-linear model. The linearity of the response over the entire CO_2 regime from 25 to 37 Pa allows the fossil CO_2 estimation by using a classical linear regression, the most conservative statistical approach (Fig. 7.1B).

All *Tsuga* and *Betula* data presented hereafter are calibrated according to the models above. As a consequence of the adjusted model for *Betula*, the CO_2 reconstructions based on this genus may differ slightly from initial publications (Wagner et al., 1999a; Wagner et al., 2002).

PALAEOATMOSPHERIC CO_2 RECONSTRUCTIONS

Based on the well defined response rates of *Betula* and *Tsuga*, palaeoatmospheric CO_2 records have been established for three key periods of climate change during the Holocene (Wagner et al., 1999a; Wagner et al., 2002; Chapter 4). Additional CO_2 records from other species are available for the Preboreal oscillation (McElwain et al, 2002; Rundgren and Björck, 2003), the 8.2 kyrs cool pulse (Rundgren and Beerling, 1999), and the Little Ice Age (van Hoof et al., this study). The present study focusses on the comparability of independent stomatal frequency records in terms of trends in atmospheric CO_2 and the temporal synchroneity of the records. In order to emphasize the amplitude of reconstructed atmospheric CO_2 changes associated with the three Holocene cool pulses, all available records are given in normalized CO_2 concentrations (ppmv); whereas all ages are given in calibrated calendar years BP.

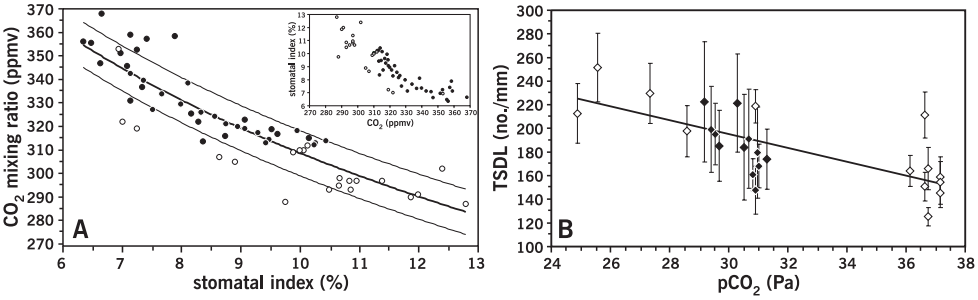

Figure 7.1: Modelled relation between atmospheric CO_2 concentration and stomatal frequency in training sets consisting of leaves from herbaria and subfossil deposits calibrated against historical CO_2 concentrations. CO_2 mixing ratios of 290–315 ppmv were derived from shallow Antarctic ice cores (http://cdiac.esd.ornl.gov/trends/co2/siple.htm; Neftel et al., 1985), mixing ratios of 315–368 ppmv are annual means from instrumental measurements at Mauna Loa (http://cdiac.esd.ornl.gov/ndps/ndp001.html).

A: Thick black line: Model for CO_2 estimates based on linear regression of log-transformed stomatal index (SI) data for *Betula pendula/pubescens* ($CO_2 = 10^{2.802} - [0.313 + \log(SI_f)]$; $r^2 = 0.79$); thin lines indicate ± 1 RMSE (= 9.6 ppmv). Inset: historical response of SI to global atmospheric CO_2. Training set includes leaf remains from modern peats (black circles) and herbarium specimens (open circles).

B: Response of number of stomata per mm needle lenght (TSDL) of *Tsuga heterophylla* to a pCO_2 increase from 24 to 38 Pa. CO_2 partial pressure was calculated by multiplying the CO_2 mixing ratio by local barometric pressure P_B (Pa), estimated according to Jones (1992): $P_B = 101.325/e^{[(z/29.3)/T]}$ where z is altitude above sea level and T air temperature in K (estimated from mean annual temperature at the closest weather station, corrected by a temperature lapse rate appropriate for the region in case of significant altitudinal difference between site and station). Black diamonds represent subfossil and modern needles from Jay Bath (Mount Rainier, WA), open diamonds modern and herbarium needles from other localities. Error bars indicate ± 1 SE. Solid line indicates best fit in classical regression analysis. TSDL: true stomatal density per mm needle length (TSDL = $-5.8581 \times pCO_2 + 371.14$; $r^2 = 0.5124$; RMSE = 42.8 ppmv).

The Preboreal oscillation (Fig. 7.2A)
The Preboreal stage of the Holocene is represented in three different stomatal frequency records. *B. pubescens* and *B. pendula* leaf remains were obtained from a peat section temporarily exposed at the Borchert archaeological excavation site in Denekamp, The Netherlands (52°23'N, 7°00'E; 30 m a.s.l., Fig. 7.2A). The section spans the period from 11,620 cal. BP to 10,920 cal. BP, with a high-resolution age assessment based on wiggle matching of 18 ^{14}C datings over the 35 cm peat section (Appendix A3). The stomatal index values from this record are calibrated according to the model in Fig. 7.1A and provide evidence for a short-term CO_2 decrease between 11,350 cal BP and 11,080 cal. BP with a CO_2 minimum at 11,120 cal BP (Fig. 7.2D).

This distinct minimum is supported by stomatal frequency analysis on *Larix laricina* needles preserved in a lake in New Brunswick, Canada (Fig. 7.2A, D, Splan Pond, 45°14'N, 67°06'W, 106 m a.s.l., age assessment based on two AMS ^{14}C datings for this interval; McElwain et al., 2002). The timing of the CO_2 decrease documented in both records parallels the Preboreal oscillation sensu Björck et al. (1997) which is equivalent to the GH 11.2 kyrs temperature decline documented in Greenland ice cores (INTIMATE, 1998).

Further evidence for a CO_2 decrease during this time is provided by a stomatal frequency record based on *Salix herbacea*, *Salix polaris*, and *Betula nana* leaves from Lake Madtjärn in southwestern Sweden (58°35'N, 12°10'E; 135 m a.s.l.; Rundgren and Björck, 2003). The age assessment for this record is based on the age depth model for the entire Madtjärn profile, in which the early Preboreal is covered by six AMS ^{14}C datings. A slight temporal offset of 100 calendar years between this record and the two records above might be an artifact of the selected age-depth model for the earliest Holocene (see Rundgren and Björck, 2003 for original data).

Consistent in all records, the shifts in stomatal frequency indicate a change in the atmospheric CO_2 concentration of 20 - 30 ppmv associated with the Preboreal oscillation.

The 8.2 kyrs BP cooling event (Fig.7.2B)
For the time slice of the 8.2 kyrs cool pulse, two stomatal frequency based CO_2 reconstructions are available (Fig. 7.2E). The first record (Wagner et al., 2002) is based on the stomatal index values from European tree birch leaves derived from organic rich gyttja deposits from Lille Gribso, a small kettle hole lake North of Copenhagen, Denmark (55°58'N, 12°18'E; 45 m a.s.l.). Well preserved *B. pubescens* and *B. pendula* leaf remains occur continuously through an interval corresponding to the period between 8700 cal. BP and 6800 cal. BP. Chronological control is provided by a series of six AMS ^{14}C dates measured on single birch leaves (Wagner et al., 2002).

The second record is based on *S. herbacea* leaf material from ten horizons accumulated in a small lake close to Abisko, Northern Sweden (Lake Njulla, 68°22'N, 18°42'E; 999 m a.s.l.; Rundgren and Beerling, 1999). For the time interval of interest three ^{14}C datings are available. The two data sets consistently reveal a century-scale interval of 30 ppmv CO_2 concentration changes with lowest CO_2 levels centred around 8.2 kyrs BP.

Little Ice Age (Fig. 7.2C)
For the period between 1000 and 1500 AD, covering part of the Little Ice Age, two independent stomatal frequency reconstructions are shown in Fig. 7.2F.

Tsuga heterophylla needle assemblages were obtained from a 91 cm sediment core drilled in Jay Bath, a shallow pond on the southern flank of Mount Rainier (Washington, USA; 46º46'N 121º46'W; Fig. 7.2C). The age assessment for this site is established on five AMS ^{14}C datings and one tephra layer at 1481 AD (Chapter 4). The stomatal frequency results in this study are calibrated according to the modern training set shown in Fig. 7.1B. Two CO_2 minima are evident in the record, a smaller one around 1050 AD and a very pronounced minimum centred around 1150 AD (Fig. 7.2F). Maximum CO_2 levels are registered during the 14th century, followed by a steady CO_2 decrease.

These initial results are confirmed by a high resolution record of fossil *Quercus robur* leaves from an oxbow lake of the river Roer, near Sint Odilienberg, The Netherlands (51°08'N, 6°00'E; 25 m a.s.l., Fig. 7.2C; Van Hoof in prep.). Wiggle match dating of eleven AMS ^{14}C datings provides a precise age assessment of the 60 leaf-rich layers in this section, covering the period from 1000 AD to 1500 AD. The CO_2 reconstruction based on *Q. robur* leaves reproduces and substantiates in detail the short-term CO_2 decrease around 1050 AD. The second minimum in this high resolution record is assigned to the late 12th to early 13th century. In good agreement with the *T. heterophylla* record, the *Q. robur* data indicate decreasing CO_2 concentrations during the late 14th and 15th century. Both records provide independent evidence for rapid CO_2 fluctuations on time-scales varying from decades to centuries. While the estimated amplitudes of 20 ppmv to 30 ppmv in the *Q. robur* record are in good agreement with the fluctuations documented for the Preboreal oscillation and the 8.2 kyrs event, the maximum change of up to 60 ppmv estimated in the *T. heterophylla* record exceeds the other records. The difference, however, is well within the standard error of the *Q. robur* record and may be caused by the comparably lower accuracy of the modern training set for *T. heterophylla* (Fig. 7.1B).

Temperature reconstructions for the period of the Little Ice Age based on marine and terrestrial evidence show a series of short, moderately cool pulses rather than the very pronounced single century-scale coolings of the Preboreal oscillation and the 8.2 kyrs event. This pattern is also evident in the stomatal frequency based CO_2 reconstructions.

A
B
C
D
E
F
norm. CO2 (ppmv)
cal. year BP
cal. year BP
cal. year AD

Figure 7.2: Localities of the fossil assemblages (A, B, C) used for stomatal frequency records (D, E, F).
A: SP = Splan Pond (Canada), B = Borchert (Netherlands) and LM = Lake Madtjärn (Sweden). **B**: LG = Lille Gribsø (Denmark) and LN = Lake Njulla (Sweden). **C**: JB = Jay Bath (Washington, USA) and R = Roer river (Netherlands).

D: Reconstructed normalized CO_2 mixing ratios from three stomatal records (deviations from the long term average in each record) centred around the time of the Preboreal Oscillation. The thick black line represents unsmoothed normalized mixing ratios based on stomatal index measurements of *Betula pubescens* leaves from the Borchert section (Wagner et al., 1999). The black dashed line represents unsmoothed normalized mixing ratios based on stomatal number per mm needle length of *Larix laricina* from Splan Pond (McElwain et al., 2002). The thin grey line represents a locally weighted average of normalized mixing ratios based on stomatal indeces of *Salix herbacea*, *Salix polaris* and *Betula nana* from Lake Madtjärn (Rundgren & Björk, 2003). The time scale at the bottom of the figure is based on the age-assessment of the Borchert and Splan Pond records. The original time-scale of the Lake Madtjärn record is shown at the top of the figure and has been shifted by 100 years (within one ^{14}C standard deviation) to facilitate comparison. The grey confidence interval represents ± 1 SE (standard error of the samples per depth) in the Borchert record.

E: Reconstructed normalized CO_2 mixing ratios based on two different stomatal frequency records (deviations from the long term average in each record) around the 8.2 kyr cooling event. The black line represents unsmoothed normalized mixing ratios based on stomatal index of *Betula pendula/pubescens* from Lille Gribsø (Wagner et al., 2002). The grey line represents a five point moving average of normalized mixing ratios based on stomatal index of *Salix herbacea* from Lake Njulla (Rundgren & Beerling, 1999). The stomatal index of the training set was calibrated against CO_2 partial pressure and also expressed in Pa in the original study. Here, the reconstructed partial pressures were converted to mixing ratios using the estimated local barometric air pressure at the site (Fig 7.1; Jones, 1992) to allow comparison with the other records. Both records are plotted on a common time scale and the confidence interval represents ± 1 SE (standard error of the samples per depth) in the Lille Gribsø record.

F: Reconstructed normalized mixing ratios based on two different stomatal frequency records around the onset of the Little Ice Age. The black line represents a 3 point moving average of normalized mixing ratios based on stomatal index of *Quercus robur* leaves from the Roer river area (Van Hoof et al., in prep.). The black interrupted line represents a three point moving average of normalized mixing ratios based on stomatal numbers per mm needle length (TSDL) of *Tsuga heterophylla* needles from Jay Bath (Chapter 4). The TSDL of the modern training set was calibrated against CO_2 partial pressure and the reconstructed partial pressures were converted to mixing ratios using the estimated local barometric air pressure (Fig 7.1; Jones 1992). The grey confidence interval represents ± 1 SE (standard error of the samples per depth in the unsmoothed data) in the Roer record.

DISCUSSION

The compilation and detailed comparison of the seven records provides an indirect but powerful assessment of the reliability of stomatal frequency analysis as a proxy for paleoatmospheric CO_2 concentrations. So far, the validation of stomatal frequency as a sensitive parameter to changing CO_2 concentrations has basically been performed for individual species (see Royer, 2001 for review). Potential influences of environmental factors other than CO_2, e.g. light, water availability and temperature have frequently been tested in experiments under controlled growth conditions. The results obtained in a controlled and artificial environment in growth experiments, however, can not unambiguously be transferred to responses under the natural growth conditions in the field. Field studies, on the other hand, provide insight into the intrinsic variability under natural growth conditions but observed variations are often a response to a combination of different environmental parameters.

By directly comparing the generated CO_2 estimates based on independent stomatal frequency records, species-specific uncertainties may be minimized, which permits testing the overall reliability of the CO_2 reconstructions.

Taking into account the wide geographical area the investigated leaf material originates from, the difference in photoperiod over the covered latitudinal range from 45°N to 68°N could potentially affect the stomatal frequency records. Light intensity and photoperiod have been long known to strongly affect stomatal frequency (Schürmann, 1959; Kürschner et al., 1996; Poole et al., 1996, Wagner et al., 2000). While light intensity primarily regulates epidermal cell expansion and, therefore, influences stomatal densities, prolonged photoperiods lead to enhanced stomatal initiation rates quantified in the stomatal index (Schürmann, 1959; Wagner, 2000). The dependency on photoperiod may consequently cause erroneous data when stomatal index values from contrasting latitudes are compared to data from a restricted latitudinal range (Wagner et al., 1999b).

CO_2 estimates from high and mid-latitudes are combined in the second case study, the 8.2 kyrs event, where stomatal index data of *Betula* leaves from Denmark and *Salix herbacea* data from northern Sweden are available. The calibration data for *Betula* (Fig. 7.1A) are based solely on leaf material from Denmark and the Netherlands, since field studies have demonstrated the high sensitivity of birch to changes in photoperiod (Wagner et al., 2000). No such dependency is known for *Salix*, and calibration data are derived from a wide latitudinal range (Rundgren and Beerling, 1999). Independent of the different approaches, the good correspondence of paleo-CO_2 estimates from the high and mid- latitude records strongly suggests that latitudinal differences in photoperiod did not bias these data sets.

Only very sparse information is available so far on the potential influence of temperature on stomatal frequency. Controlled-environment experiments with *B. pendula* under (extremely) different growth temperatures provide evidence for a positive correlation between the sto-

matal index and temperature for this particular species (Wagner, 1998). No interaction between stomatal frequency and temperature was observed in experiments with cotton (Reddy et al., 1998). Comparison of spring and annual temperatures near Jay Bath with the stomatal frequency of the subfossil *T. heterophylla* needles during the past ninety years showed no correlation. Although the available data are not unequivocal, they suggest that the temperature changes are unlikely to have caused the observed changes in the individual stomatal frequency records. The three periods discussed here are commonly referred to as cool pulses, but the regional temperature changes have not been uniform over the Northern Hemisphere. The good agreement of stomatal frequency records from sites located at different altitude, latitude, and longitude with their individual temperature ranges minimizes the possibility of temperature changes as the responsible factor for the observed parallel changes in the record.

Effects of water availability on epidermal morphology are well known. Drought stress for instance leads to the development of distinct xeromorphic features during leaf development (Bosabalidis and Kofidis, 2003; Li and Wang, 2003). One of the most common and pronounced effects observed in growth experiments, is the reduced lateral epidermal cell expansion under drought conditions (Bosabalidis and Kofidis, 2003; Li and Wang, 2003). The stomatal index, however, is not influenced by water shortage in these performed experiments. Under natural growth conditions, the comparison of modern precipitation data for the past seventy years and the stomatal frequency of *T. heterophylla* shows no correlation (Chapter 2).

This observational evidence for the independence of the stomatal frequency parameters from precipitation is corroborated by the good agreement between the CO_2 records in spite of the highly regional precipitation surpluses or deficits associated with the periods of climate change studied. Again, as with temperature, the broad geographical distribution of the sites studied provides evidence for the independence of the CO_2 records from precipitation changes associated with the Preboral oscillation, the 8.2 kyrs event, and the Little Ice Age.

Besides the potential impact of environmental factors other than CO_2 concentrations, genetic variations within individual plant species or hybridization of related species could be a potential cause for the changing stomatal frequency patterns. Studies on genetically controlled leaf material from *B. pendula* and *B. pubescens*, however, have shown that at least for these two species the influence of genetic difference can be neglected (Wagner, 2000; Fig. 7.1A). In cases where the species specific stomatal frequency response does not allow a grouping, single-site CO_2 reconstructions based on multiple species can be derived by developing separate calibration data sets as demonstrated for *S. polaris* and *S. herbacea* (Rundgren and Björck, 2003). The approach of combining CO_2 estimates including a wide range of taxonomically contrasting plant types in this study a priori excludes any influence of taxonomic or genetic nature as shown by the consistency of CO_2 reconstructions derived from broad-leaved trees, herbaceous shrubs, and conifers, or a combination of those.

CONCLUSIONS

The successful replication of stomatal frequency records in terms of timing and duration in the seven compared records provides strong evidence for the integrity of the leaf-based proxy for atmospheric CO_2 concentrations. The general coherence of the reconstructed amplitudes of atmospheric CO_2 fluctuations corroborates the assumption that a wide range of terrestrial plants show a common response to this environmental factor independent of geographical setting, habitat conditions or taxonomy.

The agreement between stomatal frequency records from the Atlantic realm and sites located in the Pacific Northwest of the USA indicates that the observed stomatal parameter shifts are not restricted to the circum North Atlantic sector, but are at least northern hemispheric in nature. The demonstrated ability of stomatal frequency analysis to generate independent but highly comparable proxy records clearly meets the requirements for a paleoproxy in the field of global atmospheric CO_2 dynamics.

REFERENCES

Alexander RR. 1987. Ecology, silviculture, and management of the Engelmann spruce-subalpine fir type in the central and southern Rocky Mountains. *USDA Forest Serv ice Agricultural Handbook* 659.

Alexander RR, Shearer RC and WD Shepperd. 1984. Silvical characteristics of subalpine fir. *USDA Forest Service Technical Report* RM-115.

Allard P, Carbonelle J, Dajlevic D, Le Bronec J, Morel P, Robe MC, Maurenas JM, Faivre-Pierret R, Martin D, Sabroux JC and P Zettwoog. 1991. Eruptive and dif fuse emissions of CO_2 from Mount Etna. *Nature* 351: 387–391.

Alley RB, Mayewski PA, Sowers T, Stuiver M, Taylor KC and PU Clark. 1997. Holocene climatic instability: a prominent, widespread event 8200 years ago. *Geology* 25: 483–486

Anklin RB, Barnola JM, Schwander J, Stauffer B and D Raynaud. 1995. Processes af fecting the CO_2 concentrations measured in Greenland ice. *Tellus* 47B: 461–470.

Apple ME, Olszyk DM, Ormrod DP, Lewis J, Southworth D and DT Tingey. 2000. Mor phology and stomatal function of Douglas fir needles exposed to climate change: elevated CO_2 and temperature. *International Journal of Plant Sciences* 161: 127–132.

Barber DC, Dyke A, Hillaire-Marcel C, Jennings AE, Andrews JT, Kerwin MW, Bilodeau G, McNeelly R, Southon J, Morehead MD and J-M Gagnon. 1999. Forc ing of the cold event of 8,200 years ago by catastrophic drainage of Laurentide lakes. *Nature* 400: 344–348.

Barnola JM, Anklin M, Porcheron J, Raynaud D, Schwander J and B Stauffer. 1995. CO_2 evolution during the last millennium as recorded by Antarctic and Greenland ice. *Tellus* 47B: 264–272.

Baubron JC, Allard P and JP Toutain. 1990. Diffuse volcanic emissions of carbon dioxide from Volcano Island, Italy. *Nature* 344: 51–53.

Beerling DJ. 1997. Carbon isotope discrimination and stomatal responses of mature *Pinus sylvestris* L. trees exposed in situ for three years to elevated CO_2 and temperature. *Acta Oecologica* 18: 697–712.

Beerling DJ, Birks HH and FI Woodward. 1995. Rapid late-glacial atmospheric CO_2 changes reconstructed from the stomatal density record of fossil leaves. *Journal of Quater nary Science* 10: 379–384.

Bender JM 1971. Variations in the $^{13}C/^{12}C$ ratios of plants in relation to the pathway of photosynthetic carbon dioxide fixation. *Phytochemistry* 10: 1239–1244.

Birks HJB. 1995. Quantitative palaeoenvironmental reconstructions. *In:* D Maddy and JS Brew (eds.) Statistical modelling of Quaternary environmental data. *Technical Guide, Quaternary Research Association, Cambridge* 5: 161–254.

Birks HH, Eide W, and HJB Birks. 1999. Early Holocene atmospheric CO_2 concentrations. *Science* 286: 1815.

Björck S, Rundgren M, Ingólfsson O and S Funder. 1997. The Preboreal Oscillation around the Nordic Seas: terrestrial and lacustrine responses. *Journal of Quaternary Science* 12: 455–465.

Boetsch J, Chin J, Ling M and J Croxdale. 1996. Elevated carbon dioxide affects the patterning of subsidiary cells in *Tradescantia* stomatal complexes. *Journal of Ex perimental Botany* 47: 925–931.

Bosabalidis AM and G Kofidis. 2002. Comparative effects of drought stress on leaf anatomy of two olive cultivars. *Plant Science* 163: 375–379.

Briffa KR. 2000. Annual climate variability in the Holocene: interpreting the message of ancient trees. *Quaternary Science Reviews* 19: 87–105.

Bronk Ramsey C. 1995. Radiocarbon calibration and analysis of stratigraphy: the OxCal program. *Radiocarbon* 37: 425–430.

Brouwer R. 1963. The influence of the suction tension of the nutrient solutions on growth, transpiration and diffusion pressure deficit of bean leaves (*Phaseolus vulgaris*). *Acta Botanica Neerlandica* 12: 248–261.

Bruns M, Levin I, Münnich KO, Hubberten HW and S Fillipakis. 1980. Regional sources of volcanic carbon dioxide and their influence on ^{14}C content of present-day plant material. *Radiocarbon* 22: 532–536.

Buchmann N, Kao W-Y and JR Ehleringer. 1997. Influence of stand structure on carbon-13 of vegetation, soils, and canopy air within deciduous and evergreen forests in Utah, United States. *Oecologia* 110: 109–119.

Casadevall TJ and LP Greenland. 1981. The chemistry of gases emanating from Mount St. Helens, May-September 1980. *In*: PW Lipman and DR Mullineaux (eds.) The 1980 eruptions of Mount St. Helens, Washington. *U.S. Geological Survey Professional Papers* 1250: 221–226.

Charlton WA. 1990. Differentiation in leaf epidermis of *Chlorophytum comosum* Baker. *Annals of Botany* 66: 567–578.

Chin J, Wan Y, Smith J and J Croxdale. 1995. Linear aggrevations of stomata and epider mal cells in *Tradescantia* leaves: evidence for their group patterning as a function of cell type. *Developmental Biology* 168: 39–46.

Craig H. 1953. The geochemistry of stable carbon isotopes. *Geochimica et Cosmochimica Acta* 3: 53–92.

Cronin TM, Dwyer GS, Kamiya T, Schwede S and DA Willard. 2003. Medieval Warm Period, Little Ice Age and 20th century temperature variability from Chesapeake Bay. *Global and Planetary Change* 36: 17–29.

Croxdale J. 1998. Stomatal patterning in monocotyledons: *Tradescantia* as a model sys tem. *Journal of Experimental Botany* 49: 279–292.

Croxdale J. 2000. Stomatal Patterning in Angiosperms. *American Journal of Botany* 87: 1069–1080.

CROXDALE J, JOHNSON B, SMITH J AND B YANDELL. 1992. Stomatal patterning in *Tradescantia*: an evaluation of the cell lineage theory. *Developmental Biology* 93: 1078–1082.

CWYNAR L. 1987. Fire and forest history of the North Cascade Range. *Ecology* 68: 791–802.

DE LUCIA EH. 1986. Effect of low-root temperature on net photosynthesis, stomatal con ductance and carbohydrate concentration in Engelmann spruce (*Picea engelmannii* Parry ex Engelm.) seedlings. *Tree Physiology* 2: 143–154.

DEMENOCAL P, ORTIZ J, GUILDERSON T AND M SARNTHEIN. 2000, Coherent High- and Low-Latitude Climate Variability During the Holocene Warm Period. *Science* 288: 2198–2202.

DIXON M, LE THIEC D AND JP. GARREC. 1995. The growth and gas exchange responses of soil-planted Norway spruce (*Picea abies* (L.) Karst) and red oak (*Quercus rubra* L.) exposed to a naturally occurring drought. *New Phytologist* 129: 265–273.

DORE JE, LUKAS R, SADLER DW AND DM KARL. 2003. Climate-driven changes to the atmos pheric CO_2 sink in the subtropical North Pacific Ocean. *Nature* 424: 754–757.

DUNWIDDIE PW. 1985. Dichotomous Key to Conifer Foliage in the Pacific Northwest. *North west Science* 59: 185–191.

DUNWIDDIE PW. 1986. A 6000-year record of forest history on Mount Rainier, Washington. *Ecology* 67: 58–68.

DUNWIDDIE PW. 1987. Macrofossil and pollen representation of coniferous trees in modern sediments from Washington. *Ecology* 69: 1–11.

EHLERINGER JR, HALL AE AND GD FARQUHAR. 1993. Stable isotopes and plant carbon-water relations. San Diego, Academic Press. 555 p.

ESAU K. 1977. Anatomy of Seed Plants. John Wiley and Sons, New York, NY, USA. 550 p.

ESPER J, COOK ER AND FH SCHWEINGRUBER. 2002. Low-Frequency Signals in Long Tree-Ring Chronologies for Reconstructing Past Temperature Variability. *Science* 295: 2250–2253.

ETHERIDGE DM, STEELE LP, LANGENFELS RL, FRANCEY RJ, BARNOLA JM AND VI MORGAN. 1996. Natural and anthropogenic changes in atmospheric CO_2 over the last 1000 years from air in Antarctic ice and firn. *Journal of Geophysical Research* 101: 4115–4128.

EVANS WC, BANKS NG AND LD WHITE. 1981. Analyses of gas samples from the summit crater. *In:* PW Lipman and DR Mullineaux (eds.) The 1980 eruptions of Mount St. Helens, Washington. *U.S. Geological Survey Professional Papers* 1250: 227–231.

FARQUHAR GD, EHLERINGER JR AND KT HUBICK. 1989. Carbon isotope discrimination and photosynthesis. *Annual Review of Plant Physiology and Plant Molecular Biology* 40: 503–537.

FARRAR CD, SOREY ML, EVANS WC, HOWLE JF, KERR BD, KENNEDY BM, KING C-Y AND JR SOUTHON. 1995. Forest-killing diffuse CO_2 emission at Mammoth Mountain as a sign of magmatic unrest. *Nature* 376: 675–678.

FERNANDEZ MD, PIETERS A, DONOSO C, TEZARA W, AZUKE M, HERRERA C, RENGIFO E AND A HERRERA.1998. Effects of a natural source of very high CO_2 concentration on the leaf gas exchange, xylem water potential and stomatal characteristics of plants of *Spatiphylum cannifolium* and *Bauhinia multinervia. New Phytologist* 138: 689–697.

FISCHER WC AND AF BRADLEY 1987. Fire ecology of western Montana forest habitat types. *USDA Forest Service Technical Report* INT-223.

FISCHER H, WAHLEN M, SMITH J, MASTROIANNI D AND B DECK. 1999. Ice core records of atmospheric CO_2 around the last three glacial terminations. *Science* 283: 1712–1714.

FLORIN R. 1931. Untersuchungen zur Stammengeschichte der Coniferales und Cordaitales. *Kungliga Svenska Vetenskapsakademiens Handlingar* 10: 1–588.

FLÜCKIGER J, MONNIN E, STAUFFER B, SCHWANDER J AND TF STOCKER. 2002. High-resolution Holocene N_2O ice core record and its relationship with CH_4 and CO_2. *Global Biogeochemical Cycles* 16: 1010.

FOXWORTHY B AND M HILL. 1982. Volcanic eruptions of 1980 at Mount St. Helens: The first 100 days. *U.S. Geological Survey Professional Papers* 1249: 1–125.

FRANCEY RJ, TANS PP, ALLISON CE, ENTING IG, WHITE JWC AND M TROLIER. 1995. Changes in the oceanic and terrestrial carbon uptake since 1982. *Nature* 373: 326–330.

FRANCIS P, HORROCKS L AND C OPPENHEIMER. 2000. Monitoring gases from andesite volca noes. *Philosophical Transactions of the Royal Society of London* 358: 1567–1584.

FRANK D. 1995. Surficial extent and conceptual model of hydrothermal system at Mount Rainier, Washington. *Journal of Volcanology and Geothermal Research* 65: 51–80.

FRANKLIN JF.AND RG MITCHELL. 1967. Successional status of subalpine fir in the Cascade Range. *USDA Forest Service Research Paper* PNW-46.

FRANKLIN JF AND CT DYRNESS. 1973. Natural vegetation of Oregon and Washington. *USDA Forest Service Technical Report* PNW-8.

GAY AP AND RG HURD. 1975. The influence of light on stomatal density in the tomato. *New Phytologist* 75: 37–46.

GERBER S, JOOS F, BRÜGGER P, STOCKER TF, MANN ME, SITCH S AND M SCHOLZE. 2003. Con straining temperature variations over the last millennium by comparing simulated and observed atmospheric CO_2. *Climate Dynamics* 20: 281–299.

GERLACH TM AND KA MCGEE. 1998. Rates of volcanic CO_2 degassing from airborne determinations of SO_2 emission rates and plume CO_2/SO_2: Test study at Pu'u 'O'o cone, Kilauea volcano, Hawaii. *Geophysical Research Letters* 25: 2675–2678.

GERLACH TM, DOUKAS MP, MCGEE KA AND R KESSLER. 1999. Airborne detection of diffuse carbon dioxide emissions at Mammoth Mountain, California. *Geophysical Research Letters* 26: 3661–3664.

GLOVER BJ. 2000. Differentiation in plant epidermal cells. *Journal of Experimental Botany* 51: 497–505.

GRAUMLICH LJ AND LB BRUBAKER. 1986. Reconstruction of annual temperature (1590-1979) for Longmire, Washington, derived from tree rings. *Quaternary Research* 25: 223–234.

GRAY JE, HOLROYD GH, VAN DER LEE F, SIJMONS PC, WOODWARD FI, SCHUCH W AND AM HETHERINGTON. 2000. The HIC signalling pathway links CO_2 perception to stomatal development. *Nature* 408: 713–715.

GUEHL JM, PICON C, AUSSENAC G AND P GROSS. 1994. Interactive effects of elevated CO_2 and soil drought on growth and transpiration efficiency and its determinants in two Euro pean tree species. *Tree Physiology* 14: 707–724.

HARRIS DM, SATO M, CASADEVALL TJ, ROSE JR. WI AND TJ BORNHORST. 1981. Emission rates of CO_2 from plume measurements. *In:* PW Lipman and DR Mullineaux (eds.) The 1980 eruptions of Mount St. Helens, Washington. *U.S. Geological Survey Profes sional Papers* 1250: 201–207.

HEMSTROM MA AND JF FRANKLIN. 1982. Fire and other disturbances of the forests of Mount Rainier National Park. *Quaternary Research* 18: 32–54.

HOUGHTON, JT, DING Y, GRIGGS DJ, NOGUER M., VAN DER LINDEN PJ AND D XIAOSU. 2001. Climate Change 2001: The Scientific Basis Contribution of Working Group I to the Third Assessment Report of the Intergovernmental Panel on Climate Change (IPCC). Cambridge, UK, Cambridge University Press, 944 p.

HULTINE KR AND JD MARSHALL. 2000. Altitude trends in conifer leaf morphology and stable carbon isotope composition. *Oecologia* 123: 32–40.

INDERMÜHLE A, STOCKER TF, JOOS F, FISCHER H, SMITH HJ, WAHLEN M., DECK B, MASTROIANNI D, TSCHUMI J, BLUNIER T, MEYER R AND B STAUFFER. 1999a. Holocene carbon_cycle dynamics based on CO_2 trapped in ice at Taylor Dome, Antarctica. *Nature* 398:121–126.

INDERMÜHLE A, STAUFFER B, STOCKER TF, RAYNAUD D AND JM BARNOLA. 1999b. Early Holocene atmospheric CO_2 concentrations. *Science* 286: 1815

INDERMÜHLE A, MONNIN E, STAUFFER B, STOCKER TF AND M WAHLEN. 2000. Atmospheric CO_2 concentration from 60 to 20 kyr BP from Taylor Dome ice core, Antarctica. *Geo physical Research Letters* 27: 735–738.

JAMES ER, MANGA M AND TP ROSE. 1999. CO_2 degassing in the Oregon Cascades. *Geology* 27: 823–826.

JANIK CJ, NEHRING NL AND AH TRUESDELL. 1983. Stable isotope geochemistry of thermal fluids from Lassen Volcanic National Park, California. *Geothermal Resources Coun cil Transactions* 7: 295–300.

JONES, HG. 1992. Plants and Microclimate. University Press, Cambridge, UK.

JOOS F, PLATTNER GK, STOCKER TF, MARCHAL O AND A SCHMITTNER. 1999. Global warming and marine carbon cycle feedbacks on future atmospheric CO_2. *Science* 284: 464–467.

KEELING CD AND TP WHORF. 2002. Atmospheric CO_2 Concentrations—Mauna Loa Observa tory, Hawaii, 1958–2001. Website: http://cdiac.esd.ornl.gov/ndps/ndp001.html

KOROL RL. 2001. Physiological attributes of 11 Northwest conifer species. *USDA Forest Service General Technical Report* RMRS–GTR–73.

KOUWENBERG LLR, MCELWAIN JC, KÜRSCHNER WM, WAGNER F, BEERLING DJ, MAYLE FE AND H VISSCHER. 2003 (Chapter 2). Stomatal frequency adjustment of four conifer species to historical changes in atmospheric CO_2. *American Journal of Botany* 90: 610–619.

KÜRSCHNER, WM. 1997. The anatomical diversity of recent and fossil leaves of the durmast oak (*Quercus petraea* Lieblein/ *Quercus pseudocastanea* Goeppert): implications for their use as biosensors of paleoatmospheric CO_2 levels. *Review of Palaeobotany and Palynology* 96: 1–30.

KÜRSCHNER, WM, VAN DER BURGH J, VISSCHER H AND DL DILCHER. 1996. Oak leaves as biosensors of late Neogene and early Pleistocene paleoatmospheric CO_2 concentra tions. *In:* R Poore and LC Sloan (eds.) Pliocene climates. *Marine Micropaleontology* 27: 299–312.

KÜRSCHNER, WM, WAGNER F, VISSCHER EH AND H VISSCHER. 1997. Predicting the response of leaf stomatal frequency to a future CO_2-enriched atmosphere: constraints from his torical observations. *Geologische Rundschau* 86: 512–517.

LAMBERS, H, CHAPIN III, FS AND TL PONS. 1998. Plant physiological ecology. New York, Springer Verlag. 540 p.

LARKIN, JC, MARKS DM, NADEAU J AND F SACK. 1997. Epidermal cell fate and patterning in leaves. *The Plant Cell* 9: 1109–1120.

LI C AND K WANG. 2003. Differences in drought response of three contrasting *Eucalyptus microtheca* F. Muell. Populations. *Forest Ecology and Management* 179: 377–385.

LICHTENTHALER HK. 1985. Differences in morphology and chemical composition of leaves grown at different light intensities and qualities. *In:* NR Baker, WJ Davies and CK Ong (eds.) Control of leaf growth. Cambridge University Press, Cambridge, UK: 201–221.

LIN J, JACH ME AND R CEULEMANS. 2001. Stomatal density and needle anatomy of Scots pine (*Pinus sylvestris*) are affected by elevated CO_2. *New Phytologist* 150: 665–674.

LOWDON JA. 1969. Isotopic fractionation in corn. *Radiocarbon* 11: 147–161.

MALONE SR, MAYEUX HS, JOHNSON HB AND HW POLLEY. 1993. Stomatal density and aperture length in four plant species grown across a subambient CO_2 gradient. *American Journal of Botany* 80: 1413–1418.

MAN RZ AND VJ LIEFFERS. 1999. Effects of shelterwood and site preparation on microclimate and establishment of white spruce seedlings in a boreal hardwood forest. *Forestry Chronicle* 75: 837–844.

MANN ME AND PD JONES. 2003. Global surface temperatures over the past two millennia. *Geophysical Research Letters* 30: doi: 10.0129/2003GL017814 10.0129.

MARCHAL O, STOCKER TF AND F JOOS. 1998. Impact of oceanic reorganizations on the ocean carbon cycle and atmospheric carbon dioxide content. *Paleoceanography* 13: 225–244.

MARCHAL O, STOCKER TF, JOOS F, INDERMÜHLE A, BLUNIER T AND J TSCHUMI. 1999. Modelling the concentration of atmospheric CO_2 during the Younger Dryas climate event. *Cli mate Dynamics* 15: 341–354.

MAYLE FE AND L CWYNAR.1995. Impact of Younger Dryas cooling event upon lowland veg etation of maritime Canada. *Ecological Monographs* 65: 129–154.

MCELWAIN JC, MAYLE FE AND DJ BEERLING. 2002. Stomatal evidence for a decline in atmos pheric CO_2 concentration during the Younger Dryas stadial: A comparison with Ant arctic ice core records. *Journal of Quaternary Science* 17: 21–29.

MCGEE KA, DOUKAS MP AND TM GERLACH. 2001. Quiescent hydrogen sulfide and carbon dioxide degassing from Mount Baker, Washington. *Geophysical Research Letters* 28: 4479–4482.

Medlyn BE, Barton CVM, Broadmeadow MSJ, Ceulemans R, De Angelis P, Forstreuter M, Freeman M, Jackson SB, Kellomäki S, Laitat E, Rey A, Roberntz P, Sigurdsson BD, Strassemeyer J, Wang K, Curtis PS and PG Jarvis. 2001. Stomatal conduct ance of forest species after long-term exposure to elevated CO_2 concentration: a syn thesis. *New Phytologist* 149: 247–264.

Mellander P-E. 2003. Spring Water Stress in Scots Pine: Interaction of snow and soil - temperature. Thesis. Acta Universitatis Agriculturae Sueciae, *Sylvestria* 287. Swed ish University of Agricultural Sciences, Uppsala

Miglietta F and A Raschi. 1993. Studying the effect of elevated CO_2 in the open in a natu rally enriched environment in Central Italy. *In:* J Rozema, H Lambers, SC van de Geijn and ML Cambridge (eds.) CO_2 and Biosphere. *Vegetatio* 104–105: 391–400.

Moran SC, Qamar A. and SD Malone. 1995. Seismicity at Mount Rainier. *IUGG XXI General Assembly Abstracts*: A453.

Mullineaux DR. 1974. Pumice and other pyroclastic deposits in Mount Rainier National Park, Washington. *Geological Survey Bulletin* 1326: 1–83.

Mullineaux DR. 1996. Pre-1980 Tephra-fall deposits erupted from Mount St. Helens, Wash ington. *U.S. Geological Survey Professional Papers* 1563.

Neftel, A, Moor E, Oeschger H and B Stauffer. 1985. Evidence from polar ice cores for the increase in atmospheric CO_2 in the past two centuries. *Nature* 315: 45–47.

Nestsyarovich MD, Panamarova AV and TF Dzyarugina. 1963. Zmyanenne anatamichnai budovy khvoi nekatorykh drevavykh parod u zalezhnastsi ad yae uzrostu i vyshyni prymatsavannya [Changes in anatomical structure of needles in some woody plants as affected by age and insertion level]. *Ser. biyal. Navuk* 1963: 5–13.

Nordhausen M. 1903. Über Sonnen- und Schattenblätter. *Berichte der Deutschen Botanischen Gesellschaft* 21: 30–45.

Osborne C. 1991. Statistical calibration: a review. *International Statistical Review* 59: 309–336.

Oskarsson N, Pálsson K, Olafsson H and T Ferreira. 1999. Experimental monitoring of carbon dioxide by low power IR-sensors: soil degassing in the Furnas Volcanic Cen tre, Azores. *Journal of Volcanology and Geothermal Research* 92: 181–193.

Owens JN. 1968. Initiation and development of leaves in Douglas fir. *Canadian Journal of Botany* 46: 271–278.

Packee EC. 1990. Tsuga heterophylla (Raf.) Sarg. western hemlock. *In*: RM Burns and BH Honkala (eds.) Silvics of North America. Volume 1. Conifers. *USDA Forest Service Agricultural Handbook* 654: 613-622.

Paoletti E and R Gellini. 1993. Stomatal density in beech and holm oak leaves collected over the last 200 years. *Acta Ecologica* 14: 173–178.

Park R and S Epstein. 1960. Carbon isotope fractionation during photosynthesis. *Geochimica et Cosmochimica Acta* 21: 110–126.

Parlange JY and PE Waggoner. 1970. Stomatal dimension and resistance to diffusion. *Plant physiology* 46: 337–342.

PASQUIER-CARDIN A, ALLARD P, FERREIRA T, HATTÉ C, COUTINHO R, FONTUGNE M AND M JAUDON. 1999. Magma-derived CO_2 emissions recorded in ^{14}C and ^{13}C content of plants grow ing in Furnas caldera, Azores. *Journal of Volcanology and Geothermal Research* 92: 195–207.

PEÑUELAS J AND R MATAMALA. 1990. Changes in N and S leaf content, stomatal density and specific leaf area of 14 plant species during the last three centuries of CO_2 increase. *Journal of Experimental Botany* 41: 1119–1124.

PETIT JR, JOUZEL J, RAYNAUD D, BARKOV NI, BARNOLA J-M, BASILE I, BENDER M, CHAPPELLAZ J, DAVIS M, DELAYGUE G, DELMOTTE M, KOTYAKOV VM, LEGRAND M, LIPENKOV VY, LORIUS C, PÉPIN L, RITZ C, SALTZMAN E AND M STIEVENARD.1999. Climate and atmos pheric history of the past 420,000 years from the Vostok ice core, Antarctica. *Nature* 399: 429-436.

PLATTNER GK, JOOS F, STOCKER TF AND O MARCHAL. 2001. Feedback mechanisms and sensi tivities of ocean carbon uptake under global warming. *Tellus* 53B: 564–592.

POOLE I, WEYERS JDB, LAWSON T AND JA RAVEN. 1996. Variations in stomatal density and index: implications for paleoclimatic reconstructions. *Plant, Cell and Environment* 19, 705–712.

POOLE I AND WM KÜRSCHNER. 1999. Stomatal density and index: the practice. *In:* TP Jones and NP Rowe (eds.) Fossil plant and spores: modern techniques. The Geological Society, London: 257–260.

PRITCHARD SG, MOSJIDIS C, PETERSON CM, RUNION GB AND HH ROGERS. 1998. Anatomical and morphological alterations in longleaf pine needles resulting from growth in el evated CO_2: interactions with soil resource availability. *International Journal of Plant Sciences* 159: 1002–1009.

QIANG W, WANG X, CHEN T, FENG H, AN L HE Y AND G WANG. 2003. Variations of stomatal density and carbon isotope values of *Picea crassifolia* at different altitudes in the Qilian Mountains. *Trees* 17: 258–262.

RAVEN JA AND PG FALKOWSKI. 1999. Oceanic sinks for atmospheric CO_2. *Plant, Cell and Environment* 22: 741–755.

RAYNAUD D, JOUZEL J, BARNOLA JM, CHAPPELLAZ J, DELMAS RJ AND C LORIUS. 1993. The ice record of greenhouse gases. *Science* 259: 926–934.

REDDY KR, ROBANA RR, HODGES HF, LIU XJ AND JM MCKINION. 1998. Interactions of CO_2 enrichment and temperature on cotton growth and leaf characteristics. *Environmen tal and Experimental Botany* 39, 117–129.

ROYER DL. 2001. Stomatal density and stomatal index as indicators of paleoatmospheric CO_2 concentration. *Review of Palaeobotany and Palynology* 114: 1–28.

ROYER DL, WING SL, BEERLING DJ, JOLLEY DW, KOCH PL, HICKEY LJ AND RA BERNER. 2001. Paleobotanical evidence for near-present-day levels of atmospheric CO_2 during part of the Tertiary. *Science* 292: 2310–2313.

RUBIN M, LOCKWOOD JP AND I FRIEDMAN. 1987. Effects of volcanic emanations on carbon-isotope content of modern plants near Kilauea volcano. *In:* RW Decker, TL Wright and PH Stauffer (eds.) Volcanism in Hawaii. *U.S. Geological Survey Professional Papers* 1350: 209–211.

Rundgren M and DJ Beerling. 1999. A Holocene CO_2 record from the stomatal index of subfossil *Salix herbacea* L. leaves from northern Sweden. *The Holocene* 9: 509–513.

Rundgren M and S Björck. 2003. Late-glacial and early Holocene variations in atmos pheric CO_2 concentration indicated by high-resolution stomatal index data. *Earth and Planetary Science Letters* 213: 191–204.

Ryan S. 1995. Quiescent Outgassing of Mauna Loa Volcano 1958-1994. *Geophysical Mono graphs* 92: 95–115.

Salisbury EJ. 1927. On the causes and ecological significance of stomatal frequency, with special reference to the woodland flora. *Philosophical Transactions of the Royal Society of London B* 216: 1–65.

Sarmiento JL and JC Orr. 1991. Three-dimensional simulations of the impact of Southern Ocean nutrient depletion on atmospheric CO_2 and ocean chemistry. *Limnology and Oceanography* 36: 1928–1950.

Saupé F, Strappa O, Coppens R, Guillet B and R Jaegy. 1980. A possible source of error in ^{14}C dates: volcanic emanations (examples from the Monte Amiata district, provinces of Grosseto and Sienna, Italy). *Radiocarbon* 22: 525–531.

Saxe HD, Ellsworth S and J Heath. 1998. Tree and forest functioning in an enriched CO_2 atmosphere. *New Phytologist* 139: 395–436.

Schoch PG. 1972. Effect of shading on structural characteristics of the leaf and the yield of fruit in *Capsicum annuum* L. *Journal of the American Society of horticultural sci ence* 97: 461–464.

Schoettle AW and SG Rochelle. 2000. Morphological variation of *Pinus flexilis* (Pinaceae), a bird-dispersed pine, across a range of elevations. *American Journal of Botany* 87: 1797–1806.

Schürmann B. 1959. Über den Einfluß der Hydratur und des Lichtes auf die Ausbildung der Stomata-Initialien. *Flora* 147: 471–520.

Schwander J. 1996. Gas diffusion in firn. *In:* EW Wolff and RC Bales (eds.) Chemical exchange between the atmosphere and polar snow: *NATO ASI Series* 143: 527–539.

Serna L, Torres-Contreras J and C Fenoll. 2002. Specification of stomatal fate in *Arabidopsis*: evidence for cellular interactions. *New Phytologist* 153: 399–404.

Sherrod DR and JG Smith. 1990. Quaternary extrusion rates of the Cascade Range, north western United States and southern British Columbia. *Journal of Geophysical Re search* 95: 19465–19474.

Siegenthaler U and T Wenk. 1984. Rapid atmospheric CO_2 variations and ocean circula tion. *Nature* 308: 624–626.

Siegenthaler U, Friedli H, Lötscher H, Moor A, Neftel A, Oeschger H and B Stauffer. 1988. Stable-isotope ratio and concentration of CO_2 in air from polar ice core. *Annals of Glaciology* 10: 151–156.

Smith BN and S Epstein. 1970. Biogeochemistry of the stable isotopes of hydrogen and carbon in salt marsh biota. *Plant physiology* 46: 738–742.

Sorey ML, Evans WC, Kennedy BM, Farrar CD, Hainsworth LJ and B Hausback. 1998. Carbon dioxide and helium emissions from a reservoir of magmatic gas beneath Mammoth Mountain, California. *Journal of Geophysical Research* 103: 15303–15323.

SPAHNI R, SCHWANDER J, FLÜCKIGER J, STAUFFER B, CHAPPELLAZ J AND D RAYNAUD. 2003. The attenuation of fast atmospheric CH_4 variations recorded in polar ice cores. *Geophysi cal Research Letters*: doi:10.129/2003GL017093.

STAUFFER B, BLUNIER T, DÄLLENBACH A, INDERMÜHLE A, SCHWANDER J, STOCKER TF, TSCHUMI J, CHAPPELLAZ J, RAYNAUD D, HAMMER CU AND HB CLAUSEN. 1998. Atmospheric CO_2 concentration and millennial-scale climate change during the last glacial period. *Nature* 392: 59–62.

STAUFFER B AND J TSCHUMI. 2000. Reconstruction of past atmospheric CO_2 concentrations by ice core analyses. *In:* T Hondoh (ed.) Physics of Ice Core Records. Sapporo, Hokkaido University Press: 217–241.

STEWART GH. 1986. Population dynamics of a montane conifer forest, western Cascade Range, Oregon, USA. *Ecology*. 67: 534-544.

STEWART JD AND J HODDINOTT. 1993. Photosynthetic acclimation to elevated atmospheric CO_2 and UV radiation in *Pinus banksiana*. *Physiologia Plantarum* 88: 493–500.

STRAND M, LUNDMARK T, SÖDERBERGH I AND P-E MELLANDER. 2002. Impact of seasonal air and soil temperatures on photosynthesis in Scots pine trees. *Tree Physiology* 22: 839–847.

STUIVER M, REIMER PJ, BARD E, BECK JW, BURR GS, HUGHEN KA, KROMER B, MCCORMAC G, VAN DER PLICHT J AND M SPURK. 1998. INTCAL98 radiocarbon age calibration, 24.000-0 cal. BP. *Radiocarbon* 40: 1041–1084.

SULERZHITZKY LD. 1970. Radiocarbon dating of volcanoes. *Bulletin Volcanologique* 35: 85–94.

SYMONDS RB, ROSE WI, BLUTH GJS AND TM GERLACH. 1994. Volcanic-Gas Studies: Methods, results and applications. *In:* MR Carroll and JR Holloway (eds.) Volatiles in Magma's. *Reviews in Mineralogy* 30: 1–66.

TAKAHASHI T, OLAFSSON J, GODDARD JG, CHIPMAN DW AND SC SUTHERLAND. 1993. Seasonal variation of CO_2 and nutrients in the high-latitude surface ocean: a comparative study. *Global Biogeochemical Cycles* 7: 843–878.

TARNAWSKI MG, GREEN TGA, BUEDEL B, MEYER A, ZELLNER H AND OL LANGE. 1994. Diel changes of atmospheric CO_2 concentration within, and above, cryptogam stands in a New Zealand temperate rain forest. *New Zealand Journal of Botany* 32: 329–336.

TICHÁ, I. 1982. Photosynthetic characteristics during ontogenesis of leaves. 7. Stomata den sity and sizes. *Photosynthetica* 16: 375–471.

TOGNETTI R, MINNOCCI A, PENUELAS J, RASCHI A AND MB JONES. 2000. Comparative field water relations of three Mediterranean shrub species co-occurring at a natural CO_2 vent. *Journal of Experimental Botany* 51: 1135–1146.

TOMLINSON PB. 1974. Development of the stomatal complex as a taxonomic character in the monocotyledons. *Taxon* 23: 109–128.

TUCKER, GF, HINCKLEY TM, LEVERENZ J AND S JIANG. 1987. Adjustment of foliar morphology in the acclimation of understory Pacific silver fir following clearcutting. *Forest Ecol ogy and Management* 21: 249–268.

VAN DER BURGH J , VISSCHER H, DILCHER DL AND WM KÜRSCHNER. 1993. Paleoatmospheric signatures in Neogene fossil leaves. *Science* 260: 1788–1790.

VAN DE WATER PK, LEAVITT SW AND JL BETANCOURT. 1994. Trends in stomatal density and $^{13}C/^{12}C$ ratios of Pinus flexilis during last glacial-interglacial cycle. *Science* 264: 239–242.

VAN VOLKENBURGH E. 1987. Regulation of dicotylenous leaf growth. *In:* DJ Cosgrove and DP Knievel (eds.) Physiology of cell expansion during plant growth. Rockville, The American Society of Plant Physiologists: 193–201.

VAN VOLKENBURGH E. 1999. Leaf expansion – an integrating plant behaviour. *Plant, Cell and Environment* 22: 1463–1473.

VIKTOR A AND MD CRAMER. 2003. Variation in root-zone CO_2 concentration modifies iso topic fractionation of carbon and nitrogen in tomato seedlings. *New Phytologist* 157: 45–54.

VON GUTTENBERG H. 1961. Grundzuge der Histogenese Hoheren Pflanze: II die Gymnospermen. Handbuch der Pflanzenanatomie Bd 8, Tl 4. Berlin: Gebrüder Borntraeger.

WAGNER F. 1998. The influence of environment on the stomatal frequency in Betula. PhD Thesis, Laboratory of Palaeobotany and Palynology, Utrecht University, Utrecht, The Netherlands. *LPP Contributions Series* 9: 1–102.

WAGNER F, BELOW R, DE KLERK P, DILCHER DL, JOOSTEN H, KÜRSCHNER WM AND H VISSCHER. 1996. A natural experiment on plant acclimation: lifetime stomatal frequency re sponse of an individual tree to annual atmospheric CO_2 increase. *Proceedings of the National Academy of Sciences* 93: 11705–11708.

WAGNER F, BOHNKE SJP, DILCHER DL, KÜRSCHNER WM, VAN GEEL B AND H VISSCHER. 1999a. Century-scale shifts in early Holocene atmospheric CO_2 concentration. *Science* 284: 1971–1973.

WAGNER F, BOHNCKE SJP, DILCHER DL,KÜRSCHNER WM, VAN GEEL B AND H VISSCHER. 1999b. Response to Technical Comments by Indermühle and et al. Birks et al. on "Century-scale shifts in early Holocene atmospheric CO2 concentrations". *Science* 286: 1815a.

WAGNER F, NEUVONEN S, KÜRSCHNER WM AND H VISSCHER. 2000. The influence of hybridiza tion on epidermal properties of birch species and the consequences for palaeoclimatic interpretation. *Plant Ecology* 148: 61–69.

WAGNER F, AABY B AND H VISSCHER. 2002. Rapid atmospheric CO_2 changes associated with the 8.200-years-B.P. cooling event. *Proceedings of the National Academy of Sci ences* 99: 12011–12014.

WATTS WR, NEILSON RE AND PG JARVIS. 1976. Photosynthesis in Sitka spruce (*Picea sitchensis* (Bong) Carr.) VII: Measurements of stomatal conductance and $^{14}CO_2$ uptake in a forest canopy. *Journal of Applied Ecology* 13: 623–638.

WILMER CM AND P FIRTH. 1980. Carbon isotope discrimination of epidermal tissue and mesophyll tissue from leaves of various plants. *Journal of Experimental Botany* 31: 1–5.

WOODWARD FI. 1987. Stomatal numbers are sensitive to increases in CO_2 concentration from pre-industrial levels. *Nature* 327: 617–618.

WOODWARD FI AND FA BAZZAZ. 1988. The response of stomatal density to CO_2 partial pres sure. *Journal of Experimental Botany* 39: 1771–1781.

WOODWARD FI AND CK KELLY. 1995. The influence of CO_2 concentration on stomatal den sity. *New Phytologist* 131: 311–327.

WOOLLER MJ AND ADQ AGNEW. 2002. Changes in graminoid stomatal morphology over the last glacial-interglacial transition: evidence from Mount Kenya, East Africa. *Palaeogeography, Palaeoclimatology, Palaeoecology* 177: 123–136.

YAMAGUCHI DK. 1983. New tree-ring dates for recent eruptions of Mount St. Helens. *Qua ternary Research* 20: 246–250.

YI C, GONG P, XU M AND Y QI. 2001. The effects of buffer and temperature feedback on the oceanic uptake of CO_2. *Geophysical Research Letters* 28: 751–754.

ZIMBELMAN DR, RYE RO AND GP LANDIS. 2000. Fumaroles in ice caves on the summit of Mount Rainier – preliminary stable isotope, gas, and geochemical studies. *Journal of Volcanology and Geothermal Research* 97: 457–473.

SAMENVATTING

Klimaatmodellen voorspellen een sterke toename in temperatuur als gevolg van de uitstoot van koolstofdioxide door de mens. Dit bevestigt het beeld van een koppeling tussen atmosferische CO_2-concentratie en klimaatsveranderingen. Om het effect van de huidige snelle toevoeging van CO_2 aan het klimaatsysteem te kunnen doorgronden, moeten eerst het voorkomen en de grootte van natuurlijke CO_2-veranderingen en hun klimatologische gevolgen in kaart worden gebracht. Gedurende de laatste ijstijden vertoonde het atmosferische CO_2 gehalte, gemeten aan ingesloten luchtbellen in Antarctische ijskernen, fluctuaties gelijktijdig met gereconstrueerde temperatuurschommelingen. Het is daarentegen niet duidelijk of dergelijke CO_2 veranderingen ook plaatsvinden op kortere tijdschalen, zoals bijvoorbeeld tijdens koelere periodes in het Holoceen, de huidige tussen-ijstijd van de afgelopen 10.000 jaar. Nauwkeurige en gedetailleerde reconstructies van de pre-industriële ontwikkeling van het atmosferische CO_2-niveau zijn noodzakelijk om meer inzicht te krijgen in een eventuele koppeling tussen natuurlijke CO_2-veranderingen en klimaatschommelingen op relatief korte tijdschalen van decennia tot eeuwen.

Een relatief nieuwe en vaak gebruikte methode voor de reconstructie van Holocene CO_2 niveaus op deze korte tijdschalen is de analyse van de frequentie van stomata (huidmondjes) op fossiele bladeren afkomstig uit veen- en meerafzettingen. Verschillende soorten planten.gegroeid in natuurlijke en experimentele omstandigheden, vertonen een aanpassing van de hoeveelheid huidmondjes aan de CO_2-concentratie in de lucht. Door de geopende huidmondjes in de epidermis (buitenste bladlaag) vindt de gaswisseling in een blad plaats en bij verandering van de hoeveelheid huidmondjes kan de balans tussen de opname van CO_2 voor de fotosynthese en de verdamping van water verschoven worden. Als nu de hoeveelheid huidmondjes bij een hoger atmosferisch CO_2-gehalte afneemt, kan dezelfde fotosynthese-activiteit bereikt worden met minder verdamping, wat in de meeste omstandigheden gunstig zal zijn voor een plant. Door nu de relatie tussen de hoeveelheid huidmondjes van verschillende soorten en het toegenomen CO_2-niveau in de lucht over de laatste eeuw te bepalen, is het mogelijk om aan de hand van huidmondjestellingen op fossiele bladeren de atmosferische CO_2 concentratie in het verleden te reconstrueren.

Tot nu toe zijn stomataire CO_2 reconstructies tijdens het Holoceen voornamelijk gebaseerd op loofbomen en -struiken. Coniferen domineren veelal in bossen in de gematigde en boreale klimaatzones, het gebruik van fossiele coniferennaalden zou dit soort reconstructies in nieuwe gebieden maar ook andere tijdsperiodes mogelijk maken. Hoewel fossiele naalden vaak gevonden worden in Holocene veen- en meerafzettingen zijn ze amper nog gebruikt voor

CO_2-reconstructies nadat de eerste studies suggereerden dat de stomatale frequentie bij coniferen niet meer zou veranderen bij stijging van CO_2 boven de 280 ppmv. Dit gebrek aan respons bij hogere CO_2-waarden zou daarentegen ook verklaard kunnen worden door het gebruik van van voor loofbomen ontwikkelde telmethoden in deze studies op coniferennaalden. De bladontwikkeling in coniferen verloopt immers anders dan bij loofverliezende soorten en leidt tot een ander huidmondjespatroon op de epidermis. Om het potentieel van coniferen voor CO_2-recontructies opnieuw te beoordelen is het nodig om aangepaste telmethoden te ontwikkelen, toegespitst op de specifieke bladmorfologie van coniferen. Bovendien moet voor een succesvolle toepassing van de stomataire frequentie op coniferennaalden als maat voor CO_2-concentraties ook de invloed van andere biologische - en omgevingsfactoren op de huidmondjesdichtheid bepaald worden.

De stomataire analyse van coniferen uit noordwest Amerika zou in hoge mate bij kunnen dragen aan de uitbreiding van het arsenaal aan taxonomisch, ecologisch en geografisch contrasterende soorten die te gebruiken zijn voor de reconstructie van CO_2 concentraties in het verleden. Dit proefschrift heeft daarom de volgende doelstellingen:
(1) De ontwikkeling van conifeer-specifieke telmethoden om de respons van geselecteerde coniferensoorten op de CO_2-stijging tijdens de afgelopen eeuw te kwantificeren. (2) De validatie van deze CO_2-respons door de invloed van lokale biologische en omgevingsfactoren op huidmondjesaantallen te bestuderen. (3) Het verkrijgen van hoge-resolutie CO_2-reconstructies voor het late Holoceen met behulp van stomataire frequentieanalyse op fossiele coniferennaalden, en (4) de vergelijking van zowel de hier verkregen als al bestaande Holocene CO_2-reconstructies met wereldwijde en regionale klimaatschommelingen om het verband tussen klimaat en CO_2 op kortere tijdschalen nader te bestuderen.

In **hoofdstuk 2** worden de huidmondjesaantallen op naalden van vier Noordamerikaanse coniferensoorten (*Tsuga heterophylla*, *Picea glauca*, *P. mariana* en *Larix laricina*) tijdens de CO_2-stijging gedurende de laatste eeuw gemeten. Het blijkt dat de meest gebruikte maat voor stomataire frequentie bij loofverliezende soorten, de stomataire index (SI: de verhouding tussen het aantal huidmondjes en het totaal aantal epidermiscellen), bij deze coniferen niet veranderd is. Dit kan verklaard worden door de specifieke huidmondjespatronen op coniferennaalden. Een nieuwe maat, het aantal huidmondjes per millimeter naaldlengte, is daarentegen wel afgenomen tijdens de CO_2 stijging van de laatste eeuw. Omdat deze afname bij *Tsuga heterophylla* niet te verklaren is met behulp van andere biologische of omgevingsfactoren, zoals temperatuur of neerslag, kan gesteld worden dat de stijging in CO_2 tijdens de laatste eeuw deze aanpassing in huidmondjesaantal heeft veroorzaakt. Deze duidelijke respons op CO_2-waarden van 290 tot 370 ppmv, samen met de resistentie van fossiele naalden, die goed bewaard blijven in sedimenten, maken dat de hier onderzochte coniferensoorten bij uitstek geschikt lijken voor het reconstrueren van CO_2 niveaus uit het verleden.

Tot nu toe wordt in stomataire analyse de voorkeur gegeven aan het meten van de stomataire index (SI: de verhouding tussen het aantal huidmondjes en het totaal aantal epidermiscellen) boven de stomataire dichtheid (SD: het aantal huidmondjes per mm^2 bladoppervlak), omdat de SD mede afhangt van de grootte van de tussenliggende epidermiscellen. Uit eerdere onderzoeken blijkt dat omgevingsfactoren als lichtintensiteit en beschikbare hoeveelheid water de strekkingsgraad van de epidermiscellen, en daardoor de SD, sterk beinvloeden. Dit is ook goed zichtbaar in afname van de SD in de latere fasen in de bladontwikkeling, als de sterkste strekkinggroei plaatsvindt. Omdat in coniferen de SD beter lijkt te reageren op CO_2 dan de SI, moet de invloed van strekkinggroei op huidmondjesaantallen in coniferen nauwkeurig bepaald worden. Dat kan bijvoorbeeld in jonge naalden waarvan de ontwikkeling nog niet voltooid is. In **hoofstuk 3** wordt de differentiatie van stomata en andere epidermiscellen tijdens de bladgroei van *Tsuga heterophylla* bekeken. De eerste huidmondjes verschijnen in rijen aan de top van de naald en verspreiden zich vervolgens richting de basis. Het aantal rijen stomata verandert niet meer tijdens de bladontwikkeling. De SD neemt daarentegen (niet-lineair) af tot 50% van de uiteindelijke bladlengte bereikt is, maar daarna niet meer. Het totale aantal huidmondjes op de naald neemt gedurende de hele groeiperiode toe, doordat kennelijk tot op het eind nog nieuwe stomata en epidermiscellen gevormd worden. Dit is een fundamenteel verschil met loofbomen en -struiken, waarvan de bladeren in latere fasen voornamelijk door strekkingsgroei van de epidermiscellen in oppervlakte toenemen. Aangezien zowel de huidmondjesdichtheid, het aantal rijen, als het aantal huidmondjes per millimeter naaldlengte niet meer veranderen na het bereiken van de helft van de uiteindelijke naaldlengte, heeft de mate van bladontwikkeling in de gebruikte coniferennaalden geen invloed op de betrouwbaarheid van de hieruit voorkomende CO_2 reconstructies.

Nu is duidelijk aangetoond en geverifieerd dat huidmondjesaantallen van *Tsuga heterophylla* naalden op CO_2 reageren, en deze relatie is in hoofstuk 2 gekwantificeerd. In **hoofdstuk 4** wordt deze relatie gebruikt om de atmosferische CO_2-concentratie gedurende de laatste 1200 jaar te reconstrueren op basis van fossiele naalden in meersediment afkomstig uit Jay Bath (Mount Rainier, Washington, USA). In de gereconstrueerde CO_2-concentraties zijn duidelijke schommelingen met een duur van honderden jaren te zien rond een lange-termijngemiddelde van 280-290 ppmv, en de industriële CO_2-stijging van 280 tot 370 ppmv is duidelijk aanwezig in het meest recente deel. Minimale CO_2-niveaus van 260 ppmv zijn te vinden rond 860 AD en 1160 AD, en kleinere afnames tot 275-280 ppmv vinden plaats rond 1600 AD en 1800 AD. Tussen deze lage waarden liggen CO_2-maxima van 300 ppmv rond 1000 AD, 320 ppmv rond 1300 AD en 300 ppmv rond 1700 AD. Deze fluctuaties lijken synchroon te verlopen met zowel wereldwijde temperatuursschommelingen als veranderingen in de watertemperatuur van de Noord Atlantische Oceaan; dit zou wijzen op een voortdurende koppeling tussen CO_2-niveau en klimaat in het Holoceen.

Bij uitbreiding van de stomataire frequentie dataset verder terug in de tijd tot 200 AD vertonen de naalden van *Tsuga heterophylla* onverwacht lage huidmondjesaantallen tussen 300 en 750 AD (**hoofdstuk 5**). In tegenstelling tot de fluctuaties beschreven in het vorige hoofdstuk, komen deze extreem lage hoeveelheden, die zouden wijzen op zeer hoge CO_2-concentraties,

niet overeen met bijzonder hoge temperaturen. Daarentegen vallen de lage huidmondjesaantallen wel samen met een periode van sterke verstoring van de vegetatie rond Jay Bath. Uit een reconstructie van de lokale vegetatie gebaseerd op de fossiele naalden in het sediment blijkt dat tussen 300 en 700 AD voornamelijk soorten aanwezig waren die karakteristiek zijn voor een vroege successie na een verstoring. Toen *Tsuga heterophylla* zich in die tijd uitbreidde, was dat dus in een relatief open landschap, in tegenstelling tot het gesloten bos waarin *T. heterophylla* daarna op deze plek groeide. Het open karakter van deze plek aan de rand van het natuurlijke hoogtevoorkomen van de soort zorgde waarschijnlijk voor suboptimale groeicondities voor de eerste generaties *T. heterophylla*. Met name de verlenging van de periode van koude bodemcondities zou kunnen hebben geleid tot vermindering van het aantal huidmondjes om het daaraan gekoppelde watergebrek te verminderen. Na 750 AD kwam *T. heterophylla* onafgebroken voor in een gesloten bos, zodat deze stressinvloed op huidmondjesaantallen geen rol meer speelde gedurende de laatste 1200 jaar.

Niet alleen klimatologische en ecologische factoren op hoogte compliceren de interpretatie van de stomataire frequentie data, maar ook het feit dat Mount Rainier, waar Jay Bath op ligt, een nog steeds actieve vulkaan is. Tijdens uitbarstingen, maar ook in rustige periodes, kunnen flinke hoeveelheden vulkanisch CO_2 ontsnappen uit de krater zelf, geothermische gebieden, of uit de bodem op de flanken van de vulkaan. Nu is de afstand tussen Jay Bath en de krater en huidige geothermisch actieve gebieden te groot om een significante CO_2-uitstoot uit de laatstgenoemde bronnen te verwachten (**hoofdstuk 6**). Om ook lokale vulkanische CO_2-produktie via de bodem uit te sluiten, zijn metingen aan koolstofisotopen van plantenmateriaal gedaan. Zelfs kleine hoeveelheden vulkanisch CO_2 zouden namelijk een duidelijk signaal in koolstofisotopen achterlaten bij de opname in planten via fotosynthese. Aangezien dergelijke aanwijzingen niet gevonden werden, zijn de stomataire frequentiedata van Jay Bath gedurende de laaste 2000 jaar niet beinvloed door vulkanisch geproduceerde CO_2.

In **hoofstuk 7** tenslotte worden uiteindelijk alle beschikbare stomataire CO_2-reconstructies voor bepaalde periodes van het Holoceen, waarin de meest prominente klimaatschommelingen plaatsvonden, met elkaar vergeleken, inclusief de CO_2-reconstructie over de laatste 1200 jaar van Jay Bath. Voor drie van dergelijke periodes zijn meerdere stomataire datasets beschikbaar, namelijk voor de zogenoemde Preboreale Oscillatie in het vroegste Holoceen, de koele periode rond 8200 jaar geleden, en tenslotte de Kleine IJstijd tijdens de laatste 1000 jaar. Alle stomataire data laten sterk gelijkende fluctuaties in CO_2 qua timing, duur (eeuwen) en amplitude zien tijdens deze koelere periodes, wat pleit tegen het beeld van relatief stabiele CO_2-concentraties gedurende het hele Holoceen zoals bekend uit de ijskernmetingen. Omdat de stomataire CO_2-data afkomstig zijn van totaal verschillende soorten uit ver uit elkaar gelegen gebieden, lijkt het uitgesloten dat de gevonden fluctuaties een gevolg zouden zijn van lokale klimaatsfactoren of methodologische beperkingen in de calibraties. De grote overeenkomsten in de diverse stomataire CO_2-reconstructies vormen

een sterk bewijs voor de betrouwbaarheid van stomataire analyse als maat voor CO_2 niveaus in het verleden en pleiten voor een varierend atmosferisch CO_2-gehalte tijdens kortdurende klimaatschommelingen in het Holoceen.

Samenvattend maken de studies in dit proefschrift het aannemelijk dat huidmondjesaantallen op coniferennaalden betrouwbare indicatoren voor CO_2-concentraties in het verleden kunnen zijn, en bij uitstek gebruikt kunnen worden voor de reconstructie van relatief hoge CO_2-concentraties. Wel dient in hooggelegen gebieden rekening gehouden te worden met de invloed van extreme stressfactoren in open vegetaties tijdens de vroege vegetatie-successie. Bovendien ondersteunt de op coniferen gebaseerde CO_2-reconstructie over de afgelopen 1200 jaar de uit andere stomataire CO_2-reconstructies gebleken koppeling tussen CO_2 en klimaat op korte tijdschalen gedurende het Holoceen.

ACKNOWLEDGEMENTS

Just add in equal measures of cheer, despair, and long hours of counting stomata in a dark room, stir thoroughly, and boom ! The result is this beautiful thesis right in front of you. I have many people to thank who contributed their share in the cooking process over the last five years (and a bit), so let's get started:

First of all, of course, there's the stomata-trojka: Rike Wagner, Wolfram Kürschner, and Henk Visscher. I would never have managed without them. Wolfram and Rike started the whole stomata-subsection of our department with their theses, and my work is based on the foundations they have laid. Rike, isn't it surprising how often stubborn minds do think alike ? Thank you for all the encouragement, scientific discussions and (smoking) companionship over the years. Wolfram and Henk V, I've very much enjoyed our discussions when I came up with yet another theory, and you were invaluable in shaping up this piece of work. Especially our weekend-Montfoort-sessions in the end, where we cracked our brains over "De Bult", were greatly appreciated.

A special thanks goes out to Han Leereveld. He left the lab when I got started on my PhD, but he introduced me in the world of science during my master's research and is responsible for me getting the research-bug.

I'm also indebted to many other colleagues for their help. Thank you, Andy Lotter, Bert van der Zwaan and Cathy Whitlock for reviewing this thesis, and my co-authors Jenny Mc Elwain, David Beerling and Francis Mayle. All the work done by Peter Dunwiddie in his thesis on vegetation development on Mount Rainier has proven to be an invaluable basis.

And the best part of trying to work on inter-continent comparisons is definitely getting the material yourself. I've been extremely lucky to do fieldwork in two of the most gorgeous (and wettest) country sides, the Pacific Northwest and New Zealand. Of course much help was needed and gratuitously offered. Thanks go out to Peter Dunwiddie, Cathy Whitlock, Estella Leopold, Les Cwynar, the people at Mount Rainier National Park, Johan van der Burgh and Wolfram for an unforgettable field trip to Washington.

Unfortunately the data from New Zealand could not be included in this thesis, but it will go out into the world someday. This field trip was an amazing experience, not in the least because Kiwi's turned out to be the most helpful people I've ever met. The people at GNS

(Lower Hutt), Massey University (Palmerston North), Landcare (Christchurch), Neville Moar and Marcus Vandergoes were wonderful, and my fieldwork would never have succeeded without the two hardest working technicians in the world: Ton van Druten and David Feek.

Marjolein Mullen, Leonard Bik and Jan van Tongeren helped out in all the administrative stuff, making figures and getting my computer to do what I want.

I can't acknowledge all the people working at the Laboratory of Palaeobotany and Palynology over the last five years separately, but thank you all (students, PhD's, staff and foreign guests) for making it such a great place to work. The former PhD's (Karin, Erica, Marloes, Hanneke, neighbour Ivo, and especially Cindy among them) were great in sharing their experience and lots of mental support. Tom, Timme, Merlijn, Frank, Erwin, Appy, Jeroen, Welmoed, Anja and Alice, thank you for the good company and fun (and the cheese), and good luck with finishing your own books. Ivo and Lennart, it was great to get rid of my frustration trying to beat the crap out of you in our squash-games.

Willemien, you did a wonderful job designing my cover ! Pinabeest Conceptual and Visual solutions: for all your artwork, not just thesis covers (info@pinabeest.nl).

Financial support by NWO/ALW mainly, but also the Department of Botanical Palaeo-ecology/Laboratory of Palaeobotany and Palynology and the LPP Foundation is gratefully acknowledged.

Since life is not all about work, there are many other people without whom I would never have finished this project. Too many to thank them all personally, but you know who you are !

My mom and dad, Oma Bakx, Bram, Margot, Viola and Joelle, you are the best, your care and support during the rough times means more to me than I can say.

All my friends, you've provided great diversions, entertainment and support over the last years, let's keep that up !

And a very special thanks goes out to all the people who have shared my life at IBB 143-2, making it the best place to call home.

And now it's time to celebrate !

CURRICULUM VITAE

Lenny Liesbeth Ria Kouwenberg werd op 11 oktober 1973 geboren te Leiden. In 1991 behaalde zij het gymnasium diploma aan het Stedelijk Gymnasium te Leiden. In datzelfde jaar begon zij met een studie Biologie aan de Universiteit Utrecht (UU). Zij koos voor de afstudeerrichting Paleo-ecologie en tijdens de doctoraalfase verrichtte zij twee afstudeeronderzoeken. Het eerste onderzoek werd onder begeleiding van Dr. Stella Noach uitgevoerd bij de vakgroep Populatiegenetica, en betrof een studie naar erfelijkheid van fenotypische plasticiteit in lichaamsgrootte bij verschillende omgevingstemperaturen in *Drosophila melanogaster*. Tijdens het tweede afstudeeronderzoek, bij Dr. Han Leereveld van de vakgroep Palaeobotanie en Palynologie, onderzocht zij veranderingen in het mariene afzettingsmilieu in het Mediterrane gebied ten tijde van het onder-Krijt met behulp van dinoflagellaten en pollen en sporen. In 1997 behaalde zij het doctoraal diploma in de Biologie en was vervolgens werkzaam als palynologisch consultant bij de Stichting LPP. Vanaf juni 1998 heeft zij als Onderzoeker in Opleiding (gefinancierd door NWO) het in dit proefschrift beschreven onzerzoek uitgevoerd, in dienst bij de leerstoelgroep Botanische Paleoecologie (voorheen Palaeobotanie en Palynologie), faculteit Biologie van de Universiteit van Utrecht.

APPENDICES

Table A1: statistical significance in student's T-tests for differences in stomatal parameters between developmental stages. ** $P < 0.01$; * $P < 0.05$; n.s. $P > 0.05$.

	Developmental stage	Means	Fully grown	Small	Out of bud	Just out of bud	From bud
Needle length (mm)	Fully grown	12.0 ± 0.9	–	**	**	**	**
	Small	7.2 ± 1.1	**	–	*	*	**
	Out of bud	5.8 ± 0.2	**	*	–	n.s.	**
	Just out of bud	5.1 ± 1.1	**	*	n.s.	–	*
	From bud	2.7 ± 1.5	**	**	**	*	–
Needle width (mm)	Fully grown	2.2 ± 0.13	–	n.s.	**	**	**
	Small	2.1 ± 0.16	n.s.	–	*	**	**
	Out of bud	1.8 ± 0.15	**	*	–	n.s.	**
	Just out of bud	1.7 ± 0.19	**	**	n.s.	–	*
	From bud	1.4 ± 0.09	**	**	**	*	–
Needle area (mm)	Fully grown	26.1 ± 2.7	–	**	**	**	**
	Small	15.3 ± 3.2	**	–	*	*	**
	Out of bud	10.6 ± 0.9	**	*	–	n.s.	**
	Just out of bud	8.6 ± 2.7	**	*	n.s.	–	*
	From bud	3.6 ± 0.9	**	**	**	*	–
Relative needle length (%)	Fully grown	100 ± 7.2	–	**	**	**	**
	Small	60.2 ± 9.0	**	–	*	*	**
	Out of bud	48.5 ± 1.5	**	*	–	n.s.	**
	Just out of bud	42.6 ± 9.0	**	*	n.s.	–	*
	From bud	22.2 ± 4.2	**	**	**	*	–

Table A1 continued

	Developmental stage	Means	Fully grown	Small	Out of bud	Just out of bud	From bud
Relative needle width (%)	Fully grown	100 ± 6.0	–	n.s.	**	**	**
	Small	97.3 ± 7.5	n.s.	–	*	**	**
	Out of bud	83.7 ± 6.9	**	*	–	n.s.	**
	Just out of bud	75.7 ± 8.8	**	**	n.s.	–	*
	From bud	62.5 ± 3.9	**	**	**	*	–
Relative needle area (%)	Fully grown	100 ± 10.3	–	**	**	**	**
	Small	58.8 ±12.5	**	–	*	*	**
	Out of bud	40.6 ±3.4	**	*	–	n.s.	**
	Just out of bud	32.8 ±10.5	**	*	n.s.	–	*
	From bud	14.0 ±3.4	**	**	**	*	–
SR	Fully grown	15.08 ± 0.55	–	n.s.	n.s.	n.s.	*
	Small	15.02 ± 2.22	n.s.	–	n.s.	n.s.	n.s.
	Out of bud	15.06 ± 0.66	n.s.	n.s.	–	n.s.	n.s.
	Just out of bud	14.25 ± 1.75	n.s.	n.s.	n.s.	–	n.s.
	From bud	17.33	*	n.s.	n.s.	n.s.	–
SD (mm^{-2})	Fully grown	213.1 ± 20.1	–	n.s.			
	Small	218.1 ± 10.3	n.s.	–			
SD_{top} (mm^{-2})	Fully grown	223.4 ± 19.3	–	n.s.	**	**	n.s.
	Small	226.3 ± 19.9	n.s.	–	n.s.	n.s.	**
	Out of bud	274.9 ± 7.4	**	n.s.	–	n.s.	**
	Just out of bud	313.2 ± 14.6	**	n.s.	n.s.	–	*
	From bud	558.4 ± 74.0	n.s.	**	**	*	–

Table A1 continued

	Developmental stage	Means	Fully grown	Small	Out of bud	Just out of bud	From bud
TSDL (mm^{-1})	Fully grown	213 ± 24	–	n.s.			
	Small	218 ± 43	n.s.	–			
$TSDL_{top}$ (mm^{-1})	Fully grown	223 ± 23	–	n.s.	**	*	**
	Small	227 ± 54	n.s.	–	n.s.	n.s.	**
	Out of bud	274 ± 9	**	n.s.	–	n.s.	**
	Just out of bud	289 ± 42	*	n.s.	n.s.	–	*
	From bud	704	**	**	**	*	–
SN	Fully grown	2535 ± 226	–	**	**	**	**
	Small	1562 ± 330	**	–	n.s.	n.s.	n.s.
	Out of bud	1588 ± 57	**	n.s.	–	n.s.	n.s.
	Just out of bud	1612 ± 469	**	n.s.	n.s.	–	n.s.
	From bud	1409	**	n.s.	n.s.	n.s.	–
PL (µm)	Fully grown	31.3 ± 1.4	–	n.s.			
	Small	29.1 ± 1.9	n.s.	–			
PL_{top} (µm)	Fully grown	31.3 ± 2.8	–	n.s.	**	**	**
	Small	28.4 ± 2.9	n.s.	–	*	*	**
	Out of bud	23.0 ± 1.2	**	*	–	n.s.	n.s.
	Just out of bud	22.8 ± 1.9	**	*	n.s.	–	n.s.
	From bud	20.8 ± 2.0	**	**	n.s.	n.s.	–
SL (µm)	Fully grown	71.9 ± 3.0	–	**			
	Small	66.2 ± 1.3	**	–			

Table A2: Mean number of stomata per mm needle length (TSDL), mean pore length (PL) and estimated maximum stomatal conductance (G_{max}) of *Tsuga heterophylla* needles per depth interval in the Jay Bath sediment core.

depth (cm)	age (year AD)	TSDL (n/mm)	PL (µm)	Gmax (mm s^{-1})
1	1990	185.8	27.4	9.7
3	1963	182.8	28.1	10.0
4	1946	201.1	27.7	10.7
5	1927	203.7	26.9	10.7
8	1859	241.6	26.8	12.2
9	1834	223.6	27.1	11.6
10	1807	222.7	27.3	11.7
11	1779	236.1	27.9	12.5
12	1751	202.8	29.1	11.6
13	1721	232.4	27.8	12.4
14	1690	213.1	27.5	11.9
16	1627	227.6	28.8	13.0
17	1595	215.5	26.2	10.6
18	1563	254.1	25.9	12.3
19	1530	197.7	26.2	9.8
22	1431	234.9	26.6	11.7
24	1365	224.2	26.3	11.1
25	1332	194.9	29.5	11.3
26	1299	212.6	28.0	11.5
27	1267	232.5	28.2	12.7
28	1236	226.0	28.2	12.3
29	1204	232.5	28.1	12.7

Table A2 continued

depth (cm)	age (year AD)	TSDL (n/mm)	PL (μm)	Gmax (mm s^{-1})
30	1173	255.5	24.8	12.0
31	1143	233.9	27.5	12.5
32	1113	238.7	27.3	12.3
33	1083	238.9	27.7	12.5
34	1055	208.7	28.4	11.4
35	1026	253.3	30.2	15.1
36	999	210.1	28.9	11.8
37	971	222.5	28.9	12.4
38	945	217.9	27.2	11.3
39	919	240.7	26.6	12.2
41	869	239.2	28.3	13.0
42	844	244.2	26.1	11.8
43	820	195.4	27.5	10.3
44	797	227.7	28.8	12.8
45	774	245.0	26.9	12.5
46	752	209.7	27.5	11.1
47	730	172.7	28.9	10.1
48	708	223.2	25.8	11.2
53	603	179.7	28.7	10.1
54	582	188.4	27.5	10.0
55	560	176.7	29.4	10.0
56	539	186.4	27.6	9.8
58	495	190.0	27.5	9.9

Table A2 continued

depth (cm)	age (year AD)	TSDL (n/mm)	PL (μm)	Gmax (mm s^{-1})
59	473	178.5	30.5	10.8
60	450	165.0	31.2	10.0
61	426	175.5	28.8	9.7
62	401	176.8	29.9	10.3
63	375	213.2	28.9	12.0
64	349	225.7	27.5	10.9
65	321	208.6	28.3	10.3
66	291	242.5	26.0	11.2
67	260	218.6	26.8	11.3
68	228	201.1	27.9	10.9

Table A3: AMS radiocarbon dates from the Borchert section (Van der Plicht et al., unpublished).

WMD Nr.	Sample Nr.	Depth (cm)	Material dated	Laboratory Nr.	$\delta^{13}C$	^{14}C age
18	52	499.2	*Betula*	GrA-17576	−26.72	9490 ± 60
17	50	500.8	*Betula*	GrA-17455	−26.52	9610 ± 50
16	48	502.4	*Betula*	GrA-17453	−26.70	9600 ± 50
15	45	504.8	*Betula*	GrA-17575	−27.44	9530 ± 60
14	42	507.2	*Betula* + *Populus*	GrA-1715	−26.14	9650 ± 50
13	40	508.8	*Betula* + *Populus*	GrA-1717	−26.74	9700 ± 50
12	38	510.4	*Betula* + *Populus*	GrA-1718	−25.99	9790 ± 50
11	34A	513.6	Mosses	GrA-2623	−28.28	9900 ± 60
10	34B	513.6	*Betula*	GrA-2654	−26.83	10,200 ± 200
9	33	514.4	*Betula* + Mosses	GrA-1711	−25.69	9830 ± 50
8	31	516.0	*Betula*	GrA-1714	−25.78	9860 ± 50
7	29	517.6	*Betula* + Mosses	GrA-1712	−25.72	9740 ± 50
6	28A	518.4	Mosses	GrA-2621	−28.09	10,050 ± 60
5	28B	518.4	*Betula*	GrA-2643	−27.21	10,070 ± 100
4	26B	520.0	*Betula*	GrA-2792	−27.23	10,400 ± 800
3	26A	520.0	Mosses	GrA-2620	−32.89	9990 ± 60
2	24	521.6	*Betula*	GrA-1716	−25.98	9900 ± 50
1	22	523.2	*Betula*	GrA-1713	−27.54	9860 ± 50